ADVANCED MATERIALS
www.advmat.de

Stable Metal–Organic Frameworks: Design, Synthesis, and Applications

*Shuai Yuan, Liang Feng, Kecheng Wang, Jiandong Pang, Matheiu Bosch, Christina Lollar, Yujia Sun, Junsheng Qin, Xinyu Yang, Peng Zhang, Qi Wang, Lanfang Zou, Yingmu Zhang, Liangliang Zhang, Yu Fang, Jialuo Li, and Hong-Cai Zhou**

Dedicated to Prof. Susumu Kitagawa on the occasion of his 65th birthday

Metal–organic frameworks (MOFs) are an emerging class of porous materials with potential applications in gas storage, separations, catalysis, and chemical sensing. Despite numerous advantages, applications of many MOFs are ultimately limited by their stability under harsh conditions. Herein, the recent advances in the field of stable MOFs, covering the fundamental mechanisms of MOF stability, design, and synthesis of stable MOF architectures, and their latest applications are reviewed. First, key factors that affect MOF stability under certain chemical environments are introduced to guide the design of robust structures. This is followed by a short review of synthetic strategies of stable MOFs including modulated synthesis and postsynthetic modifications. Based on the fundamentals of MOF stability, stable MOFs are classified into two categories: high-valency metal–carboxylate frameworks and low-valency metal–azolate frameworks. Along this line, some representative stable MOFs are introduced, their structures are described, and their properties are briefly discussed. The expanded applications of stable MOFs in Lewis/Brønsted acid catalysis, redox catalysis, photocatalysis, electrocatalysis, gas storage, and sensing are highlighted. Overall, this review is expected to guide the design of stable MOFs by providing insights into existing structures, which could lead to the discovery and development of more advanced functional materials.

1. Introduction

Metal–organic frameworks (MOFs) are an emerging class of porous materials constructed from metal-containing nodes and organic linkers.[1,2] Due to their structural and functional tunability as well as their ever-expanding application scope, MOFs have become one of the most fascinating classes of materials for both scientists and engineers.[3–9] They have been extensively studied not only for fundamental interests such as catalytic intermediate trapping and energy transfer, but also for potential practical applications including gas storage and separation, heterogeneous catalysis, chemical sensing, biomedical applications, and proton conduction.[10–13] Many early MOFs made from divalent metals, such as Zn^{2+} or Cu^{2+}, have shown exceptional porosity and promise for a wide variety of applications[1,14] but ultimately proved unsuitable for use under harsh conditions because of stability issues. For instance, MOF-5,[1] a prominent milestone in MOF research, decomposes gradually upon exposure to moisture in air. When MOFs are used for certain applications, their framework integrity must be guaranteed to maintain their intended functionalities and characteristics. In fact, water or moisture is usually present in industrial processes, and applications such as catalysis often require stability toward aqueous acid/base or coordinating anions. The instability of many MOFs in water or other harsh conditions has considerably limited their further application and commercialization. Therefore, the chemical stability of MOFs has been receiving more and more attention over the last five years. Researchers have started to address the stability of MOFs in different environments, understand the possible decomposition pathways, and are attempting to develop more stable framework structures.[15–17]

The stability of MOFs can be affected by multiple factors, including the operating environment, metal ions, organic ligands, metal–ligand coordination geometry, hydrophobicity of the pore surface, etc.[15,18,19] Studies on the stability of MOFs have allowed us to rationalize the effect of some factors and judiciously design stable framework structures. The relatively labile coordination bonds that support the framework structures are believed to be responsible for the limited stability of MOFs.[20] Thus a stable MOF structure should have strong coordination

S. Yuan, L. Feng, Dr. K. Wang, Dr. J. Pang, Dr. M. Bosch, C. Lollar, Y. Sun, Dr. J. Qin, X. Yang, Dr. P. Zhang, Q. Wang, Dr. L. Zou, Y. Zhang, Dr. L. Zhang, Dr. Y. Fang, J. Li, Prof. H.-C. Zhou
Department of Chemistry
Texas A&M University
College Station, TX 77843-3255, USA
E-mail: zhou@chem.tamu.edu
Prof. H.-C. Zhou
Department of Materials Science and Engineering
Texas A&M University
College Station, TX 77843-3003, USA
The ORCID identification number(s) for the author(s) of this article can be found under https://doi.org/10.1002/adma.201704303.

DOI: 10.1002/adma.201704303

bonds to survive the attack of guest molecules or possess steric hindrance to prevent the intrusion of guests to the metal nodes.

The metal–ligand bond strength determines the thermodynamic stability of MOFs under many operating environments. Therefore, the stability of MOFs can be roughly predicted by examining the strength of the bonds that form the framework. It is known that the metal–ligand bond strengths with a given ligand are positively correlated to charges of the metal cations and negatively correlated to the ionic radius. The effects of charge and radius can be combined into the concept of charge density. When the ligands and the coordination environment remain the same, high-valent metal ions with high charge densities can form stronger coordination bonds and thus a more stable framework. This trend is in line with Pearson's hard/soft acid/base (HSAB) principle and corroborated by many observations in MOF research.[16] The carboxylate-based ligands can be regarded as hard bases, which form stable MOFs together with high-valent metal ions, such as Ti^{4+}, Zr^{4+}, Al^{3+}, Fe^{3+}, and Cr^{3+}. Early stage work on high-valent metal based MOFs was established by Férey and co-workers who developed the Al^{3+}, Fe^{3+}, and Cr^{3+} based MIL series (MIL stands for Material Institut Lavoisier) including well-known MIL-53,[21] MIL-100,[22] and MIL-101.[4] The Zr^{4+} based MOFs were first synthesized in 2008 and have attracted considerable attention since 2012 because of their remarkable stability in water and even acidic conditions.[23] Following this trend, an escalating number of stable MOFs have been synthesized and reported in recent years.

According to the HSAB principle, stable MOFs can also be assembled by soft azolate ligands (such as imidazolates, pyrazolates, triazolates, and tetrazolates) and soft divalent metal ions (such as Zn^{2+}, Cu^{2+}, Ni^{2+}, Mn^{2+}, and Ag^{+}). The most representative examples are the zeolitic imidazolate frameworks (ZIFs) constructed by Zn^{2+} and imidazolate linkers.[24] In addition, Long and co-workers have developed triazole and pyrazolate-based MOFs which exhibit good stability in alkaline environments.[25,26]

Besides the influence of bond strength that determines thermodynamic stability, the stability of MOFs can also be affected by kinetic factors. A simple consideration of the bond strength of MOFs based on thermodynamics could result in inaccurate predictions that contradict experimental results. For example, UiO-66, UiO-67, and UiO-68 (UiO stands for University of Oslo) are isostructural MOFs having the same $[Zr_6(\mu_3\text{-}O)_4(\mu_3\text{-}OH)_4(COO)_{12}]$ cluster but different linker lengths.[23] Based on a thermodynamic argument, they might be expected to show similar stability according to their bond strengths.[23] However, experimental results showed decreased stability with an increase in linker length. This inconstancy can be rationalized by noting how the rigidity of linkers affects the kinetic stability. Dense and rigid structures formed by highly connected metal–oxo clusters and rigid organic linkers are usually more stable. This is in line with the good stability of high-valence metal clusters which tend to have higher coordination numbers and thus more rigid framework structures. Additionally, by specially designing hydrophobic surfaces or interfaces, water and other guest molecules can be excluded from approaching metal ions. For example, Omary and co-workers developed a series of fluorinated MOFs (FMOFs) with remarkable water stability as a result of super-hydrophobicity.[27] In addition, several publications have shown that postsynthetic treatment of labile MOFs with hydrophobic coatings can generate stable MOF composites.[28–34] However, this review will focus on the inherent stability of MOF materials. Composite materials will not be discussed.

With increased attention on stable MOFs and an improved understanding of the fundamental factors that affect the structural stability, studies on stable MOFs have flourished in the last few years. The ever-increasing number of

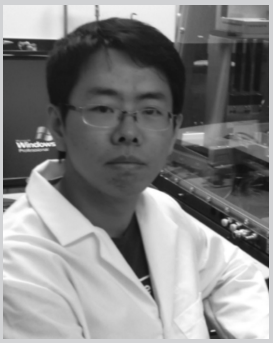

Shuai Yuan received his B.Sc. in chemistry from Shandong University in 2012. He then joined Prof. Hong-Cai Zhou's research group in the same year at Texas A&M University (TAMU). He is now a Ph.D. candidate in the Department of Chemistry at TAMU. His research is focused on the synthesis of stable metal–organic frameworks for energy conversion and storage.

Liang Feng received his B.Sc. in chemistry from Wuhan University in 2016, where he mainly worked on the synthesis of MOFs for gas storage and separation. He then joined Prof. Hong-Cai Zhou's research group in the same year at TAMU. His research interests focus on the design and synthesis of multifunctional metal–organic frameworks for catalysis.

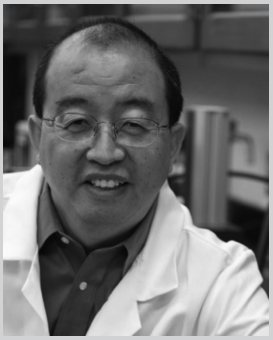

Hong-Cai Zhou obtained his Ph.D. in 2000 from TAMU under the supervision of F. A. Cotton. After a postdoctoral stint at Harvard University with R. H. Holm, he joined the faculty of Miami University, Oxford, in 2002. He moved back to TAMU and became a full professor in 2008. He was promoted to a Davidson Professor of Science in 2014 and a Robert A. Welch Chair in Chemistry in 2015. His research focuses on the discovery of synthetic methods to obtain robust framework materials with unique catalytic activities or desirable properties for clean-energy-related applications.

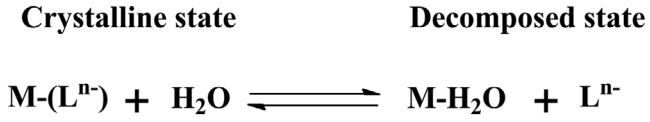

Scheme 1. Proposed decomposition mechanism of MOFs in water.

stable MOFs has significantly expanded the application of this emerging class of materials. Besides the conventional gas storage, stable MOFs have currently been applied in catalysis, biomedicine, and sensing.[15] A typical example is using MOFs as photocatalysts for catalytic water splitting and CO_2 reduction, which requires the framework to be stable in aqueous solutions with acid, base, or coordinating anions.[35,36] This review intends to provide fundamental mechanisms concerning MOF stability as well as the most recent design and synthetic strategies for stable MOFs. Important stable MOFs will be introduced, and their latest applications will be discussed. Altogether, this review provides a preliminary database for stable MOFs and their applications. It is expected to guide the design of stable MOFs by providing insights into existing structures, which could lead to the discovery and development of more advanced functional materials in respective fields.

2. Fundamentals of MOF Stability

Chemical stability is described as the ability of MOFs to maintain their long-ranged ordered structure in certain chemical environments.[37,38] It is usually confirmed by maintained powder X-ray diffraction (PXRD) pattern and Brunauer–Emmett–Teller (BET) surface area after specific treatments. The PXRD pattern characterizes the crystallinity of the sample; the BET surface area, derived from the N_2 sorption isotherm, probes the porosity. The operating environment (external factor) and the MOF structure (internal factor) are the two major aspects that affect the chemical stability of a MOF material.

2.1. In Water Vapor and Liquid Water

The procedure of MOF degradation in water vapor or liquid water can be considered as a series of substitution reactions in which the metal-coordinated linkers are replaced by water or hydroxide (**Scheme 1**).[37,39] Therefore, the direct method to prohibit this procedure is to enhance the strength of the coordination bonds between inorganic clusters and coordination groups. According to the HSAB theory, the interactions between hard Lewis acids and bases, or soft Lewis acids and bases will be much stronger than those between hard acids and soft bases, or soft acids and hard bases. Thus, to obtain stable MOFs, researchers choose to construct frameworks with carboxylate-based ligands (hard Lewis bases) and high-valent metal ions (hard Lewis acids), or azolate-based ligands (soft Lewis bases) and low-valency transition metal ions (soft Lewis acids). Guided by this strategy (**Scheme 2**), dozens of MOFs with excellent stability were obtained.[4,21,24,40–53]

2.2. In Aqueous Acid/Base

Compared to neutral water molecules, proton and hydroxide ions are much more destructive to MOFs. Therefore, it is exceedingly challenging to construct stable MOFs with good resistance to proton and hydroxide ions. Moreover, the chemical conditions of acidic and basic solutions are distinct, which leads to the different stability of MOFs in acids and bases. Many MOFs constructed from high-valent metal ions and carboxylate-based ligands exhibit excellent robustness in acids, while their resistance to base is much weaker. A typical example is PCN-222 (PCN stands for porous coordination network) or MOF-545 constructed from Zr^{4+} and carboxylate linkers.[40,54] It can maintain its crystallinity in concentrated HCl but readily decomposes in dilute alkali solution. On the other hand, MOFs constructed from low-valency metal ions and azolate-based ligands typically show great stability in basic solution but they are relatively more vulnerable in acids. For instance, PCN-601, a Ni^{2+}–pyrazolate based MOF, can survive in saturated NaOH (20 mol L^{-1}) at 100 °C, but it begins to degrade when the pH of solution falls below 4.[44]

Many efforts were made to explain the above phenomenon.[37,44,55] In acid, the degradation of MOFs is mainly caused by the competition of proton and metal ion for the coordinating linkers. In basic solutions, the major driving force of MOF decomposition is the replacement of linkers by hydroxide which competitively binds to the metal cations from MOF clusters. As shown in **Scheme 3**, in acidic conditions, although

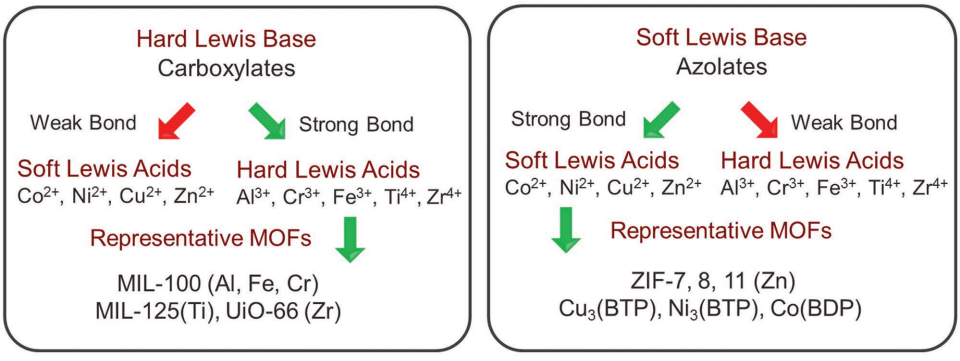

Scheme 2. Strategies to construct stable MOFs guided by HSAB theory.

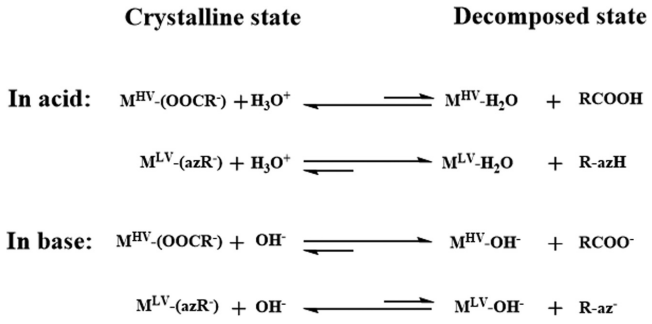

Scheme 3. Proposed decomposition mechanisms of MOFs in acid and base. (M^{HV}/M^{LV}: high/low-valency metal ions; RCOOH: carboxylate-based ligand; RazH: azolate-based ligand).

the coordination bonds between low-valency metal ions and azolate groups are strong, the pK_a values of azoles are also relatively high. This denotes a strong affinity between azolate groups and protons, which will easily push the system to the decomposed state in acidic solutions. However, for MOFs with high-valency metal ions and carboxylate-based ligands, the low pK_a of carboxylic acids and strong coordination bonds endow these MOFs with excellent stability in acids. Similar analysis can also explain the stability of MOFs in alkaline solutions. Because of the high affinity between high-valency metal ions and OH^-, MOFs constructed from high-valency metal ions and carboxylate-based ligands will easily decompose in basic solution. Low-valency metal ions have strong interactions with azolate groups and relatively low affinity to OH^-, which makes MOFs with low-valency metal ions and azolate–base ligands highly robust in basic solution.[37,44]

2.3. In Aqueous Solutions with Coordinating Anions

In addition to proton and hydroxide ions, many other coordinating anions, such as F^-, CO_3^{2-}, and PO_4^{3-}, are also destructive to MOFs. Unfortunately, these species are frequently involved in common reactions. They are usually essential reactants or work with their conjugated acids as buffer pairs to control the pH of the solution in reaction systems. Therefore, it is important to study the robustness of MOFs in aqueous solutions with these coordinating anions.[55] Because all the aforementioned coordinating anions can be classified as hard Lewis bases, they tend to interact strongly with high-valency metal ions, which is reflected by the high binding constants of these anions with Zr^{4+}, Fe^{3+}, and Al^{3+}.[56,57] For MOFs constructed from high-valency metal ions, the carboxylate ligands can be readily replaced by these coordinating anions (hard Lewis bases) that exist in the solution as competing species. An effective method to overcome the vulnerability of these materials to coordinating anions is to construct MOFs with soft metal ions and ligands. In this way, the strong coordination bonds between metal ions and ligands are maintained, while the affinity between the metal ions in the framework and the coordinating anions in solution is reduced. In 2016, our group reported a MOF constructed from a $[Ni_8(OH)_4(H_2O)_2PZ_{12}]$ (PZ = pyrazolate) cluster and a TPPP linker (TPPP = 5,10,15,20-tetrakis (4-(pyrazolate-4-yl)phenyl)porphyrin), namely PCN-602.[45] This material demonstrated excellent stability in aqueous solutions of 1 M KF, K_3PO_4, and Na_2CO_3. The N_2 sorption isotherms and PXRD patterns of the treated PCN-602 remained consistent, which confirmed the robustness of PCN-602 in these solutions. As a comparison, a Zr-cluster based analogue, PCN-224, totally decomposed in aqueous solutions containing these coordinating anions.[45]

2.4. Mechanical Stability

Mechanical stability of MOFs under vacuum or pressure is another important factor for MOF's industry and practical applications from an engineering perspective. The instability of MOF pore structure under vacuum sometimes would lead to phase changes or partial collapse of pores.[58] In order to fully activate MOFs while avoid structural collapse, solvent exchange, and solvent evacuation are usually adopted. Exchanging higher surface tension solvents with lower ones including CH_2Cl_2, *n*-hexane and liquid CO_2 and further solvent removal would help the efficient activation of MOFs. Besides, compared with zeolites, MOFs also possess a relatively low stability under mechanical pressure. For example, ZIF-8 with high chemical stability would undergo an irreversible amorphization following compression beyond 0.34 GPa and also lose porosity gradually when treated with pressures of up to 1.2 GPa.[59]

It should be noted that there is no standardized testing method to qualify the stability of a given MOF. Different standards need to be adopted depending on the operating environments. For example, some catalysis processes require acidic/basic environments or oxidizing/reducing conditions. Industrial catalysis may require stability against hydrothermal steaming. The mechanical stability of a MOF needs to be considered for industrial processing from an engineering perspective. MOFs may show dramatically different performance under different conditions. For example, MOFs with high-valency metal ions and carboxylate-based linkers have strong stability in acidic conditions but tend to be decomposed by base and coordinating anions such as CO_3^{2-}. Similarly, low-valency metal ions and azolate-based MOFs have strong resistance toward alkaline environments but can be easily decomposed by acid. MIL-88 (Fe or Cr) and MIL-53 (Fe or Cr), represent a class of chemically stable MOFs with low mechanical stability as reflected by their flexible behavior upon guest adsorption/desorption.[21] Therefore, different criteria need to be considered depending on the operating environments for certain applications.

2.5. Structural Factors Contributing to MOF Stability

2.5.1. High Connectivity of Metal Nodes and Ligands

If the connectivity of ligands or metal nodes is higher, the repair of structural defects can take place at a higher rate and prevent further decomposition, thereby enhancing the MOF stability.[44,60] This principle is applied to explain the extraordinary chemical stability of PCN-601, a 4,12-connected network. The connectivity of both the Ni_8 cluster (a 12-connected node)

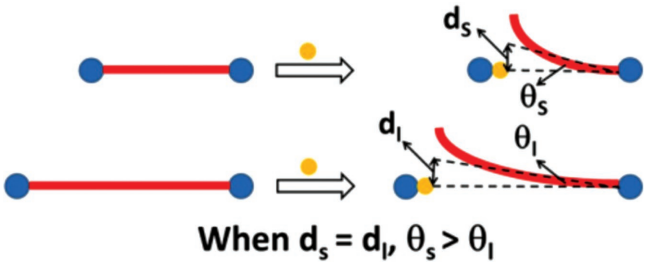

Figure 1. Illustration of the kinetic stability of MOFs with ligands of different lengths. Reproduced with permission.[44] Copyright 2016, American Chemical Society.

and the pyrazolate-based porphyrinic ligand TPP (a 4-connected linker) are relatively high among the reported inorganic clusters and organic ligands. From a kinetic perspective, the decomposition of MOFs in solutions could be regarded as successive substitution of coordination moieties with small molecules or ions. During this procedure, structural defects occur and accumulate, which finally leads to the decomposition of the framework.[39] With higher connectivity, the ligand dissociation is suppressed, while the ligand association rate is enhanced, which will lead to a faster defect reparation. This phenomenon resembles the chelating effect of multi-dentate ligands and therefore is named the 3D chelating effect. Similar conclusions can be obtained for highly connected metal nodes as well. Therefore, fragments with more connections are greatly favored for the generation of stable MOFs.

2.5.2. Rigidity of Ligands

Apart from the 3D chelating effect, the rigidity of ligands is also crucial in determining the robustness of the framework. In the work of PCN-601, Wang et al. rationalized that the length of the ligand is related to the activation energy of ligand dissociation and thus affects the decomposition of MOFs.[44,61] In **Figure 1**, two isoreticular frameworks are presented, which are constructed by a long and a short ligand. Regardless of the decomposition pathway of the framework (dissociative or associative mechanism), ligands coordinated to inorganic clusters are required to be bent in transition states. Assuming the displacements of the ligand terminals in the transition states are equal in the two scenarios ($d_s = d_l$), the short and rigid ligand would be bent to a larger angle ($\theta_s > \theta_l$). This would raise the activation energy of decomposition, which therefore leads to relatively higher inertness of the framework.[44]

2.5.3. Hydrophobic Groups

Water stability of MOFs may also be enhanced by introducing hydrophobic groups onto the ligands. ZIF-8 is a typical example to illustrate this point.[24] The methyl group on the ligand was proposed to assist in blocking water molecules from attacking the [ZnN_4] units. Similarly, in ZIF-68, 69, and 70, the hydrophobic surfaces of these ZIFs also serve to increase their water resistance.[38] In 2013, Padial et al. reported the construction of stable MOFs by using pyrazolate-based ligands with methyl groups.[62] Typically, the introduction of functional groups into MOFs will narrow the pore size of the framework, which leads to condensation of water vapor at lower pressures. However, the methyl groups were confirmed to enhance the relative pressure of water vapor condensation into frameworks substantiating the effect of methyl groups on the hydrophobicity of frameworks.[38]

The same strategy can be applied in MOFs constructed by hard Lewis acids and bases. In 2016, Wang et al. reported two isostructural Zr-MOFs, BUT-12, and BUT-13,[63] with good resistance toward boiling water, concentrated HCl, and NaOH solutions. It is proposed that the methyl groups on the organic linkers increased the hydrophobicity of the materials and therefore raised their stability in aqueous solutions.[62] The water contact angles of BUT-12 and BUT-13 with water are 138.7° and 118.3°, respectively, classifying both materials as hydrophobic. It should be noted that the liquid water wetting is likely to be a measure of MOF surface and therefore can be affected by surface termination and texture. Water isotherms for both materials bear hysteresis loops, with low uptakes at low pressures and large rises in water uptakes at high pressures.[63] All these experimental results strongly suggest a low affinity between water molecules and the surfaces of BUT-12 and BUT-13. The hydrophobic surfaces and interfaces inhibit the water molecules from attacking the inorganic clusters and enhance the stability of these MOFs.[38]

3. Design and Synthesis

3.1. Modulated Synthesis

Though there is high interest in stable MOFs, their inert metal–ligand bonds pose significant challenges in regards to synthesis. The crystallization process requires an equilibrium between the crystal formation and dissolution to allow sufficient structure reorganization or defect reparation. However, the strong coordination bonds in stable MOFs are difficult to dissociate during the MOF growth process. Therefore, direct synthesis of stable MOFs using a mixture of metal salts and organic linkers usually results in quick precipitation of low crystalline powders. To obtain highly crystalline products or single crystals, a modulated synthesis was employed. Modulated synthesis refers to the regulation of the coordination equilibrium by modulators which either competitively coordinate with the metals or suppress the deprotonation of linkers. As a result, the competitive reaction can reduce the rate of nucleation and slow down crystal growth to help produce highly crystalline products.

In fact, many early MOFs, including the divalent metal-based ones, were synthesized by adding a few drops of acid to slow down the crystal growth and obtain large crystals.[64] Strong acids with weakly coordinating counterions, such as HNO_3 or HBF_4, can reduce the pH and suppress the deprotonation of organic linkers. As the coordination of organic linkers often requires deprotonation, the rate of MOF formation is decelerated by the low pH.[33] However, it is always difficult to predict the structure of the products just by adding acid. The one-pot reaction between metal ions, organic linkers, and acids usually leads to the formation of hybrid complexes. For instance,

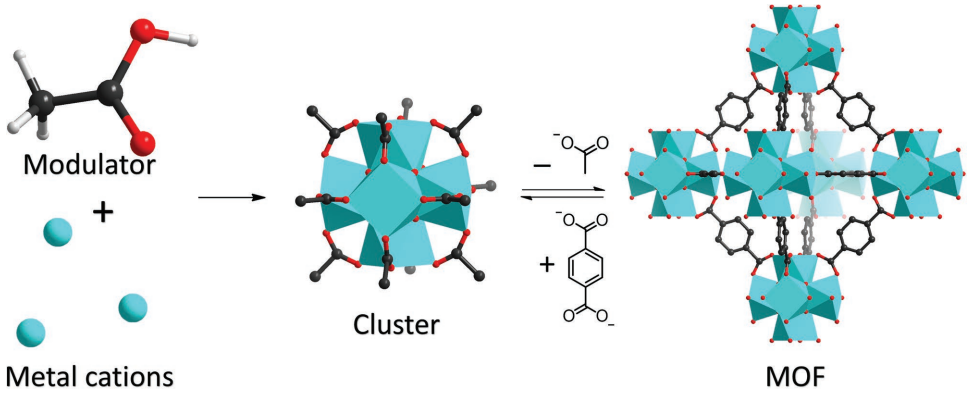

Figure 2. Representative modulated synthesis.

different metal–oxo clusters could form during the synthesis which leads to the production of impurities. The mechanism for the formation of each product is not fully understood even though some interesting structures might be obtained.

Zr-MOFs represent a prime example of rationalizing MOF formation by modulated synthesis. The first example of applying the modulated synthesis strategy to prepare Zr-MOFs was reported by Schaate et al. in 2011.[65] The effects of monocarboxylic acids on the formation of UiO-type MOFs were systematically studied. The sizes of crystals were tuned by changing the amount of monocarboxylic acid as modulating reagent. Single crystals of UiO-68-NH_2 were obtained which afforded single-crystal X-ray diffraction analysis to provide the first single-crystal structure of a Zr-MOF. This study dramatically accelerated the development of new Zr-MOFs because the single-crystalline products allow facile structural characterization, which maximizes the understanding of structure–property correlations. In situ formation of coordination complexes between the Zr(IV) cation and monocarboxylic acid modulators was proposed as the mechanism of modulated synthesis. The coordination complexes, presumably $[Zr_6(\mu_3\text{-}O)_4(\mu_3\text{-}OH)_4(RCOO)_{12}]$ clusters, act as intermediates, which form the Zr-MOFs via exchange reactions between the modulators and linkers (**Figure 2**). An excess of modulator would inhibit the replacement of modulators by linkers, therefore slowing down nucleation and crystal growth, leading to larger crystals.

Inspired by the aforementioned studies, preformed metal–oxo clusters with structures identical to the secondary building units (SBUs) of target MOFs were utilized as precursors for MOF synthesis. For example, the $[Fe_3(\mu_3\text{-}O)(OH)(H_2O)_2(RCOO)_6]$ and $[Ti_8O_8(RCOO)_{16}]$ clusters have been used as precursors to prepare MIL-88(Fe) and MIL-125(Ti)-type structures, respectively.[16,66] The use of metal–oxo clusters as precursors allows for more flexibility in experimental conditions (for example larger range of temperature) and leads to higher product yields.[67] Guillerm et al. used a $[Zr_6(\mu_3\text{-}O)_4(\mu_3\text{-}OH)_4(methacrylate)_{12}]$ cluster as a precursor to synthesize Zr-MOFs with UiO structures.[68] During the reaction process, the methacrylate ligands were replaced by dicarboxylate linkers, which potentially mimics the reaction pathway of modulated synthesis. Our group extended this modulated synthetic strategy to obtain a series of MOFs from preassembled $[Fe_2M(\mu_3\text{-}O)(H_2O)_3(RCOO)_6]$ clusters (M = $Fe^{2+,3+}$, Co^{2+}, Ni^{2+}, Mn^{2+}, and Zn^{2+}).[69] The utilization of preformed clusters avoids the in situ formation of various clusters as intermediates and therefore favors the formation of the preferred product. In addition, MOF growth can be simplified into a series of stepwise ligand substitution reactions on the preformed clusters, which facilities structural design and prediction.

3.2. Postsynthetic Modification

Postsynthetic modification (PSM) represents an important supplement to the traditional one-pot synthesis of MOFs.[70] The postsynthetic method has been proved as a versatile tool to prepare topologically identical MOFs with diverse functionalities. Stable MOFs bear an additional advantage over labile ones as they can survive harsh modification conditions while maintaining their crystallinity and porosity. This opens up the possibility of performing a wider range of PSM reactions on stable MOF platforms.

Covalent modification is the most common route of PSM that functionalizes MOFs with tailored internal surfaces for specific applications. Functional groups such as amino groups as chemical handles are usually preanchored on the linkers of MOFs for further modification reactions. The amino functionalized linkers, BDC-NH_2 (BDC-NH_2 = amino terephthalate) for example, are quite compatible with a number of MOFs, including MIL-53(Al, Cr, and Fe),[71,72] MIL-101(Al, Cr, and Fe),[73] CAU-1 (CAU = Christian-Albrechts University),[74] and UiO-66.[75] PSMs of amino groups by anhydrides, isocyanates, aldehydes, acyl chlorides, alkyl bromides, and many more complicated metal–organic complexes have been reported.[70,75–77] Click chemistry between azides and alkynes has also been widely used to modify MOFs with desired functional groups. Jiang et al. reported the covalent modification of a series of azide-functionalized Zr-MOFs through click reactions. The easily accessible and reactive azide groups in the MOF cavity allow for quantitative click reactions with alkynes to form various MOFs with tailored pore surfaces.

Besides covalent modification, dative modification of MOFs through postsynthetic metalation has also been adopted. An early example was reported jointly by Yaghi and Long groups in which an Al-based MOF with 2,2′-bipyridine (bpy) sites was synthesized and postsynthetically metalated with soft metal

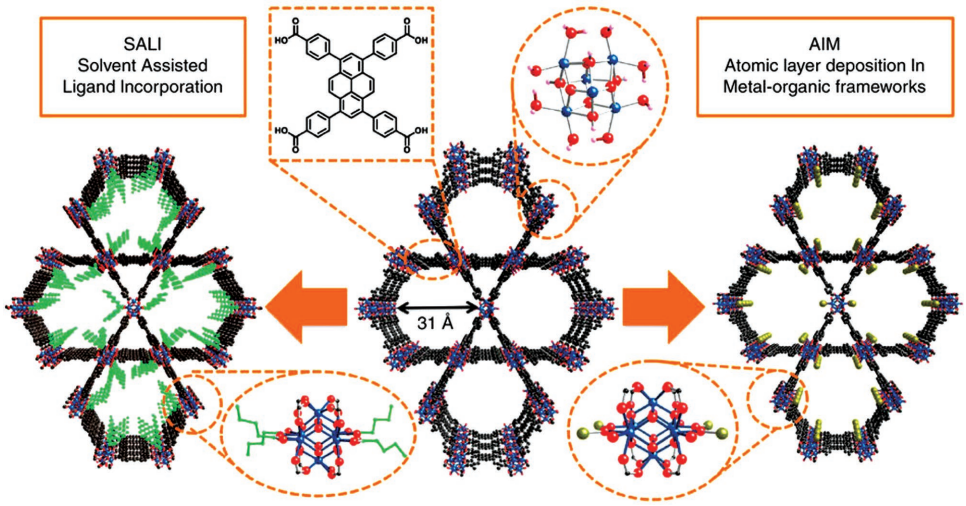

Figure 3. Postsynthetic incorporation of ligands and metal cations on the coordinatively unsaturated $[Zr_6(\mu_3\text{-}O)_4(\mu_3\text{-}OH)_4(OH)_4(H_2O)_4(COO)_8]$ node. Reproduced with permission.[83] Copyright 2017, Nature Publishing Group.

ions including Cu^{2+} and Pd^{2+}.[78] Later on, the metalation of Zr-based MOFs with bpy sites was reported. The metalated Zr-MOFs serve as efficient catalysts for a broad-scope of organic transformations such as alkene hydrogenation/hydroboration and arene C—H borylation.[79,80] The Zr_6-cluster, with amphoteric behavior, can also act as a ligand to support metal cations. NU-1000 contains octahedral $[Zr_6(\mu_3\text{-}O)_4(\mu_3\text{-}OH)_4(OH)_4(H_2O)_4(COO)_8]$ nodes, where 8 of 12 octahedral edges are connected with carboxylate ligands, while the remaining coordination sites are occupied by eight terminal $-OH^-/H_2O$ groups.[81,82] When NU-1000 samples were exposed to metal sources, the terminal $-OH^-/H_2O$ groups deprotonate to allow the binding of metal cations, which represents a special metalation approach (**Figure 3** right).[83]

The coordinatively unsaturated metal sites in MOFs can also be modified by additional ligands. For example, the vacant coordination sites in $[Cr_3(\mu_3\text{-}O)(COO)_6]$ or $[Cu_4Cl(triazolate)_6]$ MOFs could be modified with alkane amines to improve CO_2 uptake.[25,84] Similarly, functional sites possessing catalytic activity have been introduced into MIL-101(Cr) and MIL-101(Fe) through the coordination of pyridine groups to the $[M_3(\mu_3\text{-}O)(COO)_6]$ ($M = Cr^{3+}$ or Fe^{3+}) clusters.[85] The coordinatively unsaturated Zr_6-clusters can also bind with carboxylates through simple acid/base reactions. For example, the solvent-assisted ligand incorporation (SALI) method was developed to modify the coordinatively unsaturated $[Zr_6(\mu_3\text{-}O)_4(\mu_3\text{-}OH)_4(OH)_4(H_2O)_4(COO)_8]$ cluster in NU-1000 with different perfluoroalkyl carboxylate entities for enhanced CO_2 uptake (Figure 3 left).[86] Other ligands, including phosphates and sulfates, were also attached to the cluster of Zr-MOFs by similar methods.[87] A prominent example of dative PSM is the so-called linker installation method in which a coordinatively unsaturated Zr-MOF was constructed and linkers with different lengths were sequentially installed between each pair of clusters.[88,89] Systematic variation of the pore volume and decoration of pore environment were realized by sequential installation of multiple linkers with different lengths or functional groups, which resulted in synergistic effects in gas uptake.

Postsynthetic ligand and metal ion exchange have been demonstrated as an effective method to generate otherwise unobtainable MOFs. Intuitively, the inert metal bonds in stable MOFs will significantly suppress the ligand and metal ion exchange process. However, studies on the ligand and metal ion exchange of several stable MOFs suggest that the robustness of such metal–ligand bonds was overestimated.[90] Postsynthetic ligand and metal ion exchange processes were shown to readily occur in several stable MOFs, including ZIFs, MIL series, and UiO series (**Figure 4**). Compared with direct solvothermal synthesis, ligand exchange in robust MOFs provides an alternative method to incorporate

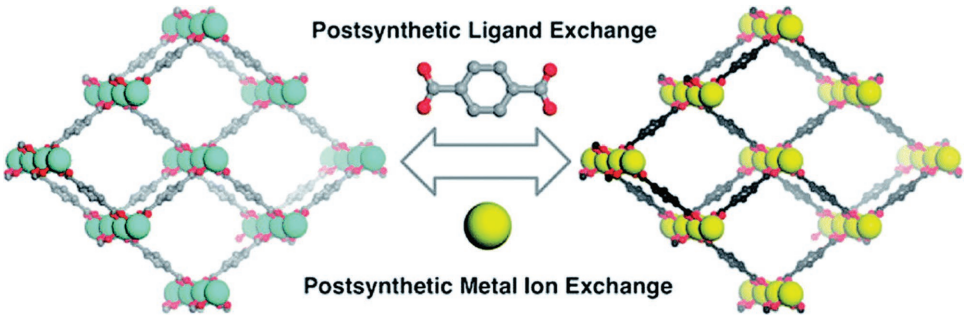

Figure 4. Postsynthetic ligand and cation exchange in robust MOFs. Reproduced with permission.[90] Copyright 2012, American Chemical Society.

functional groups, especially labile ones, into a robust MOF under relatively mild conditions. For example, a labile dinuclear iron complex, [FeFe](DCBDT)$(CO)_6$ (DCBDT = 1,4-dicarboxylbenzene-2,3-dithiolate), was incorporated into the robust UiO-66(Zr) framework as a functional mimic of the [FeFe]-hydrogenase active site.[91] On the other hand, the metal ion exchange can enhance the stability of MOFs by replacing the labile metal–ligand bond with more robust ones. Our group reported a post-synthetic metal-ion exchange and oxidation method by replacing low-valency metal in MOFs with variable-valent metal ions and further oxidizing them to higher oxidation states.[92] The resulting high-valency metal based MOFs show increased stability compared to its low-valency states. In another work, Fe-based MOFs were exchanged by Cr^{3+}, which affords more inert frameworks. The above mentioned synthetic methods together form a toolbox to prepare stable MOFs with desired functionalities.

4. Stable Metal–Organic Frameworks

The stability of MOFs can be predicted by comparing the strength of the metal–ligand bond that forms the frameworks. According to the HSAB principle, stable MOFs are mostly constructed from carboxylate-based ligands (hard Lewis bases) and high-valency metal ions (hard Lewis acids), or azolate-based ligands (soft Lewis bases) and low-valency transition metal ions (soft Lewis acids). In addition, the pore environments of MOFs can be judiciously tuned to exclude the infusion of certain reactive guests, such as water, to increase the overall chemical stability. Guided by this strategy, an increasing number of MOFs with excellent stability were reported, which were selected, classified, and summarized in this section. Some representative stable MOFs discussed herein are listed in **Table 1**.

4.1. M^{4+}–Carboxylate Based MOFs

Tetravalent metal (Ti^{4+}, Zr^{4+}, Hf^{4+}, or Ce^{4+}) and carboxylate linker-based MOFs form a relatively new field in MOF research. The first Zr-MOF was reported in 2008[23] followed by the discovery of Ti-MOFs in 2009.[93] They have drawn particular attention due to their high stability, which has made them promising for wide-scale applications. As discussed above, there are two main reasons for the excellent chemical stability of M^{4+}-based MOFs. First, the high charge and charge to radius ratio (Z/R) make them hard acids, which match to the relatively hard carboxylate ligands. The strong M^{4+}–carboxylate interaction contributes to the chemical stability of the framework. Second, tetravalent metals require more ligands to balance their charge, therefore their SBUs tend to have a high connection number. The highly connected clusters, to some extent, prevent the attack of guests such as water molecules.

4.1.1. Ti^{4+}–Carboxylate Based MOFs

Ti-MOFs are especially interesting due to their high stability and photocatalytic activity. However, only a limited number of Ti(IV)-carboxylate-based MOFs (MIL-125 and its derivatives,[93] PCN-22,[94] COK-69,[95] MOF-901,[96] and MOF-902[97]) have been reported, possibly due to synthetic difficulties. The first Ti-MOF, MIL-125, is constructed from $[Ti_8O_8(OH)_4(COO)_{12}]$ clusters and BDC linkers (**Figure 5**). It demonstrates high stability, permanent porosity, and photocatalytic activity toward alcohol oxidation.[93] Further work has been done to functionalize the BDC linker with amino groups to adjust its bandgap.[98] Recent work also demonstrates that MIL-125 and its NH_2-functionalized derivative (MIL-125-NH_2) can catalyze light-driven water splitting[99] and CO_2 reduction.[36]

PCN-22 was formed by a Ti_7-cluster and a porphyrin-based linker.[94] It presents a high permanent porosity toward N_2 with a BET surface area of 1284 m^2 g^{-1}. The combination of Ti-clusters and porphyrin linkers mimics the porphyrin-sensitized TiO_2 nanoparticles. Because of the porphyrin moieties, PCN-22 shows a broad range of light absorption with a small optical bandgap of 1.93 eV, the smallest reported to date for carboxylate based Ti-MOFs. Photocurrent measurements indicated that PCN-22 is photoactive under visible-light illumination. Finally, it acts as a heterogeneous photocatalyst that promotes the oxidation of benzyl alcohol to the corresponding aldehyde under visible light.

MOF-901 and MOF-902 are a class of unique MOFs as they combine the synthetic strategies of MOFs and covalent–organic frameworks.[96,97] A hexameric Ti-oxo-cluster, $[Ti_6O_6(OMe)_6(ABZ)_6]$ (ABZ = 4-aminobenzoate), was in situ generated which was further extended into a 2D layer through an imine condensation reaction between amino groups and dialdehyde spacers (**Figure 6**). The overall structures can be described as 2D layers with triangular apertures, stacked in an AB fashion. They exhibit permanent porosity toward N_2 with BET surface areas of 550 m^2 g^{-1} for MOF-901 and 400 m^2 g^{-1} for MOF-902.

Crystalline coordination polymers based on Ti and hydroxycarboxylate ligands have also been documented. For example, the reaction of Ti^{4+} and 2,5-dihydroxyterephthalic acid under different conditions leads to the isolation of NTU-9[100] (NTU stands for Nanyang Technological University), MIL-167, MIL-168, and MIL-169.[101] Among them, NTU-9 shows a large hexagonal cavity with a diameter of 11 Å, although the permanent porosity has not been assessed. In addition, some Ti(III)-based MOFs have been reported which can be oxidized to Ti(IV) upon exposure to air.[95,102]

4.1.2. Zr^{4+}–Carboxylate Based MOFs

Zr-based MOFs have recently been well summarized in a comprehensive review article by Yan et al.[17] Considering the large number of Zr-MOFs reported so far, we do not intend to cover all the Zr-MOFs in this section. Instead, we would like to briefly introduce the development of this field, focusing on some representative structures.

The first example of the Zr-MOF, UiO-66, was reported in 2008.[23] It is constructed from 12-connected $[Zr_6(\mu_3\text{-}O)_4(\mu_3\text{-}OH)_4(COO)_{12}]$ clusters and linear dicarboxylate linkers. Within the octahedral cluster, six vertices are occupied by Zr^{4+} and eight triangular faces are alternatively capped by four μ_3-OH and four μ_3-O. The $[Zr_6(\mu_3\text{-}O)_4(\mu_3\text{-}OH)_4]$ core is further terminated by 12 carboxylates forming $[Zr_6(\mu_3\text{-}O)_4(\mu_3\text{-}OH)_4(COO)_{12}]$ clusters.

Table 1. Summary of some representative stable MOFs.

MOFs[a)]	Clusters/cores	Linkers[b)]	BET surface area ($m^2\ g^{-1}$)	Ref.
MIL-53(Al)	$[Al(OH)(COO)_2]_n$	BDC	1181	[117]
Al-FUM	$[Al(OH)(COO)_2]_n$	FUM	1080	[182,183]
MIL-69	$[Al(OH)(COO)_2]_n$	2,6-NDC	NA	[184]
MIL-96(Al)	$[Al_3(\mu_3\text{-}O)(COO)_6]$ $[Al(OH)(COO)_2]_n$	BTC	NA	[127]
MIL-100(Al)	$[Al_3(\mu_3\text{-}O)(COO)_6]$	BTC	2152	[128]
MIL-101(Al)	$[Al_3(\mu_3\text{-}O)(COO)_6]$	$BDC\text{-}NH_2$	2100	[73]
MIL-110	$[Al_8(OH)_{15}(COO)_9]$	BTC	1400	[185]
MIL-118	$[Al(OH)(COO)_2(COOH)_2]_n$	BTEC	NA	[123]
MIL-120	$[Al(OH)(COO)_2]_n$	BTEC	308	[124]
MIL-121	$[Al(OH)(COO)_2]_n$	BTEC	162	[122]
MIL-122	$[Al(OH)(COO)_2]_n$	NTC	NA	[186]
DUT-5	$[Al(OH)(COO)_2]_n$	BPDC	1613	[118]
NOTT-300	$[Al(OH)(COO)_2]_n$	BPTA	1370	[125]
CAU-1	$[Al_8(OH)_4(OCH_3)_8(COO)_{12}]$	$BDC\text{-}NH_2$	1700[c)]	[133]
CAU-3-BDC	$[Al_{12}(OCH_3)_{24}(COO)_{12}]$	BDC	1550	[134]
CAU-3-BDC-NH_2	$[Al_{12}(OCH_3)_{24}(COO)_{12}]$	$BDC\text{-}NH_2$	1250	[134]
CAU-3-NDC	$[Al_{12}(OCH_3)_{24}(COO)_{12}]$	2,6-NDC	2320	[134]
CAU-4	$[Al(OH)(COO)_2]_n$	BTB	1520	[187]
CAU-8	$[Al(OH)(COO)_2]_n$	BeDC	600	[188]
CAU-10	$[Al(OH)(COO)_2]_n$	1,3-BDC	635	[189]
467-MOF	$[Al(OH)(COO)_2]_n$	BTTB	725	[121]
Al-PMOF	$[Al(OH)(COO)_2]_n$	TCPP	1400	[126]
PCN-333(Al)	$[Al_3(\mu_3\text{-}O)(COO)_6]$	TATB	4000	[129]
PCN-888(Al)	$[Al_3(\mu_3\text{-}O)(COO)_6]$	HTB	3700	[130]
Al-soc-MOF-1	$[Al_3(\mu_3\text{-}O)(COO)_6]$	TCPT	5585	[132]
MIL-53(Cr)	$[Cr(OH)(COO)_2]_n$	BDC	NA	[21]
MIL-88A(Cr)	$[Cr_3(\mu_3\text{-}O)(COO)_6]$	FUM	NA	[138]
MIL-88B(Cr)	$[Cr_3(\mu_3\text{-}O)(COO)_6]$	BDC	NA	[138]
MIL-88C(Cr)	$[Cr_3(\mu_3\text{-}O)(COO)_6]$	2,6-NDC	NA	[138]
MIL-88D(Cr)	$[Cr_3(\mu_3\text{-}O)(COO)_6]$	BPDC	NA	[138]
MIL-96(Cr)	$[Cr_3(\mu_3\text{-}O)(COO)_6]$ $[Cr(OH)(COO)_2]_n$	BTC	NA	[190]
MIL-100(Cr)	$[Cr_3(\mu_3\text{-}O)(COO)_6]$	BTC	3100[c)]	[22]
MIL-101(Cr)	$[Cr_3(\mu_3\text{-}O)(COO)_6]$	BDC	4100	[4]
MIL-101-NDC(Cr)	$[Cr_3(\mu_3\text{-}O)(COO)_6]$	2,6-NDC	2100	[191]
PCN-333(Cr)	$[Cr_3(\mu_3\text{-}O)(COO)_6]$	TATB	2548	[141]
PCN-426(Cr)	$[Cr_3(\mu_3\text{-}O)(COO)_6]$	TMQPTC	3155	[92]
MIL-53(Fe)	$[Fe(OH)(COO)_2]_n$	BDC	NA	[135]
MIL-68(Fe)	$[Fe(OH)(COO)_2]_n$	BDC	665	[136]
MIL-141(Fe)	$[Fe(OH)(COO)_2]_n$	TCPP	420	[137]
FepzTCPP$(FeOH)_2$	$[Fe(OH)(COO)_2]_n$	Pyrazine, TCPP	760	[137]
MIL-88A(Fe)	$[Fe_3(\mu_3\text{-}O)(COO)_6]$	FUM	NA	[138]
MIL-88B(Fe)	$[Fe_3(\mu_3\text{-}O)(COO)_6]$	BDC	NA	[138]
MIL-88C(Fe)	$[Fe_3(\mu_3\text{-}O)(COO)_6]$	2,6-NDC	NA	[138]
MIL-88D(Fe)	$[Fe_3(\mu_3\text{-}O)(COO)_6]$	BPDC	NA	[138]

Table 1. Continued.

MOFs[a)]	Clusters/cores	Linkers[b)]	BET surface area ($m^2 g^{-1}$)	Ref.
MIL-100(Fe)	$[Fe_3(\mu_3\text{-}O)(COO)_6]$	BTC	2800[c)]	[46]
MIL-101(Fe)	$[Fe_3(\mu_3\text{-}O)(COO)_6]$	BDC	2823	[131]
PCN-250(Fe)	$[Fe_3(\mu_3\text{-}O)(COO)_6]$	ABDC	1486	[192]
PCN-250(Fe_2Co)	$[Fe_2Co(\mu_3\text{-}O)(COO)_6]$	ABDC	1400	[192]
PCN-333(Fe)	$[Fe_3(\mu_3\text{-}O)(COO)_6]$	TATB	2427	[129]
PCN-600(Fe)	$[Fe_3(\mu_3\text{-}O)(COO)_6]$	TCPP	2270	[43]
$Tb_2(BDC)_3$	$[Tb(H_2O)_2(COO)_3]_n$	BDC	NA	[142]
MIL-63	$[Eu_2(\mu_3\text{-}OH)_7(COO)]_n$	BTC	15	[143]
MIL-83	$[Eu(\mu_3\text{-}O)_3(COO)_3(COOH)_3]_n$	1,3-ADC	NA	[144]
MIL-103	$[Tb(H_2O)(COO)_4]_n$	BTB	930	[145]
Y-BTC	$[Y(H_2O)(COO)_3]_n$	BTC	1080	[146]
Tb-BTC	$[Tb(H_2O)(COO)_3]_n$	BTC	786	[146]
Y-FTZB	$[Y_6(\mu_3\text{-}OH)_8(COO)_6(CN_4)_6]$	FTZB	1310	[147]
Tb-FTZB	$[Tb_6(\mu_3\text{-}OH)_8(COO)_6(CN_4)_6]$	FTZB	1220	[147]
Y-FUM	$[Y_6(\mu_3\text{-}OH)_8(COO)_{12}]$	FUM	691	[151]
Tb-FUM	$[Tb_6(\mu_3\text{-}OH)_8(COO)_{12}]$	FUM	503	[151]
Ce-Uio-66	$[Ce_6(\mu_3\text{-}O)_4(\mu_3\text{-}OH)_4(COO)_{12}]$	BDC	1282	[115]
Ce-UiO-66-$(CH_3)_2$	$[Ce_6(\mu_3\text{-}O)_4(\mu_3\text{-}OH)_4(COO)_{12}]$	BDC-$(CH_3)_2$	845	[116]
MIL-125	$[Ti_8O_8(OH)_4(COO)_{12}]$	BDC	1550	[93]
PCN-22	$[Ti_7O_6(COO)_{12}]$	TCPP	1284	[94]
COK-69	$[Ti_3O_3(COO)_6]$	CDC	NA	[95]
MOF-901	$[Ti_6O_6(OMe)_6(COO)_6]$	AB, BDA	550	[96]
MOF-902	$[Ti_6O_6(OMe)_6(COO)_6]$	AB, BPDA	400	[97]
UiO-66	$[Zr_6(\mu_3\text{-}O)_4(\mu_3\text{-}OH)_4(COO)_{12}]$	BDC	1187	[23]
UiO-67	$[Zr_6(\mu_3\text{-}O)_4(\mu_3\text{-}OH)_4(COO)_{12}]$	BPDC	3000	[23]
UiO-68	$[Zr_6(\mu_3\text{-}O)_4(\mu_3\text{-}OH)_4(COO)_{12}]$	TPDC	4170	[23]
PCN-94	$[Zr_6(\mu_3\text{-}O)_4(\mu_3\text{-}OH)_4(COO)_{12}]$	ETTC	3377	[193]
PCN-222	$[Zr_6(\mu_3\text{-}O)_4(\mu_3\text{-}OH)_4(OH)_4(H_2O)_4(COO)_8]$	TCPP	2223	[40]
PCN-223	$[Zr_6(\mu_3\text{-}O)_4(\mu_3\text{-}OH)_4(COO)_{12}]$	TCPP	1600	[103]
PCN-224	$[Zr_6(\mu_3\text{-}O)_4(\mu_3\text{-}OH)_4(OH)_6(H_2O)_6(COO)_6]$	TCPP	2600	[41]
PCN-225	$[Zr_6(\mu_3\text{-}O)_4(\mu_3\text{-}OH)_4(OH)_4(H_2O)_4(COO)_8]$	TCPP	1902	[194]
PCN-228	$[Zr_6(\mu_3\text{-}O)_4(\mu_3\text{-}OH)_4(COO)_{12}]$	TCP-1	4510	[60]
PCN-229	$[Zr_6(\mu_3\text{-}O)_4(\mu_3\text{-}OH)_4(COO)_{12}]$	TCP-2	4619	[60]
PCN-230	$[Zr_6(\mu_3\text{-}O)_4(\mu_3\text{-}OH)_4(COO)_{12}]$	TCP-3	4455	[60]
PCN-521	$[Zr_6(\mu_3\text{-}O)_4(\mu_3\text{-}OH)_4(OH)_4(H_2O)_4(COO)_8]$	MTBC	3411	[104]
PCN-700	$[Zr_6(\mu_3\text{-}O)_4(\mu_3\text{-}OH)_4(OH)_4(H_2O)_4(COO)_8]$	Me_2BPDC	1807	[89]
PCN-777	$[Zr_6(\mu_3\text{-}O)_4(\mu_3\text{-}OH)_4(OH)_6(H_2O)_6(COO)_6]$	TATB	2008	[106]
PCN-133	$[Zr_6(\mu_3\text{-}O)_4(\mu_3\text{-}OH)_4(COO)_{12}]$	BTB, DCDPS	1462	[112]
PCN-134	$[Zr_6(\mu_3\text{-}O)_4(\mu_3\text{-}OH)_4(OH)_2(H_2O)_2(COO)_{10}]$	BTB, TCPP	1946	[112]
MOF-801	$[Zr_6(\mu_3\text{-}O)_4(\mu_3\text{-}OH)_4(COO)_{12}]$	FUM	990	[37]
MOF-802	$[Zr_6(\mu_3\text{-}O)_4(\mu_3\text{-}OH)_4(OH)_2(H_2O)_2(COO)_{10}]$	PZDC	NA	[37]
MOF-808	$[Zr_6(\mu_3\text{-}O)_4(\mu_3\text{-}OH)_4(OH)_6(H_2O)_6(COO)_6]$	BTC	2060	[37]
MOF-812	$[Zr_6(\mu_3\text{-}O)_4(\mu_3\text{-}OH)_4(COO)_{12}]$	MTB	2335	[37]
MOF-841	$[Zr_6(\mu_3\text{-}O)_4(\mu_3\text{-}OH)_4(OH)_4(H_2O)_4(COO)_8]$	MTB	1390	[37]
MOF-525	$[Zr_6(\mu_3\text{-}O)_4(\mu_3\text{-}OH)_4(COO)_{12}]$	TCPP	2620	[54]

Table 1. Continued.

MOFs[a]	Clusters/cores	Linkers[b]	BET surface area ($m^2\ g^{-1}$)	Ref.
MOF-535	$[Zr_6(\mu_3\text{-}O)_4(\mu_3\text{-}OH)_4(COO)_{12}]$	XF	1120	[54]
MOF-545	$[Zr_6(\mu_3\text{-}O)_4(\mu_3\text{-}OH)_4(OH)_4(H_2O)_4(COO)_8]$	TCPP	2260	[54]
DUT-51	$[Zr_6(\mu_3\text{-}O)_4(\mu_3\text{-}OH)_4(OH)_4(H_2O)_4(COO)_8]$	DTTDC	2335	[195]
DUT-52	$[Zr_6(\mu_3\text{-}O)_4(\mu_3\text{-}OH)_4(COO)_{12}]$	2,6-NDC	1399	[107]
DUT-84	$[Zr_6(\mu_3\text{-}O)_4(\mu_3\text{-}OH)_4(OH)_6(H_2O)_6(COO)_6]$	2,6-NDC	637	[107]
DUT-67	$[Zr_6(\mu_3\text{-}O)_4(\mu_3\text{-}OH)_4(OH)_4(H_2O)_4(COO)_8]$	TDC	1064	[196]
DUT-68	$[Zr_6(\mu_3\text{-}O)_4(\mu_3\text{-}OH)_4(OH)_4(H_2O)_4(COO)_8]$	TDC	891	[196]
DUT-69	$[Zr_6(\mu_3\text{-}O)_4(\mu_3\text{-}OH)_4(OH)_2(H_2O)_2(COO)_{10}]$	TDC	560	[196]
NU-1000	$[Zr_6(\mu_3\text{-}O)_4(\mu_3\text{-}OH)_4(OH)_4(H_2O)_4(COO)_8]$	TBAPy	2320	[86]
NU-1100	$[Zr_6(\mu_3\text{-}O)_4(\mu_3\text{-}OH)_4(COO)_{12}]$	PTBA	4020	[197]
NU-1101	$[Zr_6(\mu_3\text{-}O)_4(\mu_3\text{-}OH)_4(COO)_{12}]$	Py-XP	4422	[198]
NU-1102	$[Zr_6(\mu_3\text{-}O)_4(\mu_3\text{-}OH)_4(COO)_{12}]$	Por-PP	4712	[198]
NU-1103	$[Zr_6(\mu_3\text{-}O)_4(\mu_3\text{-}OH)_4(COO)_{12}]$	Py-PTP	5646	[198]
NU-1104	$[Zr_6(\mu_3\text{-}O)_4(\mu_3\text{-}OH)_4(COO)_{12}]$	Por-PTP	5290	[198]
MIL-140A	$[ZrO(COO)_2]_n$	BDC	415	[108]
MIL-140B	$[ZrO(COO)_2]_n$	2,6-NDC	460	[108]
MIL-140C	$[ZrO(COO)_2]_n$	BPDC	670	[108]
MIL-140D	$[ZrO(COO)_2]_n$	Cl_2ABDC	701	[108]
BUT-12	$[Zr_6(\mu_3\text{-}O)_4(\mu_3\text{-}OH)_4(OH)_4(H_2O)_4(COO)_8]$	CTTA	3387	[63]
BUT-13	$[Zr_6(\mu_3\text{-}O)_4(\mu_3\text{-}OH)_4(OH)_4(H_2O)_4(COO)_8]$	TTNA	3948	[63]
Zr-ABDC	$[Zr_6(\mu_3\text{-}O)_4(\mu_3\text{-}OH)_4(COO)_{12}]$	ABDC	3000	[199]
BUT-30	$[Zr_6(\mu_3\text{-}O)_4(\mu_3\text{-}OH)_4(COO)_{12}]$	EDDB	3940	[200]
PIZOF	$[Zr_6(\mu_3\text{-}O)_4(\mu_3\text{-}OH)_4(COO)_{12}]$	PEDC	2080	[201]
Zr-BTDC	$[Zr_6(\mu_3\text{-}O)_4(\mu_3\text{-}OH)_4(COO)_{12}]$	BTDC	2207	[202]
Zr-BTBA	$[Zr_6(\mu_3\text{-}O)_4(\mu_3\text{-}OH)_4(COO)_{12}]$	BTBA	4342	[203]
Zr-PTBA	$[Zr_6(\mu_3\text{-}O)_4(\mu_3\text{-}OH)_4(COO)_{12}]$	PTBA	4116	[203]
Zr-BTB	$[Zr_6(\mu_3\text{-}O)_4(\mu_3\text{-}OH)_4(OH)_6(H_2O)_6(COO)_6]$	BTB	613	[105]
hcp UiO-67	$[Hf_{12}(\mu_3\text{-}O)_8(\mu_3\text{-}OH)_8(\mu_2\text{-}OH)_6(COO)_{18}]$	BPDC	1424	[109]
Zr_{12}-TPDC	$[Zr_{12}(\mu_3\text{-}O)_8(\mu_3\text{-}OH)_8(\mu_2\text{-}OH)_6(COO)_{18}]$	TPDC	1967	[110]
Hf_{12}-BTE	$[Hf_{12}(\mu_3\text{-}O)_8(\mu_3\text{-}OH)_8(\mu_2\text{-}OH)_6(COO)_{18}]$	BTE	NA	[111]
Cu-BTPP	$[Cu_3(\mu_3\text{-}OH)(PZ)_3]$	BTPP	660	[204]
$Ni_3(BTP)_2$	$[Ni_4(PZ)_8]$	BTP	1650	[52]
Zn(1,4-BDP)	$[Zn(PZ)_2]_n$	1,4-BDP	1710	[205]
Zn(1,3-BDP)	$[Zn(PZ)_2]_n$	1,3-BDP	820	[205]
PCN-601	$[Ni_8(OH)_4(H_2O)_2(PZ)_{12}]$	TPP	1309	[44]
ZIF-8	$[ZnN_4]$	mIM	1947	[24]
ZIF-11	$[ZnN_4]$	bIM	1676	[24]
ZIF-67	$[CoN_4]$	mIM	1587	[156]
ZIF-90	$[ZnN_4]$	ICA	1270	[206]
ZIF-68	$[ZnN_4]$	nIM, bIM	1220	[5]
ZIF-69	$[ZnN_4]$	nIM, 5cbIM	1070	[5]
ZIF-70	$[ZnN_4]$	IM, nIM	1970	[5]

[a]Note that a large number of MOFs can be obtained by functionalizing existing structures. For example, the functionalization of BDC with amino, nitro, methyl, halogen, or hydroxyl groups can lead to the formation of UiO-66 analogues. These MOFs are not included in this table; [b]Linkers are abbreviated as: BDC = terephthalate; FUM = fumarate; 2,6-NDC = naphthalene-2,6-dicarboxylate; BTC = benzene-1,3,5-tricarboxylate; BDC-NH_2 = 2-aminoterephthalate; BTEC = 1,2,4,5-benzenetetracarboxylate; NTC = 1,4,5,8-naphthalenetetracarboxylate; BPDC = biphenyl-4,4′-dicarboxylate; BPTA = biphenyl-3,3′,5,5′-tetracarboxylate; BTB = 1,3,5-benzenetrisbenzoate;

Table 1. Continued.

BeDC = 4,4′-benzophenonedicarboxylate; 1,3-BDC = isophthalate; BTTB = 4,4′,4″-[benzene-1,3,5-triyl-tris(oxy)]tribenzoate; TCPP = meso-tetrakis(4-carboxylatephenyl) porphyrin; TATB = 4,4′,4″-s-triazine-2,4,6-triyl-tribenzoate; TCPT = 3,3″,5,5″-tetrakis(4-carboxyphenyl)-*p*-terphenyl; TMQPTC = 2′,3″,5″,6′-tetramethyl-[1,1′:4′,1″:4″,1‴-quaterphenyl]-3,3‴,5,5‴-tetracarboxylate; ABDC = 4,4-azobenzenedicarboxylate; 1,3-ADC = 1,3-adamantanedicarboxylate; FTZB = 2-fluoro-4-(tetrazol-5-yl)benzoate; CDC = trans-1,4-cyclohexanedicarboxylate; AB = 4-aminobenzoate; BDA = benzene-1,4-dialdehyde; BPDA = 4,4′-biphenyldicarboxaldehyde; TPDC = [1,1′:4′,1″-terphenyl]-4,4″-dicarboxylate; ETTC = 4′,4″,4‴,4⁗-(ethene-1,1,2,2-tetrayl)tetrabiphenyl-4-carboxylate; MTBC = 4′,4″,4‴,4⁗-methanetetrayltetrabiphenyl-4-carboxylate; PZDC = 1*H*-pyrazole-3,5-dicarboxylate; MTB = 4,4′,4″,4‴-methanetetrayltetrabenzoate; XF = 4,4′-((1E,1′E)-(2,5-bis((4-carboxylatephenyl)ethynyl)-1,4-phenylene)bis(ethene-2,1- diyl))dibenzoate; DTTDC = dithieno[3,2-b;2′,3′-d]-thiophene-2,6- dicarboxylate; TDC = 2,5-thiophenedicarboxylate; TBAPy = 1,3,6,8-tetrakis(*p*-benzoate)pyrene; PTBA = 4-[2-[3,6,8-tris[2-(4-carboxylatephenyl)-ethynyl]-pyren-1-yl]ethynyl]-benzoate; Py-XP = 4′,4‴,4⁗,4⁗′-(pyrene-1,3,6,8-tetrayl) tetrakis(2′,5′-dimethyl-[1,1′-biphenyl]-4-carboxylate; Por-PP = meso-tetrakis-(4-carboxylatebiphenyl)- porphyrin; Py-PTP = 4,4′,4″,4‴-((pyrene-1,3,6,8-tetrayltetrakis(benzene-4,1-diyl))tetrakis(ethyne-2,1-diyl))tetrabenzoate; Por-PTP = meso-tetrakis-(4-((phenyl)ethynyl)benzoate)porphyrin; EDDB = 4,4′-(ethyne-1,2-diyl)dibenzoate; CTTA = 5′-(4-carboxyphenyl)-2′,4′,6′-trimethyl-[1,1′:3′,1″-terphenyl]-4,4″-dicarboxylate; TTNA = 6,6′,6″- (2,4,6-trimethylbenzene-1,3,5-triyl)tris(2-naphthoate)); PEDC = 4,4′-(1,4-phenylenebis- (ethyne-2,1-diyl))dibenzoate; BTDC = 2,2′-bithiophene-5,5′-dicarboxylate; BTBA = 4,4′,4″,4‴-(biphenyl-3,3′,5,5′-tetrayltetrakis(ethyne-2,1-diyl))tetrabenzoate; PTBA = 4-[2-[3,6,8-tris[2-(4-carboxylatephenyl)-ethynyl]-pyren-1-yl] ethynyl]-benzoate; BTE = 4,4′,4″-(benzene-1,3,5-triyl-tris(ethyne-2,1-diyl))tribenzoate; BTPP = 1,3,5-Tris((1*H*-pyrazol-4-yl)phenyl)benzene; BTP = 1,3,5-tris(1*H*-pyrazol-4-yl) benzene; 1,4-BDP = 1,4-benzenedi(4′-pyrazolyl); 1,3-BDP = 1,3-benzenedi(4′-pyrazolyl); TPP = 10,15,20-tetra(1*H*-pyrazol-4-yl)-porphyrin; mIM = 2-methylimidazolate; bIM = benzimidazolate; nIM = 2-nitroimidazolate; 5cbIM = 5-chlorobenzimidazolate; ICA = imidazolate-2-carboxyaldehyde; 5-mTz = 5-methyltetrazolate; 2-mbIM = 2-methylbenzimidazolate; [c]Langmuir surface area.

Topologically, each cluster can be simplified into a 12-connected cuboctahedral node, which is extended into an **fcu** network by linear linkers. Two types of micropores, tetrahedral and octahedral, are observed in the structure, leading to a BET surface area close to 1200 $m^2\ g^{-1}$. At the same time, two isoreticular structures, UiO-67 and UiO-68, were also synthesized by the elongation of linkers (**Figure 7**). After the discovery of UiO-66, the field of Zr-MOFs stayed silent for three years, with only a few new structures reported. This is due to the difficulties in the synthesis and structural characterization of Zr-MOFs. Indeed, most Zr-MOFs including UiO-66 are obtained as polycrystalline powders, which requires complicated Rietveld refinement of synchrotron PXRD data to characterize the structure.

These problems were solved by Schaate et al. in 2011 who introduced the modulated synthetic strategy to prepare Zr-MOFs with controllable particle sizes.[65] With modulated synthesis, single crystals of UiO-68-NH_2 were obtained and examined by single-crystal X-ray diffraction, providing the first single-crystal structure of a Zr-MOF. This study dramatically accelerates the development of Zr-MOFs because single crystalline samples allow facile and precise structural determination by single-crystal X-ray diffraction. Following this study, many Zr-MOFs were synthesized and their applications were extensively explored. Over the last few years, UiO-66 as a representative example of Zr-MOFs, has almost dethroned MOF-5 and HKUST-1 (HKUST stands for Hong Kong University of Science and Technology) as a benchmark MOF material.

Although numerous isostructural analogues of UiO-66 based on elongated or functionalized linkers have been reported, they are mostly based on the same $[Zr_6(\mu_3\text{-}O)_4(\mu_3\text{-}OH)_4(COO)_{12}]$ inorganic building unit. Zr-MOFs based on tetratopic linkers, TCPP, were systematically studied by our group.[40–42,60,103] Interestingly, different phases were obtained which contain clusters with similar $[Zr_6(\mu_3\text{-}O)_4(\mu_3\text{-}OH)_4]$ core but different connection numbers. For example, an 8-connected $[Zr_6(\mu_3\text{-}O)_4(\mu_3\text{-}OH)_4(OH)_4(H_2O)_4(COO)_8]$ cluster was observed in PCN-222, in which four equatorial carboxylates were replaced by four pairs of terminal $-OH^-/H_2O$ ligands.[40] Following this work, some structures based on similar 8-connected Zr-clusters and square planar, tetrahedral, or linear carboxylate linkers were discovered.[86,89,104] Although the connection number is reduced, the stability of Zr-MOFs with 8-connected Zr-clusters is not compromised. For example, PCN-222 and its isostructural analogue, NU-1000, can survive

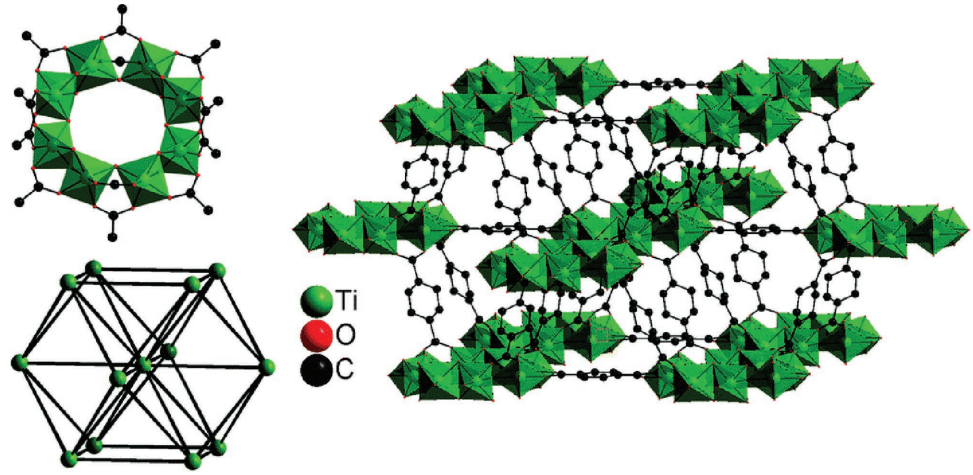

Figure 5. Structure of MIL-125. Top left: $Ti_8O_8(OH)_4(CO_2)_{12}$ unit; right: crystal structure; bottom left: **fcu** topology. Reproduced with permission.[16] Copyright 2014, Royal Society of Chemistry.

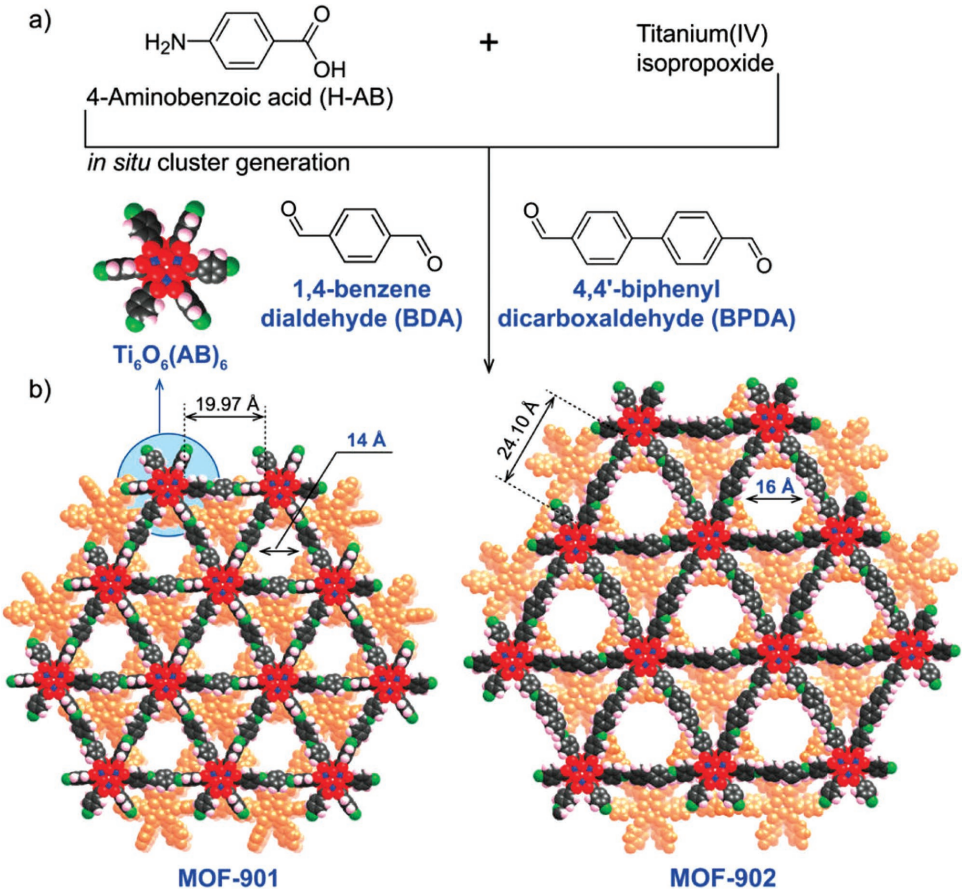

Figure 6. Synthesis of MOF- 901 and MOF-902. a) The in situ generation of Ti–oxo clusters and formation of imine bonds. b) The space filling model of crystal structures of MOF-901 and MOF-902. Atom colors: Ti, blue; C, black; O, red; N, green; H, pink; and second layer, orange. Reproduced with permission.[97] Copyright 2016, American Chemical Society.

in concentrated HCl solutions. The coordinatively unsaturated Zr-clusters also allow the tethering of external ligands or metals, acting as a versatile platform for a variety of applications.[81,87]

Later on, 6-connected $[Zr_6(\mu_3\text{-}O)_4(\mu_3\text{-}OH)_4(OH)_6(H_2O)_6(COO)_6]$ clusters were also observed, demonstrating the strong tolerance of Zr-clusters toward the elimination of linkers.[37,41] Two types of 6-connected Zr-clusters were documented, which have a hexagonal and an octahedral geometry. A few Zr-MOFs based on the hexagonal Zr-clusters were reported, including a rare 2D Zr-MOF with a triangular linker and a **kgd** topology.[105] The octahedral Zr-clusters, on the other hand, can be extended to a zeotype **mtn** topology by triangular linkers.[37,106] More recently, MOFs based on 10-connected Zr-clusters were also found.[107] In these studies, analogues based on Hf were often isolated and usually showed similar structure and properties as

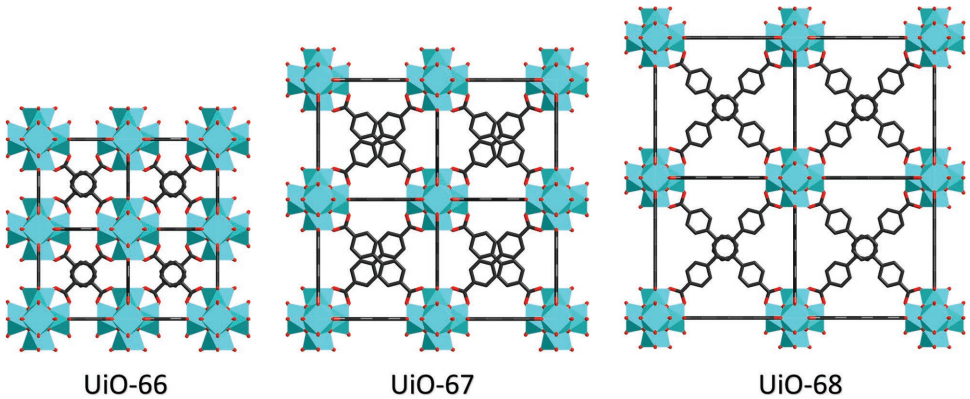

Figure 7. Structures of UiO-66, 67, and 68.

their Zr-based counterparts except for the increase in formula weight. Therefore, the structures and properties of the Hf-based MOFs will not be discussed in detail.

Although most Zr-MOFs are based on the robust $[Zr_6(\mu_3\text{-}O)_4(\mu_3\text{-}OH)_4]$ core, other Zr-clusters were also observed in Zr-MOFs. For example, MIL-140 series are composed of polymeric double chains of edge sharing ZrO_7 polyhedra connected through linear ligands.[108] Very recently, a few MOFs were discovered with $[Zr_{12}(\mu_3\text{-}O)_8(\mu_3\text{-}OH)_8(\mu_2\text{-}OH)_6(COO)_{18}]$ or $[Hf_{12}(\mu_3\text{-}O)_8(\mu_3\text{-}OH)_8(\mu_2\text{-}OH)_6(COO)_{18}]$ clusters, which could be regarded as a face-to-face linking of two Zr_6/Hf_6 clusters by six μ_2-OH groups.[109–111] Finally, constructing Zr-MOFs with multiple linkers (different lengths or symmetries) brings new opportunity to enrich the structures and their ensuing properties.[112] Considering the variable connection number and the abundant molecular Zr-clusters in the literature, numerous new members of the Zr-MOF family are envisioned in the near future.

4.1.3. Ce^{4+}–Carboxylate Based MOFs

Ce-MOFs are very attractive because of their redox properties and potential catalytic applications. For instance, a mixed-valency Ce-MOF containing Ce^{3+} and Ce^{4+} has shown intrinsic oxidase-like catalytic properties.[113] Furthermore, pure Ce^{4+}-based MOFs with hexanuclear $[Ce_6(\mu_3\text{-}O)_4(\mu_3\text{-}OH)_4(COO)_{12}]$ clusters have recently been synthesized. These Ce^{4+}-based frameworks are isoreticular to their Zr^{4+} based analogues with 6-connected, 8-connected, or 12-connected Ce_6-clusters.[114] The connectivity and symmetry of Ce_6-clusters enable the formation of networks with **fcu**, **reo**, **spn**, and **scu** topologies. Most of the Ce-MOFs are stable in polar, aprotic solvents, but they begin to degrade slowly in water. One of the representative Ce-MOFs, Ce-UiO-66, is reported to be stable in aqueous solution with pH range of 1 to 11.[115] Additionally, by introducing hydrophobic groups into the framework, the stability of Ce^{4+}-MOFs toward water and acid can be enhanced. Indeed, the resulting MOF, Ce-UiO-66-$(CH_3)_2$, is reported to be stable in 1 M HCl aqueous solution.[116]

4.2. M^{3+}–Carboxylate Based MOFs

Two main SBUs can be found in MOFs built from M^{3+} cations (Al^{3+}, Cr^{3+}, Fe^{3+}, Sc^{3+}, V^{3+}, Ga^{3+}, and In^{3+}) and carboxylates: (a) the $[M_3(\mu_3\text{-}O)(COO)_6]$ cluster, which contains a μ_3-oxo-centered trimer of MO_6 octahedra; (b) the $[M(OH)(COO)_2]_n$ chain, which has a μ_2-hydroxo corner sharing MO_6 octahedral unit (Figure 6a). Note that the trinuclear $[M_3(\mu_3\text{-}O)(COO)_6]$ cluster is usually terminated by two H_2O and one OH^- to balance the charge, giving rise to a theoretical formula of $[M_3(\mu_3\text{-}O)(OH)(H_2O)_2(COO)_6]$. The terminal H_2O can be replaced by neutral ligands such as pyridine and DMF, while the OH^- can be replaced by F^-, NO_3^-, or other counterions. In this review, they are all named as $[M_3(\mu_3\text{-}O)(COO)_6]$ for simplicity.

4.2.1. Al^{3+}–Carboxylate Based MOFs

One of the most well-known Al-MOFs is MIL-53(Al) with the formula Al(OH)(BDC).[117] MIL-53(Al) contains infinite linear zigzag chains of $AlO_4(OH)_2$ octahedra. The 1D lozenge-shaped channels are obtained by linking the parallel chains and BDC linkers (**Figure 8**b). A breathing phenomenon in MIL-53(Al) was observed in which the framework adapted its structure in response to the adsorption of guest molecules. The "np" (narrow pore) and "lp" (large pore) forms could be obtained by reversible removal and incorporation of guest molecules. Additionally, several MOFs based on the MIL-53(Al)-type structure were developed by using functionalized or extended linkers, including DUT-4[118] (DUT stands for Dresden University of Technology) and DUT-5.[118] MIL-68(Al),[119] another MIL-53(Al) isomer, has a more rigid **kgm** net. Further elongation of linker in MIL-68(Al) leads to a mesoporous Al-MOF, CYCU-3[120] (CYCU stands for Chung-Yuan Christian University). Linking the $[Al(OH)(COO)_2]_n$ chains and tritopic carboxylate ligands, BTTB, leads to the formation of 467-MOF,[121] which shows good stability in aqueous solutions with pH values ranging from 1 to 11 for 36 h, and in boiling water for 9 d (BTTB = 4,4′,4″-[benzene-1,3,5-triyl-tris(oxy)]tribenzoate).

Al-MOFs based on $[Al(OH)(COO)_2]_n$ chains and tetratopic carboxylic ligands are also explored. For example, linking $[Al(OH)(COO)_2]_n$ chains and BTEC results in three different phases of Al-MOFs with different connectivities of Al^{3+}. The three phases are named as MIL-121,[122] MIL-118,[123] and MIL-120[124] with 4, 6, and 8 oxygen atoms from carboxyl group coordinated to Al^{3+}, respectively. NOTT-300[125] (NOTT stands for University of Nottingham) is comprised of $[Al(OH)(COO)_2]_n$ chains bridged by four-connected BPTA linker. The structure remains stable when exposed to air, moisture, and common solvents. Moreover, the combination of $[Al(OH)(COO)_2]_n$ chains and porphyrin linker, TCPP, leads to the formation of Al-PMOF.[126] In the structure, the $[Al(OH)(COO)_2]_n$ chains are arranged into a nearly perfect square array due to the square porphyrin unit, which forms an interlaced pore structure. Al-PMOF remains stable in water and aqueous solutions with pH values from 5 to 8.

It is necessary to realize that Al-MOFs based on the $[Al_3(\mu_3\text{-}O)(COO)_6]$ cluster are scarce when compared to their Fe(III) or Cr(III) based analogues. A possible explanation is that the $[Al_3(\mu_3\text{-}O)(COO)_6]$ cluster-based structure is usually a kinetic product, which is not thermodynamically favored under most synthetic conditions. The first example of an Al-MOF containing the $[Al_3(\mu_3\text{-}O)(COO)_6]$ cluster is MIL-96.[127] MIL-96 contains two types of isolated clusters, the $[Al_3(\mu_3\text{-}O)(COO)_6]$ cluster and infinite chains with $AlO_4(OH)_2$ units. The two building blocks are connected to BTC, which induces corrugated chains of $AlO_4(OH)_2$ octahedra and forms three types of cages.

The combination of the $[Al_3(\mu_3\text{-}O)(COO)_6]$ clusters and tricarboxylate linkers leads to a series of structures with **mtn** topology. MIL-100(Al),[128] isostructural to reported MIL-100(Cr, Fe),[22,46] was synthesized within a very narrow pH range (0.5–0.7) through the hydrothermal reactions (Figure 8d). This structure is built up from supertetrahedral blocks based on $[Al_3(\mu_3\text{-}O)(COO)_6]$ SBUs and BTC linkers. The framework exhibits two types of cavities with pore sizes of 25 and 29 Å. Furthermore, an extended form of MIL-100, PCN-333(Al),[129] is built from $[Al_3(\mu_3\text{-}O)(COO)_6]$ SBUs and TATB linkers with D_{3h} symmetry. Two types of mesoporous cages are generated with pore sizes of 42 and 55 Å. The larger hexacaidecahedral pore is built of 24 supertetrahedra with both pentagonal windows and

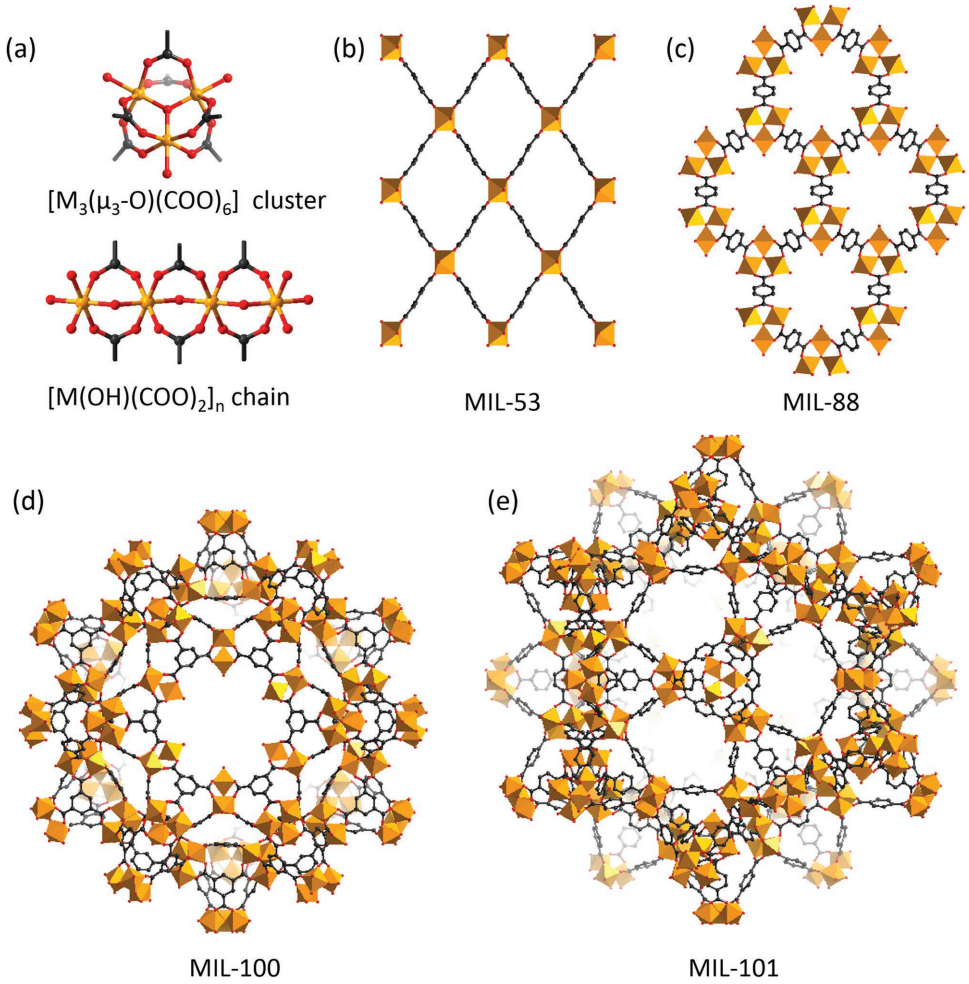

Figure 8. Structures of a) $[M_3(\mu_3\text{-}O)(COO)_6]$ cluster and $[M(OH)(COO)_2]_n$ chain, b) MIL-53, c) MIL-88, d) MIL-100, and e) MIL-101.

hexagonal windows, while the smaller one is surrounded by 20 supertetrahedra with pentagonal windows only. PCN-333(Al) shows high stability in aqueous solutions with pH range from 3 to 9. Further extension of the tricarboxylate linker leads to the formation of PCN-888 with two hierarchal mesoporous cages of 50 and 62 Å.[130]

The combination of the $[Al_3(\mu_3\text{-}O)(COO)_6]$ clusters and linear linkers can also give rise to **mtn** type of network. For example, MIL-101-NH_2(Al)[73] is composed of $[Al_3(\mu_3\text{-}O)(COO)_6]$ clusters and BDC-NH_2 linkers, which is isostrucural to MIL-101(Cr, Fe) (Figure 8e).[4,131] This structure shows a high thermal and chemical stability. One should notice that unfunctionalized MIL-101(Al) has not been successfully synthesized. This is tentatively attributed to the effect of amino groups that prevent hydrolysis of Al^{3+} and help to stabilize the framework. The $[Al_3(\mu_3\text{-}O)(COO)_6]$ clusters and tetratopic TCPT ligands form a framework with **soc** topology, namely Al-soc-MOF.[132] This MOF is well-known for its extremely high total uptake for carbon dioxide and deliverable uptake for oxygen.

In addition to $[Al_3(\mu_3\text{-}O)(COO)_6]$ clusters and $[Al(OH)(COO)_2]_n$ chains, the intrinsic characteristics of the Al^{3+} cation lead to another two Al-cluster types: an octanuclear wheel $[Al_8(OH)_4(OCH_3)_8(COO)_{12}]$ and a dodecanuclear wheel $[Al_{12}(OCH_3)_{24}(COO)_{12}]$. In CAU-1, the 12-connected octanuclear wheels are linked by BDC linkers with four linkers in the plane of the wheel, four above the wheel, and four below the wheel.[133] The resulting structure contains a distorted octahedral cage with diameter of approximately 1 nm and a distorted tetrahedral cage with diameter of approximately 0.45 nm. In CAU-3, the distorted **fcu** net is built from 12-connected $Al_{12}(OCH_3)_{24}$ dodecanuclear wheels and BDC linkers, and contains strongly distorted tetrahedral and octahedral cavities.[134]

4.2.2. Fe^{3+}–Carboxylate Based MOFs

The combination of BDC and chains of $FeO_4(OH)_2$ octahedra leads to the flexible structure, MIL-53(Fe),[135] or the rigid triangular and hexagonal shaped MIL-68(Fe).[136] Compared with MIL-68(Fe), MIL-53(Fe) is more easily synthesized and functionalized. Further, two water-stable MOFs with TCPP linkers, MIL-141(Fe) and FepzTCPP$(FeOH)_2$, are obtained based on the same $[Fe(OH)(COO)_2]_n$ chain as SBU.[137] Both materials are stable in water which can contribute to the resistance to hydrolysis of an extended SBU.

When dealing with $[Fe_3(\mu_3\text{-}O)(COO)_6]$ SBUs, topologies of Fe-MOFs exhibit high diversity because of various symmetries of the ligands. The MIL-88 series (Figure 8c) are built from $[Fe_3(\mu_3\text{-}O)(COO)_6]$ clusters and linear dicarboxylate ligands of different lengths.[138] The bipyramidal cages of the MIL-88 series exhibit reversible "breathing" motion during physical, chemical or thermal treatments. One should note that the MIL-88 series have nearly no porosity when tested for N_2 adsorption at 77 K because of the stacking of linkers in the narrow pore conformation. Interestingly, combining $[Fe_3(\mu_3\text{-}O)(COO)_6]$ SBUs and BDC linkers results in another **mtn**-type structure, MIL-101(Fe), which is isostructural to MIL-101(Al, Cr).[131] Nevertheless, MIL-101(Fe) shows relatively low thermodynamic stability and will gradually transform into denser forms, such as MIL-53(Fe) or MIL-88(Fe), when exposed to strongly polar solvents.[139]

Although MIL-101(Fe) and other dicarboxylate Fe-MOFs remain stable under exposure to air or moisture, they might become unstable under hydrothermal conditions. One alternative to rectify this is to utilize the tri- or tetracarboxylate linkers to build frameworks with high connectivity, which can improve hydrothermal stability. For example, MIL-100(Fe), a zeolite **mtn**-type structure, is constructed from $[Fe_3(\mu_3\text{-}O)(COO)_6]$ clusters and BTC linkers, leading to the formation of hybrid supertetrahedra with two types of mesoporous cages of free apertures of 25 and 29 Å.[46] PCN-333(Fe) is an extended version of MIL-100(Fe). It is stable in aqueous solutions with a pH range from 3 to 9 as confirmed by PXRD and N_2 sorption isotherms.[129]

PCN-250(Fe), built from 6-connected $[Fe_3(\mu_3\text{-}O)(COO)_6]$ clusters and rectangular tetracarboxylate linkers, is isostructural to a reported In-MOF with the **soc** topology.[140] MIL-100(Fe) and PCN-250(Fe) are both hydrothermally resistant due to the increasing connectivity of linkers. The replacement of one Fe^{3+} in the $[Fe_3(\mu_3\text{-}O)(COO)_6]$ cluster with a softer Lewis acid M^{2+} (M^{2+} = Fe^{2+}, Co^{2+}, Ni^{2+}, Mn^{2+}, and Zn^{2+}) does not significantly reduce the chemical stability of the PCN-250 series. For instance, PCN-250(Fe_2Co) remains stable upon immersion in glacial acetic acid, aqueous solutions with pH values ranging from 1 to 11 for 24 h, and in H_2O for six months. Another example of a tetracarboxylate linker-based Fe-MOF is PCN-600(M) (M = Mn, Fe, Co, Ni, Cu) with a **stp-a** network.[43] In PCN-600, channels as large as 3.1 nm are created by linking six-connected $[Fe_3(\mu_3\text{-}O)(COO)_6]$ clusters and four-connected porphyrinic linkers (TCPP). This structure shows high stability in aqueous solutions with pH from 2 to 11, representing a rare example of Fe-based mesoporous MOFs that are stable under basic aqueous conditions.

4.2.3. Cr^{3+}–Carboxylate Based MOFs

The structures of Cr-MOFs bear a close resemblance to Fe-MOFs. Most Cr-MOFs including MIL-53(Cr),[21] the MIL-88(Cr) series,[138] MIL-100(Cr),[22] MIL-101(Cr),[4] and PCN-333(Cr),[141] have isostructural Fe(III)-based counterparts. For instance, MIL-101(Cr), a highly stable MOF with very large pore sizes and surface areas, is made from the linkage of BDC linkers and $[Cr_3(\mu_3\text{-}O)(COO)_6]$ clusters. One should also notice that the synthetic conditions and stabilities vary significantly when comparing Cr^{3+} and Fe^{3+} based MOFs, which may be attributed to the kinetic inertness of Cr—carboxylate bonds. For example, PCN-333(Cr) exhibits more remarkable stability than the isostructural PCN-333(Fe) and remains intact in aqueous solutions with a wide pH range from 0 to 12.

Other M^{3+} ions including V^{3+}, In^{3+}, Sc^{3+}, and Ga^{3+}, can also form similar structures based on $[M(OH)(COO)_2]_n$ chains or $[M_3(\mu_3\text{-}O)(CO_2)_6]$ clusters, however, these frameworks are usually less stable than their Al^{3+}, Fe^{3+}, or Cr^{3+} based analogues. Therefore, these structures will not be discussed here.

4.2.4. RE^{3+}-Carboxylate Based MOFs

In the form of coordination complexes, a majority of rare earth (RE) elements are known to exist in the +3 oxidation state, although particularly stable 4f configurations can also give +4 (Ce, Tb) or +2 (Eu, Yb) ions. The structures of RE clusters are abundant, with mononuclear clusters, binuclear clusters, tetranuclear clusters, hexanuclear clusters, nonanuclear clusters, and chains. An early example of RE-MOFs, $[Tb_2(BDC)_3(H_2O)_4]_n$, shows permanent microporosity and good thermal stability up to 450 °C, although the chemical stability was not assessed.[142] Later on, many RE-MOFs were synthesized with permanent porosity, good thermal stability, and modest water resistance.[143–146] Note that RE-based MOFs are usually less stable than other M^{3+} (Al^{3+}, Fe^{3+}, or Cr^{3+}) based MOFs. This is attributed to the large radius of RE^{3+} which results in lower charge to radius ratios (Z/R) and weaker RE–carboxylate interactions. Recently, RE-MOFs based on hexanuclear clusters[147–149] and nonanuclear clusters[150] are developed which show better stability as a result of high connection numbers of the clusters. For example, RE-FTZB based on $[RE_6(\mu_3\text{-}OH)_8(COO)_6(\text{tetrazolate})_6]$ clusters and RE-FUM based on $[RE_6(\mu_3\text{-}OH)_8(COO)_{12}]$ clusters both exhibit a **fcu** topology; these building blocks are similar to $[Zr_6(\mu_3\text{-}O)_4(\mu_3\text{-}OH)_4(COO)_{12}]$ in UiO-66 and other Zr-MOFs. The chemical stability of these two MOFs was improved compared to other RE-based MOFs possibly due to hydrophobic F-functionalized linker, the rigidity of short linkers and dense structures.[151]

4.2.5. Stability of M^{3+}–Carboxylate Based MOFs

The stability of M^{3+} cation-based MOFs is highly related to the nature of the SBUs and linkers. In general, thermal stability decreases in the order of Al-MOF>Cr-MOF>Fe-MOF>V-MOF. This trend may be explained by the strengths of the metal–oxygen bond in corresponding the metal oxides (Al_2O_3, Cr_2O_3, Fe_2O_3, and V_2O_5). Some redox active metals may induce the decomposition of organic linkers and therefore reduce the stability. In addition, if we compare the thermal stability of M^{3+}-based MOFs with different SBUs, it appears that $[M(OH)(COO)_2]_n$ chains will leads to higher thermal stabilities.

Chemical stability to water, acids, and bases usually decreases in the order of Cr-MOF>Al-MOF>Fe-MOF, with decreasing inertness of the metal–oxygen bonds. Compared to

Al/Cr/Fe-MOFs, other M(III)-MOFs such as V-MOFs readily degrade in water.[152] When exposed to alkaline environments, MIL-53(Al) starts to decompose slowly, however, MIL-53(Cr) shows high stability and no change is observed in surface area and PXRD intensity. Similar phenomena were also reported in aqueous acidic solution.[153] In regard to the hydrothermal stability of MOFs, the ligand exchange constant is a critical factor. If the SBUs have smaller ligand exchange constants, the resulting MOFs are usually more stable. For instance, Cr^{3+} has a much lower ligand exchange constant than Fe^{3+} [2.4×10^{-6} s^{-1} for $Cr(H_2O)_6^{3+}$ versus 1.6×10^{2} s^{-1} for $Fe(H_2O)_6^{3+}$], so Cr^{3+}-based MOFs tend to have higher stabilities than Fe^{3+}-based MOFs. The type of SBU in MOFs also plays an important role in MOFs' chemical stabilities. M^{3+}-MOFs with $[M(OH)(COO)_2]_n$ chains tend to be more stable than MOFs constructed from $[M_3(\mu_3\text{-}O)(COO)_6]$ clusters. For example, MIL-101(Fe)[131] is unstable in aqueous solution and can be transformed into MIL-53 or MIL-88 when exposed to strongly polar solvents. This might be explained by the fact that M^{3+}-based MOFs with $[M_3(\mu_3\text{-}O)(COO)_6]$ clusters sometimes have giant voids in the framework, which may lead to the collapse of the framework, while M^{3+}-based MOFs with $[M(OH)(COO)_2]_n$ chains usually have dense structures, which tend to be more stable. Another example concerning the transformation from MIL-101-NH_2(Al) to MIL-53-NH_2(Al) also shows that the M^{3+}-based MOFs with $[M(OH)(COO)_2]_n$ chains could be a stable state during the synthesis.[73]

4.3. M^{2+}-Azolate Based MOFs

According to the HSAB principle, another class of stable MOFs can be formed by soft divalent metal ions and soft azolate-based ligands. Imidazole (HIM), pyrazole (HPZ), triazole (HTZ and HVTZ), and tetrazole (HTTZ) are coordinating moieties for azolate-based linkers.[154] Similar to carboxylic acids, the azoles are usually deprotonated in order to coordinate with the metal cations. In contrast to carboxylic acids, the azoles are mostly known as bases and the coordination behaviors of the sp^2 N-donors in azoles and pyridines are basically identical (**Scheme 4**).

4.3.1. M^{2+}-Imidazolate Based MOFs

Yaghi and co-workers introduced imidazole to coordination polymer chemistry of divalent first-row transition-metal ions and developed a new type of porous materials, namely zeolitic imidazolate frameworks (ZIFs).[24] The two N-donors in imidazolate point outward from the five-membered ring with an angle of ≈145°, which makes the M–IM–M angle coincident with the Si–O–Si angle in zeolites. This angle is essential for the generation of open-framework zeolite-like structures. The divalent transition-metal ions in ZIFs adopt square-planar or tetrahedral coordination geometries instead of the common octahedral coordination geometries. If the tetrahedral metal centers are bridged by linear bidentate ligands, the **dia** topology is expected in most cases. However, diverse structures based on 4-conected topologies can be obtained using bent

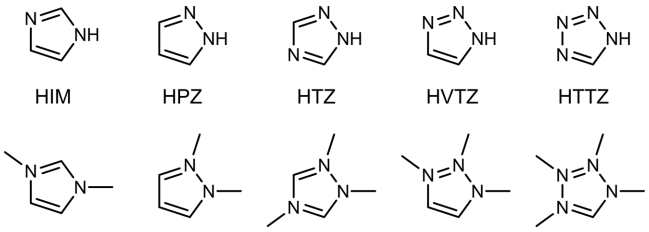

Scheme 4. Structures and typical coordination modes of azolates.

linkers, which break the perfect tetrahedral T_d symmetry of **dia** topology.

In the first paper on ZIFs published by the Yaghi group in 2006, eight topologies of the ZIF structures were reported which were all synthesized as crystals by copolymerization of either Zn(II) or Co(II) with imidazolate-type linkers.[24] Among the first 12 ZIFs, the **sod** topology ZIF-8 ($Zn(mIM)_2$) and the **rho** topology ZIF-11 ($Zn(bIM)_2$) were shown to be thermally and chemically stable (**Figure 9**). Although these ZIFs adopt the same topology with the corresponding zeolites, they possess large pores (11.6 and 14.6 Å in diameter for ZIF-8 and -11, respectively) connected through small apertures (3.4 and 3.0 Å across for ZIF-8 and -11, respectively). Due to the longer IM linking units, the pore sizes of ZIF-8 and -11 are approximately twice as large as those of their zeolite counterparts. The remarkable thermal stability of ZIF-8 and ZIF-11 were confirmed by thermal gravimetric analysis (TGA) which shows no weight loss before 550 °C in N_2.[155] ZIF-8 and ZIF-11 both stay intact in water at 50 °C for 7 d. ZIF-8 can even maintain its structure in boiling water for 7 d, whereas ZIF-11 transforms into another phase after 3 d in boiling water. ZIF-8 is also stable in 8 M aqueous NaOH solution at 100 °C, even superior to MCM (MCM stands for Mobil composition of matter) and SBA-types (SBA stands for Santa Barbara) ordered mesoporous silica. Willis et al. showed that the hydrothermal stability (50% steam at 350 °C) and activation energy (58.5 KJ mol^{-1}) of ligand displacement in ZIF-8 are higher than other typical MOFs.[39] This is attributed to the bond between the soft acid Zn^{2+} and the soft base IM. In addition, the hydrophobic pore and surface of ZIFs prevent

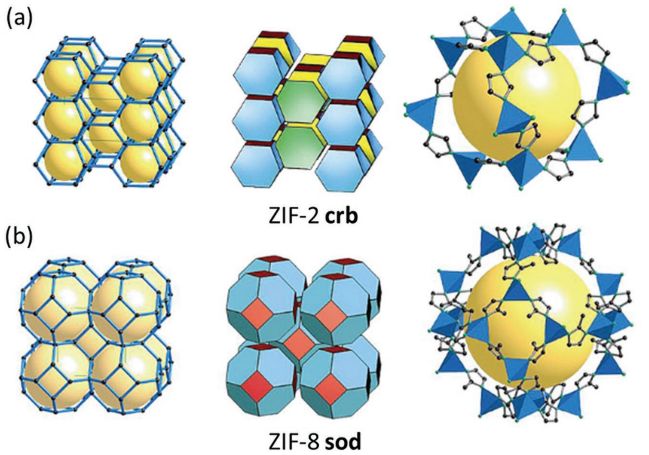

Figure 9. Structures and topologies of ZIF-2 and ZIF-8. Reproduced with permission.[24] Copyright 2006, National Academy of Sciences.

water molecules from attacking the [ZnN_4] units, which further enhances the overall stability.

ZIF-67, Co(bIM)$_2$, has a crystal structure similar to ZIF-8 with a zeolite sodalite topology.[156] Long and co-workers reported the synthesis of uniform and nonaggregated ZIF-67 dodecahedra. ZIF-67 is stable in room temperature water, boiling ethanol, and boiling toluene for 7 d. However, ZIF-67 undergoes a gradual structural transformation to Co_3O_4 and $Co(OH)_2$ in boiling water, confirmed by PXRD patterns, indicating a lower stability in boiling water compared to ZIF-8. ZIF-90 is another analogue of ZIF-8 with aldehyde groups on the imidazole ligands (imidazolate-2-carboxyaldehyde, ICA) which allows for further covalent modification. ZIF-90 shows excellent chemical stability in boiling water, toluene, and methanol for 24 h. A superhydrophobic ZIF-90 analogue is prepared through postsynthetic functionalization by pentafluorobenzylamine via an amine condensation reaction. Importantly, the modified ZIF-90 keeps high crystallinity unaltered in boiling water and steam for 24 h.

Using high-throughput methods, three mixed-linker ZIFs (ZIF-68, ZIF-69, and ZIF-70) with **gme** topology and large pores were obtained (7.2, 10.2, and 15.9 Å in diameter for ZIF-69, ZIF-68, and ZIF-70, respectively).[5] ZIF-68, ZIF-69, and ZIF-70 retained their structures in boiling benzene, methanol, and water for 7 d which was evidenced by well-maintained PXRD patterns. When the methyl group of the HmIM ligand in ZIF-8 was replaced by an ethyl group, MAF-5 and MAF-6 (MAF stands for metal azolate framework) were obtained.[157] Variable temperature PXRD analysis of MAF-5 showed that the framework was stable up to 400 °C.

4.3.2. M^{2+}-Tetrazolate/Triazolate/Pyrazolate Based MOFs

Pyrazolate possesses a rather small bridging angle (≈70°) compared with the isomer imidazolate, which in turn fixes two metal ions in a short distance of each other (≈3.5–4.7 Å depending on the ionic radius). The coordination geometry of pyrazolates is rather similar to the bidentate mode of carboxylates, which is the basis of paddle-wheel [$M_2(RCOO)_4$], trigonal-prismatic [$M_3O(RCOO)_6$], and octahedral [$M_4O(RCOO)_6$] SBUs commonly encountered in porous metal carboxylate frameworks. In contrast to imidazolates, the simple pyrazolate unit is difficult to form 3D frameworks. Thus, a variety of polypyrazolate ligands are designed and synthesized to build stable 3D MOFs. There are several typical SBUs based on bidentate coordinated pyrazolates. The most well-known SBUs are (a) octahedral [$M_4(\mu_4\text{-O})(\mu\text{-PZ})_6$], (b) cubic [$M_8(\mu_4\text{-OH})_6(\mu\text{-PZ})_{12}$], (c) triangular [$M_3(\mu_3\text{-O})(\mu\text{-PZ})_3(H_2O)_3]^+$, (d) double zigzag chain with square-planar metal ions, (e) double zigzag chain with tetrahedral metal ions, and (f) triple zigzag chain with octahedral metal ions (**Figure 10**).

In the year 2011, Navarro and co-workers reported a metal–azolate–carboxylate (MAC) framework based on bifunctional pyrazolate–carboxylate ligands and octahedral [$Zn_4(\mu_4\text{-O})(COO)_3(\mu\text{-PZ})_3$] clusters. The crystal structure of this MOF resembles that of MOF-5 and IRMOFs. This cubic **pcu-a** topology MOF shows excellent stability. No change in PXRD pattern was observed after suspension in water at room temperature or in boiling organic solvent (methanol, benzene, or cyclohexane)

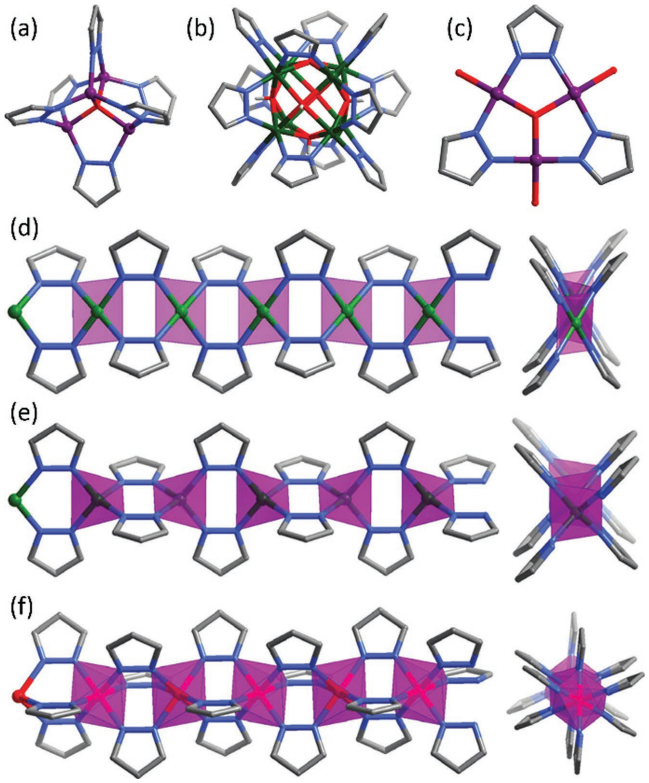

Figure 10. Structures of a) octahedral [$M_4(\mu_4\text{-O})(\mu\text{-PZ})_6$], b) cubic [$M_8(\mu_4\text{-OH})_6(\mu\text{-PZ})_{12}$], c) triangular [$M_3(\mu_3\text{-O})(\mu\text{-PZ})_3(H_2O)_3]^+$, d) double zigzag chain with square-planar metal ions, e) double zigzag chain with tetrahedral metal ions, and f) triple zigzag chain with octahedral metal ions. Reproduced with permission.[154] Copyright 2012, American Chemical Society.

for 24 h.[158] Janiak and co-workers, also reported some MAC frameworks with [$Zn_4(\mu_4\text{-O})(\mu\text{-PZ})_6$] clusters (Figure 10a) which showed high stabilities.[159] When the carboxylate group in the azolate–carboxylate ligand was replaced by another pyrazolate, a MOF-5 analogue with pure pyrazolate ligands can be obtained. In addition, MFU-1 (MFU stands for metal–organic framework Ulm-University) consisting of 1,4-bis[(3,5-dimethyl)-pyrazol-4-yl] benzene (H_2BDPB) and [$Zn_4(\mu_4\text{-O})(\mu\text{-PZ})_6$] clusters is also structurally similar to MOF-5.[160]

From a topological point of view, the cubic [$Ni_8(\mu_4\text{-OH})_6(\mu\text{-PZ})_{12}$] cluster (Figure 10b) is equivalent to the well-known [$Zr_6O_4(OH)_4(RCOO)_{12}$] cluster, which is also a 12-connected node. When the linear dicarboxylic acid ligands are replaced by linear bipyrazole ligands, a class of **fcu** networks analogous to UiO-66 can be obtained. Bordiga and co-workers reported two highly stable MOFs based on the cubic Ni_8-clusters and polypyrazolate ligands.[161] These MOFs are stable from room temperature up to 410 °C. In addition to the linear bipyrazole ligands, planar tetrapyrazole ligands can also be used to bridge the Ni_8-clusters into stable frameworks. PCN-601 and 602 are composed of Ni_8-clusters and pyrazolate-based porphyrinic ligands.[45,162] Similar to the Zr-porphyrin MOF-525, PCN-601 and 602 also adopt a **ftw-a** topology featuring large cubic cages within the frameworks (**Figure 11**). The diameter of the cages in PCN-601 and 602 are 1.5 and 2.1 nm, respectively.

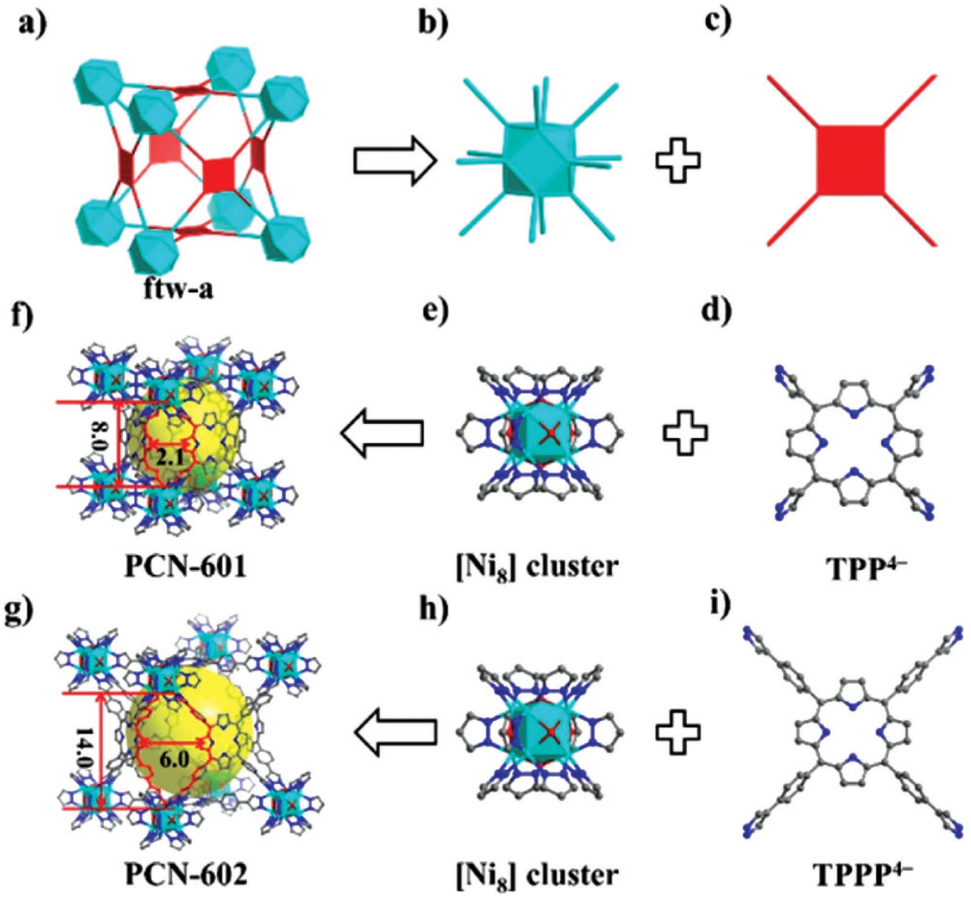

Figure 11. Reticular design and construction of PCN-601 and PCN-602: a) **ftw** net; b) 12-connected node; c) 4-connected node; d) TPP ligand; e,h) [Ni_8] cluster; f) structure of PCN-601; g) structure of PCN-602; and i) TPPP ligand. Reproduced with permission.[45] Copyright 2017, American Chemical Society.

However, the window sizes of the cages in PCN-601 are too small for catalytic applications (≈2.1 × 8.0 Å after deducting van der Waals radii). Luckily, PCN-602 with elongated tetrapyrazole ligands has a larger window size (6.3 × 14.2 Å). The BET surface area and total pore volume of PCN-602 (2219 $m^2\ g^{-1}$ and 1.36 $cm^3\ g^{-1}$, respectively) are also significantly larger than those of PCN-601 (1309 $m^2\ g^{-1}$ and 0.78 $cm^3\ g^{-1}$). The crystallinity of PCN-602 persists in aqueous solutions of HCl and NaOH with pH between 4 and 14, and shows good stability in 1 M KF, 1 M Na_2CO_3, and 1 M K_3PO_4 aqueous solutions at room temperature. Moreover, PCN-601 shows outstanding stability even in boiling saturated NaOH solution.

In 2008, the Long group reported a flexible MOF Co(BDP) based on 1,4-benzenedi(4′-pyrazolyl) (H_2BDP) and double zigzag chains with tetrahedral metal ions (Figure 10e).[163] A broad hysteresis loop is observed in the H_2 adsorption and desorption isotherms of Co(BDP) at 77 K, which suggests that adsorption occurs with a structural transformation from small to large pores. Further exploration on Co(BDP) shows that the flexible MOF exhibits a large methane storage working capacity at 5–65 bar, due to the stability and flexibility of the frameworks.[164] Additionally, flexible frameworks based on similar linear bipyrazole ligands and double zigzag chains have been widely investigated by other groups.[165–167] When the tetrahedral metal ions were replaced by octahedral metal ions, a rigid framework $Fe_2(BDC)_3$ based on the 1,4-benzenedi(4′-pyrazolyl) ligands and triple zigzag chains (Figure 10f) can be obtained, featuring triangular channels rather than the square channels present in the flexible Co(BDP). According to the PXRD data, $Fe_2(BDC)_3$ remains stable after 14 d of soaking in aqueous acid or base solutions of pH = 0 or 14 at 298 K and pH = 2 or 10 at 398 K.

In many cases, triazolate and tetrazolate-based linkers form structures similar to their pyrazole based analogues. For example, three linkers with triangular geometry (benzentripyrazolate, benzenetritriazolate, and benzenetritetrazolate[168]) can form the same 8-connected [Mn_4Cl(azolate)$_8$(H_2O)$_4$] cluster, and therefore the same **sod** network. However, triazolate-based linkers can form unique clusters in some cases. For example, MAF-X27-Cl ([Co_2(μ-Cl)$_2$(BBTA)]) (BBTA = 1*H*,5*H*-benzo(1,2-*d*:4,5-*d*′)bistriazolate) was formed by zigzag chain SBUs and ditopic triazolate-based linkers. This MOF possesses a hexagonal channel surrounded by open metal sites, bearing a close resemblance to MOF-74.[169] While tetrazolates may have more N-donors and versatile coordination modes than other azolates, they also have much lower basicity and relatively weaker coordination ability. As a result, MOFs with tetrazolate

ligands are usually less stable than those based on other five-membered aromatic nitrogen heterocycle ligands with fewer nitrogen atoms.

4.3.3. M^+-Azolate Based MOFs

Some M^+-azolate based MOFs were also documented with good chemical stability, partially due to their hydrophobicity. MOFs based on $[M_3(\mu\text{-PZ})_3]$ ($M^+ = Cu^+$ or Ag^+) SBUs were reported. Interestingly, the triangular $[Cu_3(\mu\text{-PZ})_3]$ SBU in the polypyrazolate and Cu(I)-containing frameworks can be transformed to $[Cu_3(\mu_3\text{-OH})(OH)_2(H_2O)(\mu\text{-PZ})_3]$ upon oxidation.[170] Xiang and co-workers have also reported the FJU-66 based on the triangular $[Cu_3(\mu\text{-PZ})_3]$ cluster and linear bipyrazole ligand.[171] Unlike previously described MOFs, two adjacent $[Cu_3(\mu\text{-PZ})_3]$ clusters are combined into a six-connected $[Cu_6(\mu\text{-PZ})_6]$ cluster via Cu–Cu contacts. FJU-66 can maintain its structure up to 803 K. The high thermal stability is superior to any other extended $[Cu_3(\mu\text{-PZ})_3]$ polymers, demonstrating that the extra stability results from the intertrimer cuprophilicity. Furthermore, FJU-66 remains stable in aqueous solutions with pH values in the range of 3–14 over 12 h. Another example is the FMOFs constructed from Ag(I) and 3,5-bis(trifluoromethyl)-1,2,4-triazolate. The framework has large (12.2×7.3 Å) interconnected tubes with hydrophobic cavities coated with $-CF_3$ groups of the perfluorinated ligands. It shows remarkable water stability as a result of super-hydrophobicity.

4.4. MOFs Based on Mixed Donor Linkers

Mixed donor linkers with both N- and O-donor atoms in the coordination groups have been adopted to enrich the structural abundance of MOFs. Indeed, the combination of N-donor groups (such as azolates) and O-donor groups (such as carboxylates) has led to the discovery of numerous intriguing structures. For example, the carboxylate and azolate moieties from a linker can form two different supermolecular building blocks respectively, which facilitates the design and discovery of new MOF structures.[172,173] A series of MOFs with zeolitic topologies have been reported using 4,5-imidazoledicarboxylate as a linker.[174] In addition, different donor groups can bind to different metals to form a mixed-metal MOF, which further diversifies the overall structure.[175,176] Generally, inorganic SBUs formed by high-valency metal ions and carboxylate-based linkers tend to have strong stability in acidic conditions because of the low pK_a of carboxylic acids. On the other hand, inorganic SBUs composed of low-valency metal ions and azolate-base linkers are usually robust in basic solution. The mixed-component MOFs with both azolate and carboxylate based SBUs seem to be less stable than the MOFs based on single SBUs. This could be rationalized by the fact that the overall stability of the framework is determined by the most labile bond at a given condition. For example, a series of isostructural MOFs with **fcu** topology were synthesized using either pure pyrazolate-based linkers or pyrazolate–carboxylate mixed donor linkers. MOFs with mixed carboxylate–pyrazolate linkers are sensitive to moisture, whereas those containing pyrazolate linkers exhibit a high stability in environmental moisture and water.[62]

MOFs have also been constructed using mixed-linker synthetic strategy in which O-donor linkers and N-donor are used simultaneously. Although the stability of these MOFs has not been commonly studied, they are expected to show relatively weaker stability compared to the MOFs with only one linker, which is similar to the trend of mixed donor linkers based MOFs. However, some stable mixed ligand MOFs based on +2 metal cations, pyridyl ligands and coordinating anions were documented.[177–181] For example, a series of isoreticular MOFs, SIFSIX-*n*-Cu ($n = 1$, 2, and 3), NbOFFIVE-1-Ni, and AlFFIVE-1-Ni, have shown great potentials toward gas storage and separation. Among them, hydrolytically stable AlFFIVE-1-Ni, also known as $[Ni(pyr)_2(AlF_5)]$, could selectively remove water vapor from gas streams and making it an ideal candidate for energy-efficient dehydration.

5. Properties and Applications

5.1. Catalysis

5.1.1. Lewis Acid Catalysis

Coordinatively unsaturated metal sites in MOFs have been found to act as Lewis acidic sites for catalysis. For gas phase catalysis, these sites can be exposed by the activation process (e.g., heating and evacuation) to remove the coordinated solvent molecules. In solution, the active metal sites can interact with the substrate by replacing the coordinated solvent molecules with substrate molecules. For stable MOFs based on high-valency metals and carboxylates, the metal nodes provide inherent Lewis acidic sites. Studies have shown that the Lewis acidic sites in MOFs can catalyze a variety of reactions, such as the cyanosilylation of aldehydes,[207] α-pinene oxide isomerization,[208] Friedel–Crafts reaction,[46] Hetero–Diels–Alder (hDA) reaction,[103] and the cycloaddition of CO_2 and epoxides.[41,209] Some typical examples of stable MOFs for Lewis acid catalysis will be summarized based on the valence of metals in this section.

M^{3+}-based MOF catalysts: The MIL-series (e.g., MIL-47, MIL-53, MIL-88, MIL-100, and MIL-101) are among the most widely studied classes of MOFs with trivalent metals (e.g., Al^{3+}, Cr^{3+}, and Fe^{3+}) for Lewis acid catalysis. By removing terminal water molecules on the $[Fe_3(\mu_3\text{-O})(OH)(H_2O)_2(COO)_6]$ cluster, the generated metal sites in MIL-100(Fe) can act as Lewis acidic sites for catalytic reactions, including Friedel–Crafts reactions,[46] regioselective ring-opening of epoxides,[210] Claisen–Schmidt condensation,[211] and isomerization of α-pinene oxide.[208] For instance, the Friedel–Crafts benzylation catalytic tests conducted by Férey and co-workers showed that 100% benzyl chloride conversion with nearly 100% diphenylmethane selectivity was attained after 5 min, indicating high activity and selectivity for MIL-100(Fe).[46]

Similarly, the cyanosilylation of trimethylsilylcyanide to benzaldehyde catalyzed by MIL-101(Cr) was also reported, showing a yield of 98.5% within 3 h.[207] Besides the cyanosilylation, the cycloaddition of CO_2 to epoxides is another commonly

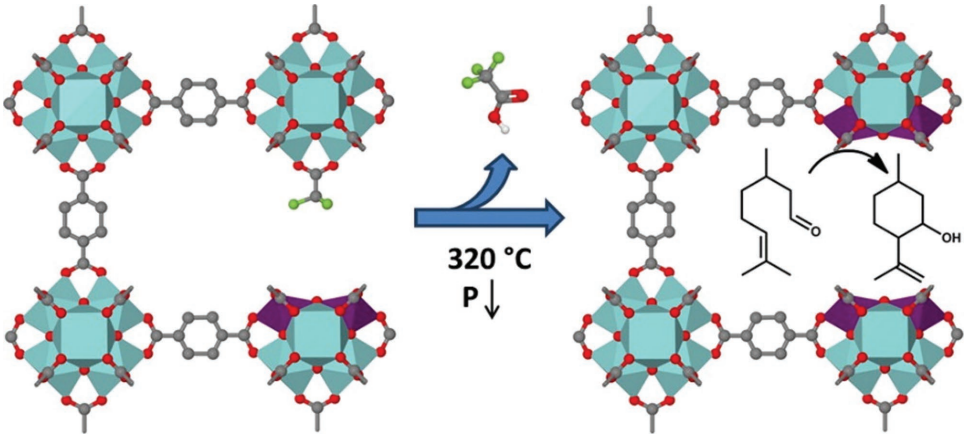

Figure 12. Removal of the coordinated trifluoroacetic acid by thermal activation. Reproduced with permission.[212] Copyright 2013, American Chemical Society.

used reaction to estimate the catalytic activity of Lewis acidic MOFs. Zalomaeva et al. reported that MIL-101(Cr) catalyzed the solvent-free coupling reaction of epoxides with CO_2 to produce cyclic carbonates.[209] Under optimal reaction conditions, the yields of propylene and styrene carbonates reached 82% and 95%, respectively. However, a decrease in catalytic activity was observed after several cycles, which may be attributed to the destruction of the framework integrity, pore blockage, and poisoning of the active sites.

M^{4+}-based MOF catalysts: Due to their high chemical stability, Zr-based MOFs have been widely studied in recent years as heterogeneous Lewis acidic catalysts. A representative example of Zr-MOFs is UiO-66 composed of $[Zr_6(\mu_3\text{-}O)_4(\mu_3\text{-}OH)_4(COO)_{12}]$ clusters and BDC linkers. With high-valency Zr^{4+} sites, UiO-66 has been studied for a variety of catalytic reactions including the aldol condensation reaction,[213] the cyclization of citronellal, etc.[212,214] Several methods have been investigated to increase the catalytic activity of UiO-66. One strategy is to create more open metal sites by defect engineering. Vermoortele et al. reported the synthesis of UiO-66 by using trifluoroacetic acid and HCl in the synthesis.[212] After dehydroxylation of the Zr_6 clusters and removal of the coordinated trifluoroacetic acid by thermal activation, a material with more defects and therefore more open metal sites can be generated (**Figure 12**). Another method to increase the catalytic activity is to introduce functionalized organic ligands. Using molecular modeling, Vermoortele et al. revealed that the presence of nitro-substituted BDC ligands can increase the rate of cyclization of (+)-citronellal to isopulegol as a result of the electron-withdrawing effect.[214] The substituents can not only affect the Lewis acidic properties of the MOF but also introduce stabilizing or destabilizing effects on the reactants based on their electronic properties.

Recently, the degradation of chemical warfare agents by MOFs has been widely investigated. Hupp and co-workers have shown that Zr-based MOFs can hydrolyze organophosphate-based nerve agents and simulants taking advantage of the Lewis acidic Zr sites as well as the extremely high chemical stability of Zr-MOFs.[215–223] For example, Mondloch et al. studied the hydrolysis of nerve agent simulant dimethyl 4-nitrophenyl phosphate (DMNP) on the $[Zr_6(\mu_3\text{-}O)_4(\mu_3\text{-}OH)_4(OH)_4(H_2O)_4(COO)_8]$ nodes of NU-1000 experimentally and computationally.[223] DMNP binds to NU-1000 by hydrogen bonding with $-H_2O/OH^-$ groups on the Zr_6-nodes as well as by weak π–π stacking interactions with the benzene ring of the organic linkers. As shown in **Figure 13**, the rate-determine step of the reaction is the dissociation of coordinated water from the Zr_6-cluster. Then, the P=O group of DMNP interacts with the Zr atom by electrostatic attraction, followed by hydrolysis of DMNP. Density functional theory (DFT) calculations provide insight into the experimental observation that the half-life for DMNP hydrolysis can be greatly reduced by heating NU-1000 to remove terminal ligands on the cluster. It is worth noting that when different organic ligands are used, Zr-MOFs containing Zr_6-clusters with various symmetries and connectivities (e.g., 12-connected, 8-connected, and 6-connected) can be generated.[216,221,223] In general, the MOFs with lower-connected Zr_6-clusters contain more Zr-OH and Zr-OH_2, leading to an increased hydrolysis rates. Another important Zr-MOF, UiO-66, has been tested for the methanolysis of methyl paraoxon and *p*-nitrophenyl diphenyl phosphate (PNPDPP).[216] The Zr-OH-Zr-containing node was proposed to be the active site, which functionally mimics the binuclear Zn^{II} active site of the phosphotriesterase enzyme for phosphate ester bonds hydrolysis.

In addition to coordinatively unsaturated metal sites on metal nodes, MOFs containing metal sites on organic ligands have been investigated. For example, PCN-223(Fe), a Zr-MOF with Fe(III)-porphyrin centers, has been used as a Lewis acid catalyst to promote the hDA between aldehydes and dienes.[103] After the treatment with $AgBF_4$, the Cl^- counterions coordinated to the Fe(III)-porphyrin centers were removed to create highly reactive Lewis acidic sites (**Figure 14**). The exposed Fe(III) center, as a Lewis acid, polarizes the aldehydes, while electron-withdrawing groups on the porphyrin further increase the electron deficiency of the Fe(III) center. As a result, the yield of the hDA reaction catalyzed by PCN-223(Fe) reached 99%, even higher than homogeneous systems.

5.1.2. Brønsted Acid Catalysis

Besides the inherent Lewis acidic sites, stable MOFs can be functionalized with Brønsted acid catalysts to extend

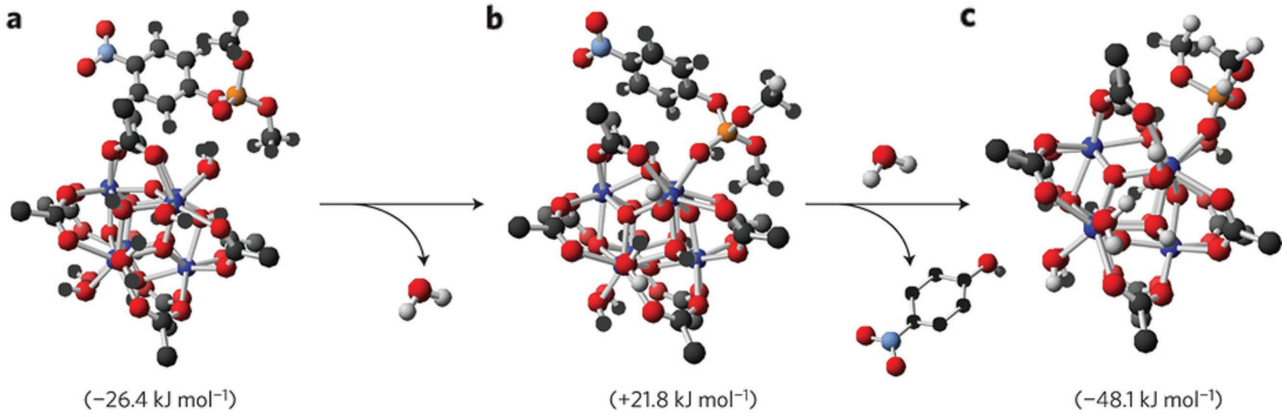

Figure 13. Association and reaction energies of the interaction of DMNP and Zr_6 cluster of NU-1000. a) DMNP binding. b) H_2O replaced by DMNP. c) Hydrolysis of DMNP. Color code: Zr (blue); O (red); C (black); H (white); P (orange); N (light blue); F (green); S (yellow). Reproduced with permission.[185] Copyright 2015, Nature Publishing Group.

the scope of catalytic reactions. Recently, stable MOFs with Brønsted acids have been investigated for various reactions including the Diels–Alder reaction,[224] acetalization,[225] isomerization,[224,226] Friedel–Craft reaction,[226,227] esterification,[228] and dehydration.[229] One strategy to introduce Brønsted acids into MOFs is to covalently bind Brønsted acidic groups to organic ligands. For example, MIL-53(Cr) and MIL-101(Cr) functionalized with sulfonic acid can be obtained by treating with triflic anhydride and sulfuric acid.[228] They showed high catalytic performance in esterification of *n*-butanol with acetic acid. The turnover frequency for sulfated MIL-53 (Cr) (0.72 min^{-1}) was higher than that of acidic polymers like Nafion NR50 (0.63 min^{-1}). In another example, Lewis acidity and Brønsted acidity coexist in the sulfated MOF-808. Substitution of terminal ligands on Zr_6-clusters with sulfate groups in a 2:1 ratio in MOF-808 forms a superacidic sulfated framework with both Lewis acidity and Brønsted acidity (**Figure 15**).[226] The sulfated MOF-808 showed activity for isomerization of methylcyclopentane at 150 °C, which represents the benchmark for MOF-based solid–acid catalysts. It is also worth noting that Brønsted acid catalysis requires a highly stable MOF platform. The catalytic process generally involves the transfer of protons from the catalytic active sites of the MOF to the substrate, which requires the MOF to be stable toward protons. As a result, compared to the large amount of MOFs explored for Lewis acidic catalysis, only a limited number of MOFs as Brønsted acidic catalysts have thus far been developed.

5.1.3. Redox Catalysis

Functionalized linkers as catalysts. The redox inertness of some stable MOFs (such as Al^{3+} and Zr^{4+}-based MOFs) limited their applications as redox catalysts. To functionalize stable MOFs for redox catalysis, one method is to adopt metallo-linkers. For example, PCN-222 with different metalloporphyrins were employed as biomimetic oxidation catalysts. Three substrates, including pyrogallol, 3,3,5,5-tetramethylbenzidine, and *o*-phenylenediamine, were adopted to estimate the catalytic activity of PCN-222(Fe). Kinetic studies have demonstrated that PCN-222(Fe) can catalyze the oxidation of a variety of substrates, acting as an effective peroxidase mimic with both excellent substrate binding affinity (K_m) and catalytic activity (k_{cat}), superior to free hemin in aqueous media. The excellent catalytic performance of PCN-222(Fe) is attributed to the stability of the framework and the large open channels, which effectively prevent the self-dimerization of porphyrin centers and facilitate the diffusion of substrates. In another example, UiO-66 was modified with molybdenum, tungsten, and vanadium for olefin epoxidation. Tan and co-workers functionalized the UiO-66-NH_2 with salicylaldehyde, pyridine-2-aldehyde, or 2-pyridine chloride by PSM and then metalated the linker with Mo(IV) catalyst. The good dispersion of the Mo(IV) catalyst and the highly accessible surface area of the MOF guarantee sufficient contact between substrate and catalytic center, facilitating the catalytic reaction. The Mo(IV)-functionalized MOFs exhibit high catalytic activity for epoxidation reactions with a conversion of 99%. In addition, Lin and co-workers constructed a series of Zr-MOFs (BPV-MOF, mBPV-MOF, and mPT-MOF) of **fcu** topology with elongated bipyridyl- and phenanthryl-containing linkers. Postsynthetic metalation of these Zr-MOFs with $[Ir(COD)(OMe)]_2$ afforded highly active, robust single-site catalysts for organic transformation reactions including tandem hydrosilylation/ortho-silylation of aryl ketones and aldehydes, tandem dehydrocoupling/ortho-silylation of *N*-methylbenzyl amines, and borylation of aromatic C—H bonds.

Encapsulated catalysts: Besides the functionalization of linkers, redox catalysts can also be incorporated into the cavity of MOFs.[230] Noble metal nanoparticles are known as efficient catalysts with a wide range of potential applications in the fields of energy conversion and storage, environmental remediation, drug research and chemical production. Immobilization of metal nanoparticles in MOF cavity provides highly accessible metal surfaces while preventing aggregation. Nobel metal nanoparticles can be introduced into MOFs by impregnation and successive reduction.[231] Metal alloy nanoparticles were also successfully embedded in the cavity of MOFs by Xu and co-workers. In 2011, they reported bimetallic AuPd NPs immobilized in MIL-101 and ethylenediamine (ED)-grafted MIL-101

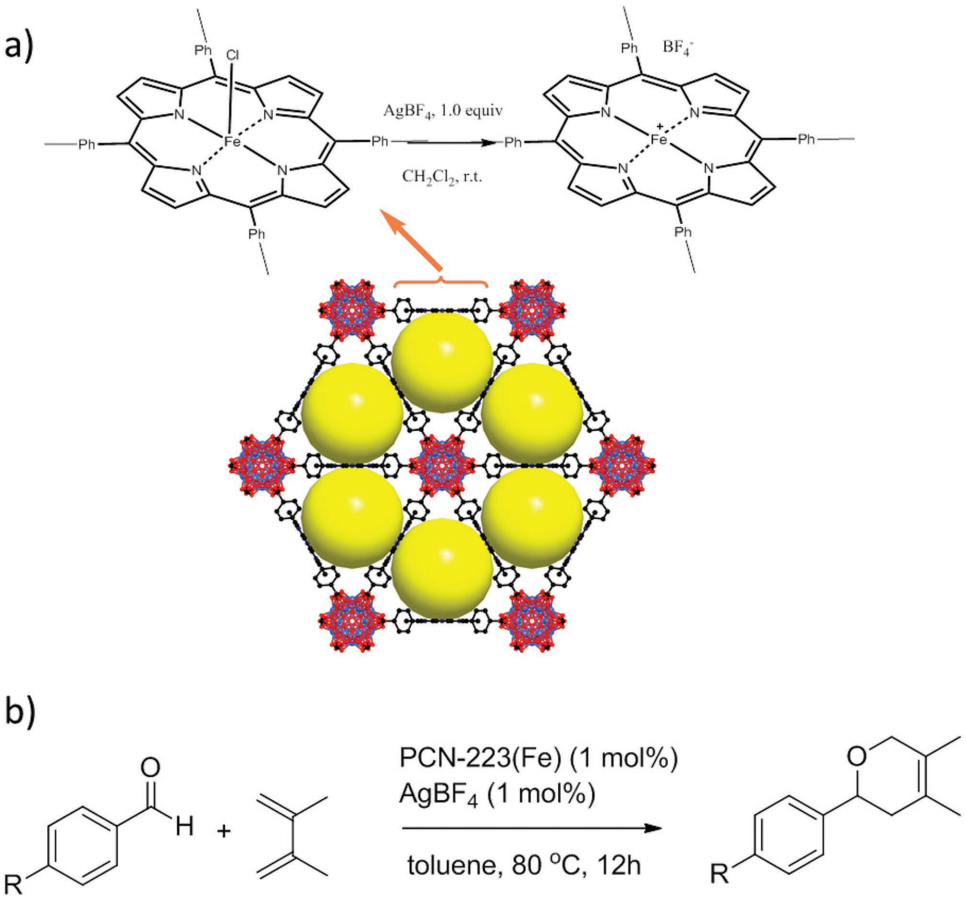

Figure 14. Illustration of the hDA reaction catalyzed by PCN-223(Fe). Reproduced with permission.[103] Copyright 2014, American Chemical Society.

(ED-MIL-101) as highly active catalysts for the conversion of formic acid to high-quality hydrogen at a convenient temperature.[232] Later on, they developed a liquid-phase concentration-controlled reduction (CCR) strategy in combination with the double solvents method (DSM) to introduce AuNi nanoparticles into MOFs and control the size and location of the immobilized AuNi nanoparticles (**Figure 16**).[233] Uniformly distributed AuNi nanoparticles encapsulated in the pores of MIL-101 were achieved which exerted high activity for hydrogen generation from the catalytic hydrolysis of ammonia borane.

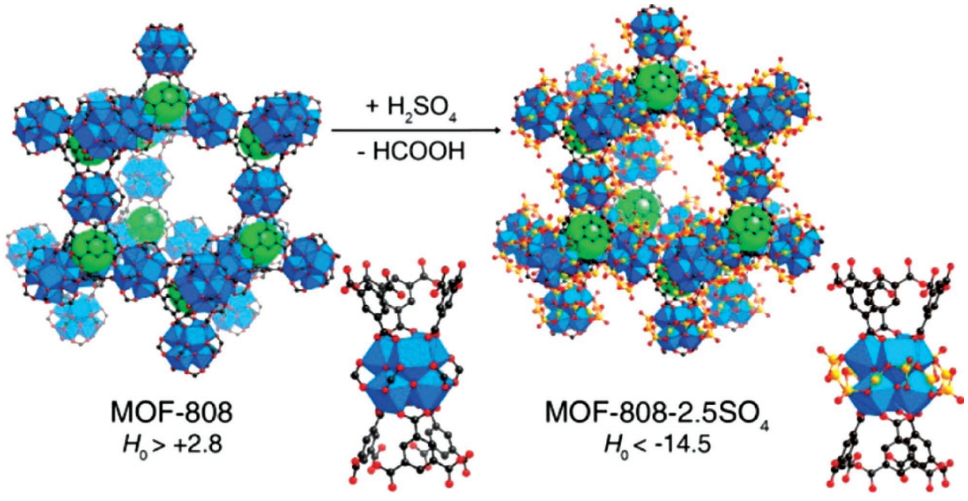

Figure 15. The preparation of sulfated MOF-808 with both Lewis acidity and Brønsted acidity. Reproduced with permission.[226] Copyright 2014 American Chemical Society.

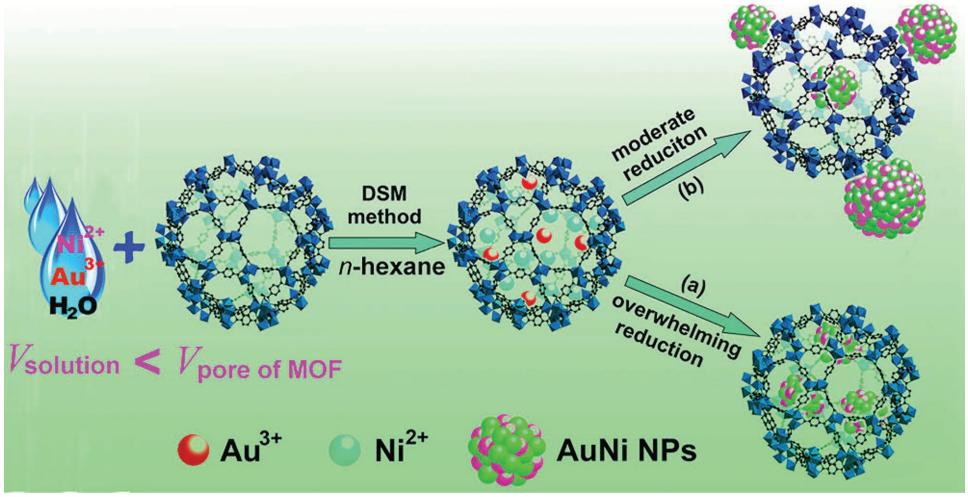

Figure 16. Schematic representation of the immobilization of AuNi nanoparticles by the MIL-101 matrix using DSM combined with a liquid-phase CCR strategy. Reproduced with permission.[233] Copyright 2013, American Chemical Society.

Recently, metal and metal oxide nanoparticles were simultaneously incorporated into a MOF for catalytic hydrogenation of CO_2 into methanol, which potentially mimics the industrialized $Cu/ZnO/Al_2O_3$ ternary catalyst.[234] A bpy-functionalized Zr-MOF, UiO-bpy, was initially synthesized. Cu^{2+} was subsequently metalated into the vacant bpy sites followed by the introduction of Zn^{2+} via reacting $ZnEt_2$ with the μ_3-OH sites on the $[Zr_6(\mu_3\text{-}O)_4(\mu_3\text{-}OH)_4(COO)_{12}]$ cluster (**Figure 17**). The Cu/ZnO_x NPs were in situ generated at 250 °C in the presence of H_2 as the reductant. The resultant Cu/ZnO_x@MOF catalysts showed high activity with a space–time yield of up to 2.59 $g_{MeOH}\ kg_{Cu}^{-1}\ h^{-1}$ and 100% selectivity for CO_2 hydrogenation to methanol.

In 2016, Tang and co-workers reported a MOF@Pt nanoparticle@MOF composite as an efficient catalyst for selective hydrogenation of α, β-unsaturated aldehydes (**Figure 18**).[235] Sandwiching platinum nanoparticles between an inner core and an outer shell composed of MIL-101 (Fe), MIL-101(Cr), or both resulted in stable catalysts that convert a range of α, β-unsaturated aldehydes with high yield and selectivity toward unsaturated alcohols. Calculations revealed that preferential interaction of MOF metal sites with the carbon–oxygen rather than the carbon–carbon group explains the selective hydrogenation of aldehydes instead of alkenes.

Metalation of clusters. Cluster metalation is a powerful tool to functionalize Zr-MOFs for redox catalysis. The terminal $-OH^-/H_2O$ groups on Zr_6-cluster can deprotonate to bind with metal cations. All the approaches for immobilization can be summarized into two categories, liquid-phase methods and gas-phase methods. In liquid-phase immobilization, metal salts and organometallic reagents are often used as metal precursors. Farha and co-workers deposited oxomolybdates on the metal nodes of NU-1000. The derived catalyst shows exceptional stability and high efficiency for cyclohexene epoxidation, which surpasses the performance of molybdenum (IV) oxide catalysts.[236] One of the advantages for metal node immobilization is the high dispersity of active species. Lin and co-workers demonstrated a single-site Mg-alkyl catalyst stabilized by Zr-MOF, which is synthesized by straightforward metalation of Zr clusters with Me_2Mg. The Mg-functionalized MOF displayed high activity for the ketone hydroboration and can be reused more than 10 times.[237] Direct structural evidence on the positions and coordination environments of the incorporated metal ions were provided by our group using PCN-700 as a platform. Along with the metalation of Zr_6 cluster, ligand migration is observed in which a Zr-carboxylate bond dissociates to form a M-carboxylate bond (M=Ni and Co).[238] Compared to liquid-phase synthesis, gas-phase immobilization is more versatile due to the high permeability of gas and easy adjustment of dosage. Farha and co-workers developed Atomic Layer Deposition (ALD) in MOFs to accurate deposit metal species onto Zr clusters. In a typical example, Ni^{2+} were immobilized on the nodes of NU-1000 using ALD. After heat treatment in H_2, the material can be used as an efficient and stable catalyst for ethylene hydrogenation and oligomerization.[239]

5.1.4. Photocatalysis

Photocatalysis is a promising pathway for the direct conversion of solar energy to clean and valuable chemical energy.[240,241] MOFs can be photoresponsive through light absorption by the organic linkers or the metal centers, attracting great interest as fascinating catalysts in this field.

Ti-based MOFs, with photoactive Ti-oxo clusters, have been exclusively studied as promising photocatalysts. A reversible photochromic behavior of MIL-125(Ti) induced UV irradiation in alcohol was initially observed by Férey and co-workers.[93] Later, Li and co-workers fabricated a NH_2-functionalized MIL-125, namely MIL-125-NH_2,[36] which not only possesses extra light absorption in visible light region but also exhibits enhanced adsorption capacity toward CO_2. Recent work has demonstrated that MIL-125-NH_2 can work as a light-driven photocatalyst for hydrogen generation[99] and CO_2 reduction.[36] In 2015, our group assembled the photocatalytic titanium-oxo cluster and photosensitizing

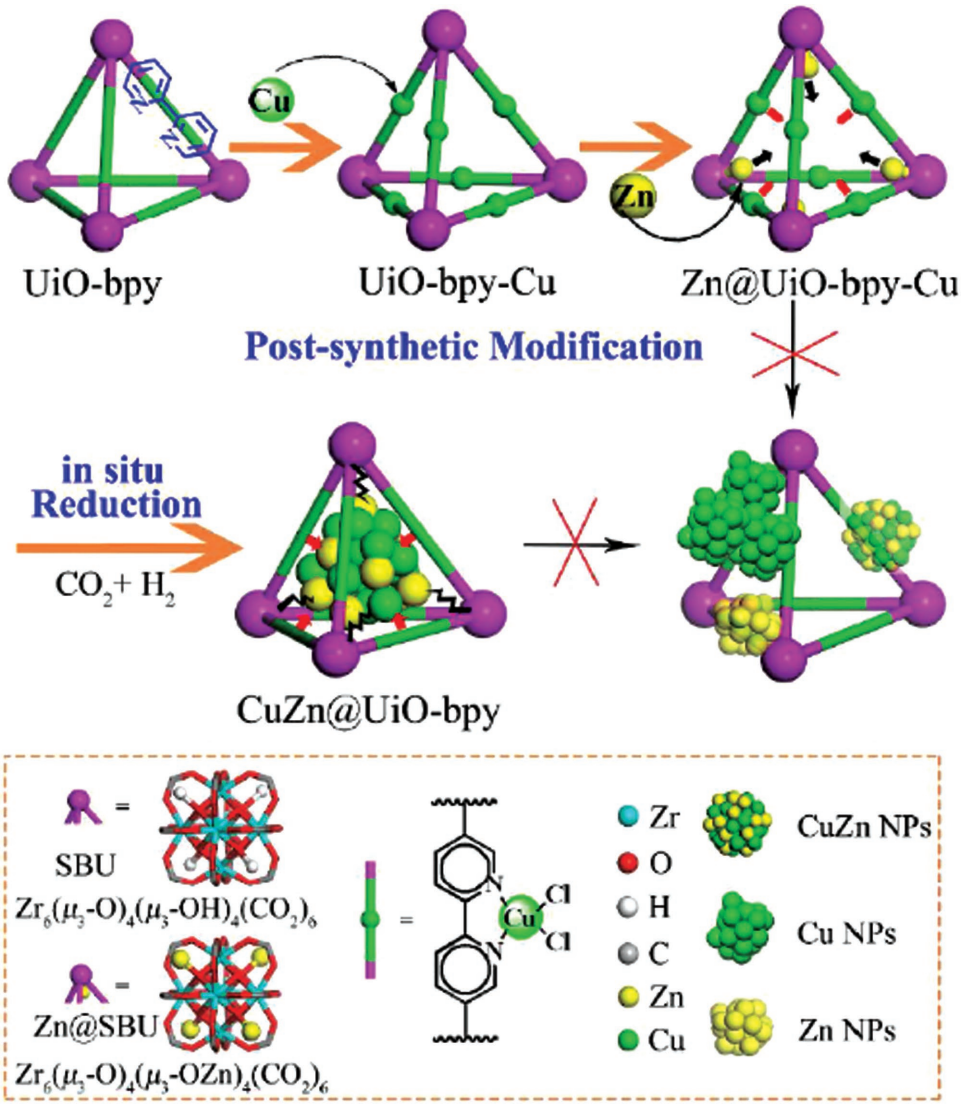

Figure 17. Preparation of CuZn@UiO-bpy via in situ reduction of postsynthetically metalated UiO-bpy. Reproduced with permission.[234] Copyright 2017, American Chemical Society.

porphyrinic linker into a MOF named PCN-22.[94] As a suitable candidate for light harvesting, PCN-22 was employed as a photocatalyst for an alcohol oxidation reaction.

Garcia and co-workers initially studied the photocatalytic activity of water stable Zr–MOFs (UiO-66 and UiO-66-NH_2) for H_2 generation in methanol or water/methanol upon irradiation at wavelengths longer than 300 nm.[242] The presence of the $-NH_2$ group in the BDC fragment induces the absorption in the wavelength longer than 300 nm due to the auxochormic and bathochromic shift, which renders UiO-66-NH_2 a better photocatalyst than UiO-66. UiO-66-NH_2 also exhibits high photocatalytic activity for the aerobic oxidation and CO_2 reduction under visible-light irradiation.[243,244] Pt nanoparticles were later incorporated inside of or supported on UiO-66-NH_2 as co-catalysts for photocatalytic hydrogen production.[245] The Zr–porphyrin MOFs, PCN-222[246] (also known as MOF-545) and MOF-525,[247] were also investigated as photocatalysts for CO_2 reduction.

In 2016, Chi et al. prepared three types of Fe-based MOFs and their amino-functionalized derivatives and utilized them as water oxidation catalysts under visible light irradiation.[248] Among them, MIL-101(Fe) exhibits excellent visible light-driven oxygen evolution activity with a high current density and early onset potential. Fe-based MOFs are promising photocatalysts for water oxidation,[248] degradation,[249] and Cr(VI) reduction.[250] Stable aluminum-based MOFs were also utilized as catalysts for visible-light driven hydrogen evolution[126] and oxygen evolution[251] from water.

Besides the inherent metal–oxo clusters, photocatalysts can also be incorporated into the organic linkers. The bpy functionalized UiO-67, as a stable and versatile platform, has been functionalized by Ir, Re, Ru, and Rh-complexes as photocatalysts.[252,253] For instance, Lin and co-workers obtained two MOFs containing phosphorescent $[Ir^{III}(ppy)_2(dcbpy)]Cl$ and $[Ru^{II}(bpy)_2(dcbpy)]Cl_2$ (ppy = 2-phenylpyridine, bpy = 2,2′-bipyridine and dcbpy = 2,2′-bipyridine-5,5′-dicarboxylic acid). They

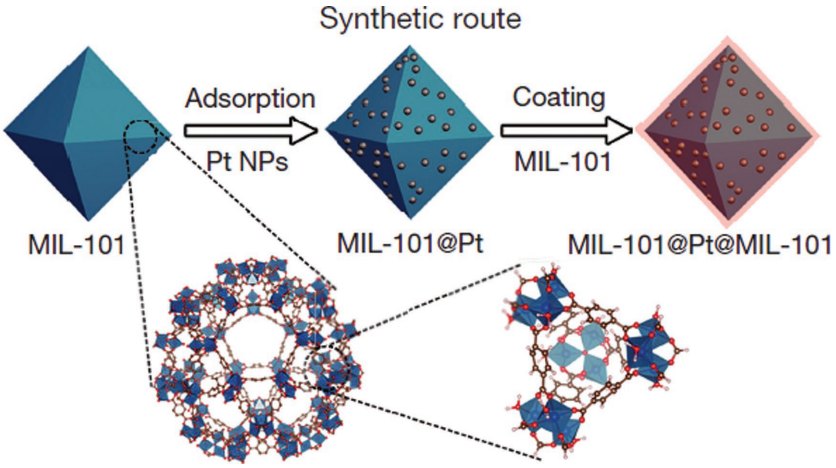

Figure 18. Illustration of the synthetic route to generate MIL-101@Pt@MIL-101, comprised of Pt nanoparticles (NPs) sandwiched between a core and a shell of MIL-101. Reproduced with permission.[235] Copyright 2016, American Association for the Advancement of Science.

were employed in three photocatalytic organic transformations (aza-Henry reaction, aerobic amine coupling, and aerobic oxidation of thioanisole), and exhibited high activities. In addition, the encapsulation of the molecular catalysts into other MOFs[91,254–256] and the modification of photoresponsive units on stable MOFs[257] were also explored. A good example is hierarchically integrating multiple components to affect synergistic functions by the impregnation method. A series of inorganic clusters as co-catalysts were encapsulated into photoactive MOFs, which showed improved activity compared with single-component references.[35,41,258–265] These composite materials have been adopted as photocatalysts for the degradation of organic dyes[266] and antibiotics,[267] oxidation of alcohols,[268] and hydrogen evolution.[269]

Compared with conventional inorganic semiconductors, it is easier to control the light-absorption properties of MOFs by tuning the light-absorption abilities of organic fragments. For instance, the introduction of $-NH_2$ groups as substituents on ligands would result in an isostructural MOF with a new band in the visible region.[270] The introduction of specific chromophores, such as porphyrin fragments, can lead to the formation of MOFs with photoresponsive characteristics derived from the corresponding chromophores. Considering the high tunability of MOFs by judicious selection of metal–oxo clusters and design of linkers, a variety of MOF based catalysts for specific applications are envisioned.

5.1.5. Electrocatalysis

Although Pt-based catalysts are currently the best electrocatalysts, widespread practical utilization is severely hampered by its prohibitive cost and low abundance. Replacement of precious Pt-group metals with efficient, low-cost catalysts holds tremendous promise for clean energy devices. Among diverse nonprecious catalysts, MOFs hold potential as highly efficient catalysts for important electrochemical reactions due to their versatile nature.

Owing to their similar electronic structures, Mo-based materials, like MoS_2 and Mo_2C, represent one of the exciting families of such catalysts. ε-Keggin polymolybdate-based MOFs were tentatively employed as electrocatalysts for the hydrogen evolution reaction (HER).[271] In 2015, our group employed two polymolybdate-based MOFs, NENU-500 and NENU-501,[272] as HER catalysts. Remarkably, NENU-500 is highly active for electrochemically generating hydrogen from water under acidic conditions with an onset overpotential of 180 mV and a Tafel slope of 96 mV dec^{-1} due to its good stability, porosity, and exposed active sites. Later, Dai et al. fabricated UiO-66-NH_2 anchored by molybdenum polysulfide (MoS_x) via chemical interactions for HER study.[273] The distinctive design of the Zr-MOF-MoS_x composite enables remarkable electrochemical HER activity and further exhibits excellent durability in acid medium.

Interestingly, Yang and co-workers introduced thin films of nanosized MOFs as atomically defined, nanoscopic catalysts for the electrochemical reduction of CO_2 in aqueous solution.[274] In situ spectroelectrochemical measurements provided insights into the cobalt oxidation state during the reaction and indicated that the majority of catalytic sites in this MOF are redox-accessible from Co(II) to Co(I) during catalysis. In 2016, Zhang, Li and co-workers employed an alkaline-stable, metal hydroxide mimicking MOF, MAF-X27-OH ($[Co_2(\mu\text{-}OH)_2(BBTA)]$), as an efficient electrocatalyst for oxygen evolution (**Figure 19**).[169] MAF-X27-OH was obtained by post-synthetic ion exchange of MAF-X27-Cl ($[Co_2(\mu\text{-}Cl)_2(BBTA)]$), which possesses open metal sites on its pore surface. After the hydroxide functionalization of MAF-X27-Cl, the electrocatalytic activity of MAF-X27-OH for the oxygen evolution reaction (OER) was drastically improved (an overpotential of 292 mV at 10.0 mA cm^{-2} in 1.0 M KOH solution). In addition, isotope tracing experiments confirmed that the hydroxide ligands are involved in the OER process to provide a low-energy intraframework coupling pathway.

The paddle-wheel type cluster, $[Co_2(RCOO)_4]$, may display high catalytic activity, however, it is highly unstable especially in water. With judicious considerations of the host/guest geometries and modular synthetic strategies, the labile $[Co_2(RCOO)_4]$ clusters were immobilized and stabilized in a Fe(III)-MOF as coordinative guests by Zhang and co-workers.[275] This thermal-, water-, and alkaline-stable MOF containing the desired dicobalt clusters exhibits high electrocatalytic oxygen evolution in water at pH = 13. In addition, the electrochemical CO_2 reduction[276] and water oxidation[277] using MOF thin films were also studied. Aside from their pristine form, MOFs have also been widely utilized as precursors for the preparation of more complicated nanostructures to fulfill the demands of catalysis.[278–280] The corresponding nanostructures derived from MOFs as catalysts toward a series of electrochemical reactions were systematically discussed in previous reviews and will not be introduced here.[281,282]

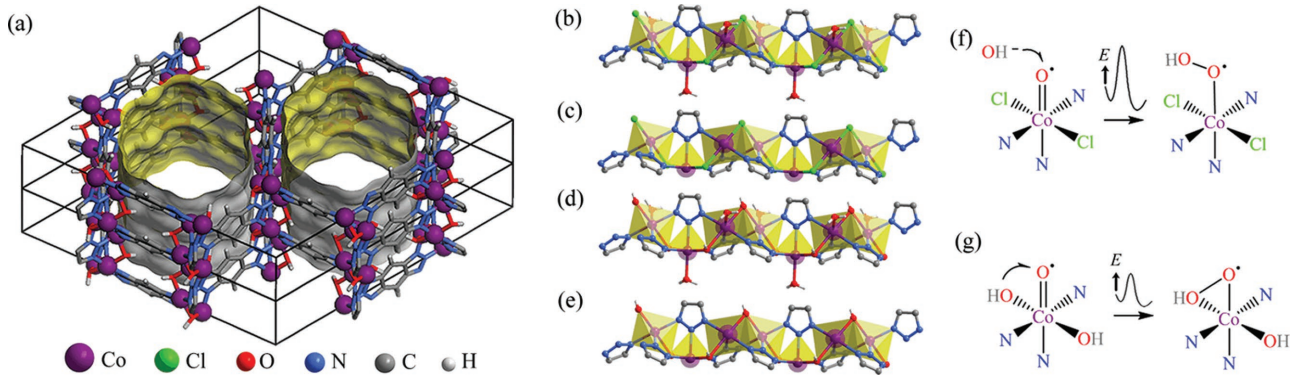

Figure 19. a) 3D Coordination network and pore surface structures of MAF-X27-OH. Local coordination environments of b) water-appended MAF-X27-Cl, c) guest-free MAF-X27-Cl, d) water-appended MAF-X27-OH, and e) guest-free MAF-X27-OH. f) Solid–liquid coupling pathway for MAF-X27-Cl. g) Intraframework coupling pathway for MAF-X27-OH. Reproduced with permission.[169] Copyright 2016, American Chemical Society.

5.2. Adsorption and Separation

Many early MOFs made from divalent metals, such as MOF-5 and HKUST-1, have shown exceptional porosity and promising H_2 and CH_4 storage capacity. For example, the Cu^{2+}-based MOF, HKUST-1, shows high performance in CH_4 storage, with a working capacity of 153 (v/v) (at 35 bar) and 200 (v/v) (at 80 bar). A Zn^{2+}-based MOF, ST-2 (ST = ShanghaiTech University) have the highest CH_4 deliverable capacity of 289 (v/v) at 200 bar. However, their practical applications in gas storage are ultimately limited by their stability. Therefore, stable MOFs with high gas storage capacities are highly desired.

Our group reported the design and synthesis of PCN-250(Fe_2M) (M = Fe, Co, Ni, Mn, and Zn), which demonstrates good chemical stability and high CH_4 uptake.[69] PCN-250(Fe_2Co) has cage sizes suitable for methane uptake and the well-dispersed, highly charged open metal sites. Hence, gas molecules in the void space can strongly interact with the framework, resulting in efficient space utilization. Additionally, the high-valence metal sites lead to an induced polarization of CH_4 molecules through charge-induced dipole interactions and this interaction can further polarize additional layers of gas molecules, enabling multiple layers of gas adsorption. PCN-250(Fe_2Co) demonstrated a total CH_4 uptake of 200 (v/v) at 35 bar and 298 K, which is among the highest in reported MOFs. More importantly, PCN-250(Fe_2Co) retained its framework integrity in water after six months. The high gas uptake and chemical stability guarantee the reusability of these materials for industrial applications.

In another work, the Long group introduced a new concept to increase the working capacity by taking advantage of S-shaped isotherms of flexible MOFs. A flexible Co-pyrazolate based MOF, Co(bdp), was selected. This MOF undergoes a reversible phase transition in response to CH_4 loading with a 'stepped' CH_4 adsorption isotherm (**Figure 20**).[164] The amount of gas adsorbed is small at low pressures but rises sharply just before the pressure reaches the desired storage pressure. Hence, the working capacity of methane uptake can be maximized compared with classical rigid adsorbents. In addition, the structural phase transition reduces the amount of heat released during adsorption and the impact of cooling during desorption, which helps to increase the working capacity. The working capacity of CH_4 for Co(bdp) is 155 (v/v) at 35 bar and 197 (v/v) at 65 bar at the desorption conditions of 298 K and 5.8 bar, which are among the highest in the literature. In addition, M^{2+}-pyrazolate based MOFs are expected to show good resistance to water and basic conditions.

The hydrostability of robust MOFs has extended their application into new areas such as water adsorption. The adsorption of water is important for many applications requiring capture and release of water, such as thermal batteries, dehumidification, and delivery of drinking water in dry areas.[18,19,283–285] The Yaghi group studied and compared the water adsorption properties of 23 materials and among them, two Zr MOFs, MOF-801 ($Zr_6O_4(OH)_4$(fumarate)$_6$) and MOF-841 ($Zr_6O_4(OH)_4(MTB)_2(HCOO)_4(H_2O)_4$), showed the best performance.[37] The water uptake of MOF-801 is higher than 20 wt% at $P/P_0 = 0.1$. The good performance can be ascribed to three symmetrically independent cavities in MOF-801 that can interact with and capture water molecules. Moreover, MOF-801 showed exceptionally stability and recyclability. At $P/P_0 = 0.3$, MOF-841 outperforms other investigated materials and the uptake is remains above 40 wt% after five cycles. Based on the outstanding performance of MOF-801, a device that captures water from the atmosphere at ambient conditions using natural sunlight was designed and demonstrated.[286] This device can harvest 2.8 L of water per kilogram of MOF daily at low relative humidity (20%) without any input of energy. Due to the high water uptake capacity, the low regeneration heat requirement, and the ability to condense water at ambient temperatures, this water harvesting strategy is quite promising.

The release of anthropogenic toxic pollutants into the atmosphere has become an increasingly concerning worldwide issues. Due to their high tunability and versatility, MOFs have also been successfully utilized to remove toxic gases from air.[219,287–290] So far several different strategies have been invented. Toxic gases can be captured in MOFs by means of rational control of pore size and functionalization of pore environments. For example, H_2S adsorption on MIL-53(Al, Cr, Fe), MIL-47(V), MIL-100(Cr), and MIL-101(Cr) has been thoroughly investigated by Weireld and

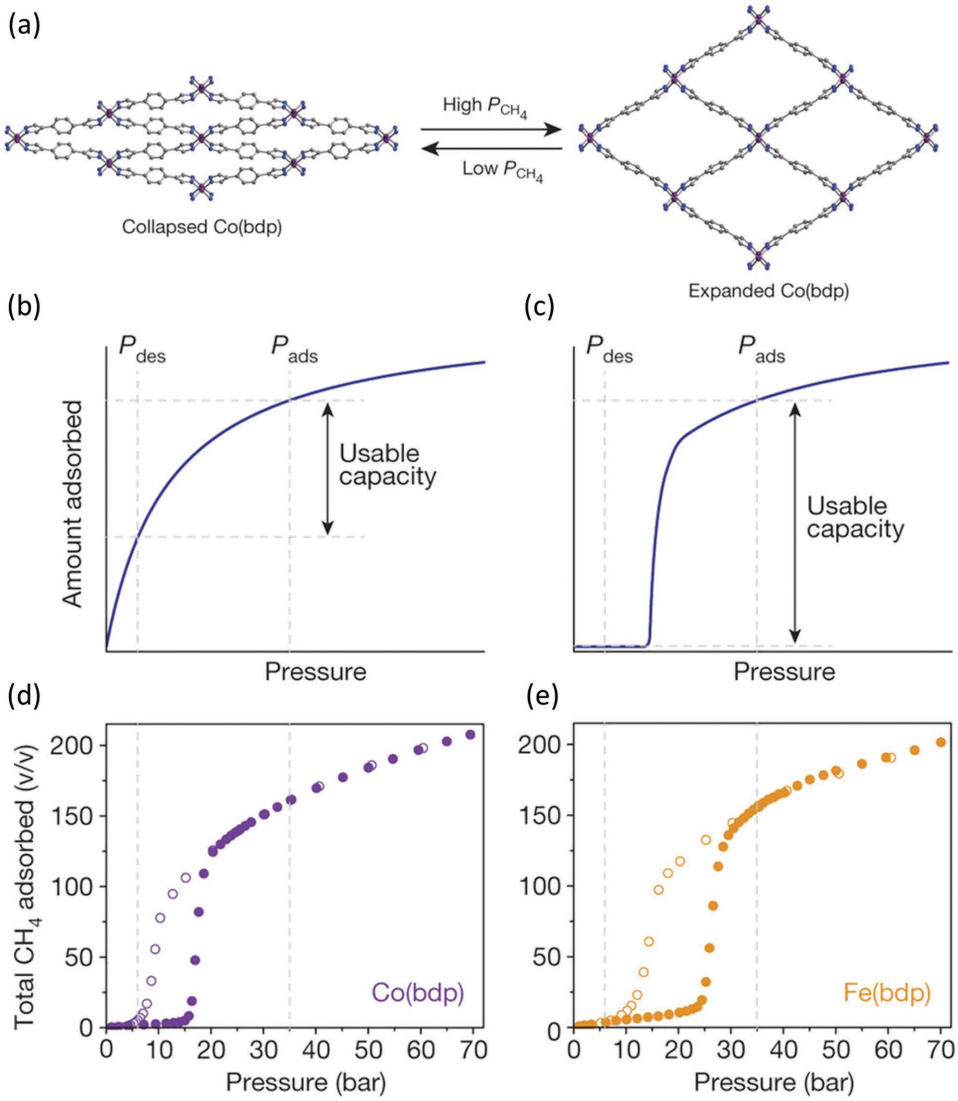

Figure 20. a) The breathing behavior of Co(bdp) upon CH_4 adsorption/desorption. b,c) A comparison of usable capacity for an idealized adsorbent exhibiting a classical Langmuir-type adsorption isotherm and an "S-shaped" adsorption isotherm. CH_4 adsorption isotherms for Co(bdp) d) and Fe(bdp) e) at 298 K. Here P_{des} = 5.8 bar and P_{ads} = 35 bar are indicated by dashed grey lines. Reproduced with permission.[164] Copyright 2016, Nature Publishing Group.

co-workers.[291,292] In addition, the catalytic degradation of toxic gases into nontoxic substances seems to be an alluring strategy.[289]

5.3. Sensing

In the field of fluorescent sensing, structural stability provides great possibilities for MOFs to perform in either aqueous surroundings or in harsh conditions, such as acid/base solutions or hyperthermic/cryogenic temperatures. Bu et al. reported a water stable Cd-MOF, $[Cd_2(TIB)_2(BDA)_2]$ (TIB = 1,3,5-tris(1-imidazolyl) benzene; BDA = 2,2′-biphenyl dicarboxylate), with a double helical structure.[293] By tightly packing the organic ligands, the stability of the MOF was enhanced toward organic solvents, water, and even acid and base (pH = 3–11). Thus, the Cd-MOF could detect various ketones in aqueous solution. In another case, two Zr-based MOFs $Zr_6O_4(OH)_8(H_2O)_4(CTTA)_{8/3}$ and $Zr_6O_4(OH)_8(H_2O)_4(TTNA)_{8/3}$ (H_3CTTA = 5′-(4-carboxyphenyl)-2′,4′,6′-trimeth-yl-[1,1′:3′,1″-terphenyl]-4,4″-dicarboxylic acid; H_3TTNA = 6,6′,6″-(2,4,6-trimethylbenzene-1,3,5-triyl)tris(2-naphthoic acid)) were synthesized by Zhou and co-workers, which are capable of detecting and removing antibiotics and explosives in water.[63] The hydrophobicity induced by the three methyl groups on the judiciously designed linkers contributes greatly to the high aqueous stability of the MOFs. As a result, they demonstrated promising sensing capabilities toward antibiotics and 2,4,6-trinitrophenol.

Recently, by taking advantage of the pH stability and pH-dependent luminescence, applications in the field of pH sensing utilizing MOFs as a platform have also been explored.

PCN-225 is an excellent example of a MOF-based pH sensor.[194] The MOF can remain intact in a wide range of pH from 1 to 11, which can be explained by the strong coordination bonds formed between the Zr^{4+} clusters and the carboxylate groups. When soaked in aqueous solutions with different pH, the emission intensity of PCN-225 changes correspondingly, due to the protonation/deprotonation of the TCPP linker.

Beyond fluorescence sensing, devices that directly converts the stimuli to electronic signals are more appealing in real applications. A fumarate-based RE-**fcu**-MOF can be made as a thin film and grown onto an electrode, showing high sensitivity toward H_2S gas.[294] This MOF adopts **fcu** topology, which is isostructural to the Zr-based MOF-801. It offers a selective H_2S detection to concentrations as low as 100 ppb with a detection limit of 5.4 ppb (**Figure 21**).

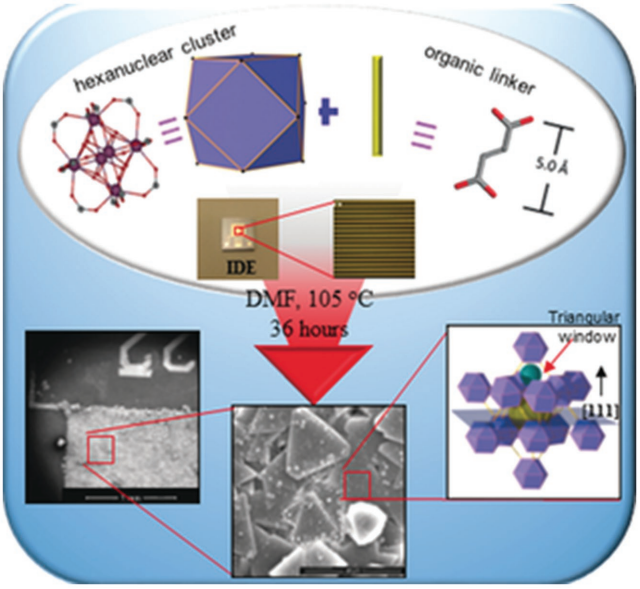

Figure 21. Schematic representation of the preparation the fumarate-based **fcu**-MOF thin film on the interdigitated electrode. Reproduced with permission.[294] Copyright 2016, Wiley-VCH.

5.4. Biological Application

Stable MOFs also have wide and promising applications in biological systems including drug delivery and enzyme immobilization. Usually nontoxic metal based MOFs such as Fe-MOFs are chosen for drug delivery systems owing to their biocompatibility and high stability in biological environment.[295] Recent development has shown that flexibility and multivariate nature of MOFs enable researchers to better control the drug release in a highly controllable and programmable manner.[296] For example, a recent report on MTV-MIL-101(Fe) indicates the controllable drug release could be achieved by well tuning interactions between drug molecules and pore environment in MTV-MOFs.[297] The high stability and tunability of MOF structures promise the future of MOFs as nanocarriers for controlled drug delivery. Enzyme immobilization in stable MOF platforms will not be discussed here since recent review has covered the topic.[298]

6. Conclusion and Prospects

With the increasing requirement for MOF stability in a variety of applications, studies on stable MOFs have been flourishing in the last few years. Constant efforts are made to disclose the structure–stability relationship, and to develop synthetic strategies for stable MOFs. First, mechanistic studies of MOF stability were introduced in this review, which allow us to predict the stability of a certain MOF based on its metal–ligand bonds and pore environments. However, the stability of a specific MOF will depend not only on the framework structure, but also on the particle size, crystal defects, operating environments, and the duration over which the MOF will face these conditions. As a result, experimental stability testing is usually required to get a fully informed decision regarding the stability of a MOF. In this respect, more systematic experimental characterization procedures are needed to obtain higher confidence in the stability of many MOFs. While PXRD measurements after the stability test can qualitatively reflect the maintenance of crystallinity, BET surface area analysis is usually more reliable to qualify the changes of porosity.

Based on the aforementioned mechanistic studies, stable MOFs were then grouped into two categories: high-valency metal–carboxylate frameworks and low-valency metal azolate frameworks. Along this line, some representative stable MOFs were introduced, their structures described, and their properties briefly discussed. Then it is shown that the increased stability of MOFs has significantly expanded their applications. Besides their role in conventional gas storage, emerging applications of stable MOFs include Lewis acid catalysis, Brønsted acid catalysis, redox catalysis, photocatalysis, electrocatalysis and fluorescent sensing. In this review, we have covered a small fraction of the great number of published MOFs, but we hope to have shown ample representation of MOFs exhibiting various applications and properties.

Regarding the discovery of new stable MOF structures, modulated synthesis has been widely used and proven successful for Zr-MOF and Fe-MOF systems. However, the modulated strategy seems less effective for the synthesis of Al/Cr/Ti-carboxylate based MOFs. In this regard, postsynthetic modification represents an important alternative to obtain otherwise unachievable MOFs. For example, some Cr-MOFs and Ti-MOFs have been synthesized by metal cation metathesis, which are difficult to realize using direct synthesis. Along with the development of synthetic strategies, new characterization techniques have also emerged to enable the discovery of new structures. Indeed, many stable MOFs are obtained as very small crystals or crystalline powders, posing challenges to structural characterization by traditional single crystal X-ray diffraction. However, in recent years, Rietveld refinements of synchrotron PXRD data has been used more frequently to characterize MOF structures. Synchrotron microdiffraction setups were used for single crystal X-ray analysis of very small single crystals. Rotation electron diffraction methods have also been applied to assist in the structural determination of MOF microcrystals.[16] The development of both new synthetic and characterization methods will continue accelerating the discovery of stable MOF structures.

Stability has been a major limitation for practical applications of MOFs since their discovery. With escalated research interest in stable MOFs, an increasing number of stable MOFs have been reported, which show good resistance to water, acid, base, and other harsh conditions. However, the stability of many so-called "stable MOFs" has yet to reach the same level of other inorganic or organic porous materials such as zeolites, mesoporous silica, and porous carbons. On the other hand, the mechanical stability of MOFs, an important consideration for the industrialization process, has not been widely studied so far.[20,61,203] Once the stability of MOFs has been addressed, stride can be taken in the industrialization of these unique materials. Although many challenges remain for practical applications of MOFs, the high designability and diversity of MOF structures suggests that such a feat is eventually feasible.

Acknowledgements

This work was supported by the Center for Gas Separations Relevant to Clean Energy Technologies, an Energy Frontier Research Center funded by the U.S. Department of Energy, Office of Science, Office of Basic Energy Sciences (DE-SC0001015), U.S. Department of Energy, Office of Fossil Energy, National Energy Technology Laboratory (DE-FE0026472), and Robert A. Welch Foundation through a Welch Endowed Chair to HJZ (A-0030). S.Y. acknowledges the Texas A&M Energy Institute Graduate Fellowship Funded by ConocoPhillips and Dow Chemical Graduate Fellowship.

Conflict of Interest

The authors declare no conflict of interest.

Keywords

heterogeneous catalysts, metal–organic frameworks, stability, structural design

Received: July 31, 2017
Revised: October 27, 2017
Published online: February 12, 2018

[1] H. Li, M. Eddaoudi, M. O'Keeffe, O. M. Yaghi, *Nature* **1999**, *402*, 276.
[2] H.-C. Zhou, J. R. Long, O. M. Yaghi, *Chem. Rev.* **2012**, *112*, 673.
[3] M. Eddaoudi, J. Kim, N. Rosi, D. Vodak, J. Wachter, M. O'Keeffe, O. M. Yaghi, *Science* **2002**, *295*, 469.
[4] G. Férey, C. Mellot-Draznieks, C. Serre, F. Millange, J. Dutour, S. Surblé, I. Margiolaki, *Science* **2005**, *309*, 2040.
[5] R. Banerjee, A. Phan, B. Wang, C. Knobler, H. Furukawa, M. O'Keeffe, O. M. Yaghi, *Science* **2008**, *319*, 939.
[6] H. Furukawa, N. Ko, Y. B. Go, N. Aratani, S. B. Choi, E. Choi, A. O. Yazaydin, R. Q. Snurr, M. O'Keeffe, J. Kim, O. M. Yaghi, *Science* **2010**, *329*, 424.
[7] W. Lu, Z. Wei, Z.-Y. Gu, T.-F. Liu, J. Park, J. Park, J. Tian, M. Zhang, Q. Zhang, T. Gentle III, M. Bosch, H.-C. Zhou, *Chem. Soc. Rev.* **2014**, *43*, 5561.
[8] N. Stock, S. Biswas, *Chem. Rev.* **2012**, *112*, 933.
[9] M. Li, D. Li, M. O'Keeffe, O. M. Yaghi, *Chem. Rev.* **2014**, *114*, 1343.
[10] L. Ma, C. Abney, W. Lin, *Chem. Soc. Rev.* **2009**, *38*, 1248.
[11] J. R. Li, R. J. Kuppler, H. C. Zhou, *Chem. Soc. Rev.* **2009**, *38*, 1477.
[12] J. Lee, O. K. Farha, J. Roberts, K. A. Scheidt, S. T. Nguyen, J. T. Hupp, *Chem. Soc. Rev.* **2009**, *38*, 1450.
[13] K. Sumida, D. L. Rogow, J. A. Mason, T. M. McDonald, E. D. Bloch, Z. R. Herm, T. H. Bae, J. R. Long, *Chem. Rev.* **2012**, *112*, 724.
[14] S. S.-Y. Chui, S. M.-F. Lo, J. P. H. Charmant, A. G. Orpen, I. D. Williams, *Science* **1999**, *283*, 1148.
[15] C. Wang, X. Liu, N. Keser Demir, J. P. Chen, K. Li, *Chem. Soc. Rev.* **2016**, *45*, 5107.
[16] T. Devic, C. Serre, *Chem. Soc. Rev.* **2014**, *43*, 6097.
[17] Y. Bai, Y. Dou, L.-H. Xie, W. Rutledge, J.-R. Li, H.-C. Zhou, *Chem. Soc. Rev.* **2016**, *45*, 2327.
[18] J. Canivet, A. Fateeva, Y. Guo, B. Coasne, D. Farrusseng, *Chem. Soc. Rev.* **2014**, *43*, 5594.
[19] N. C. Burtch, H. Jasuja, K. S. Walton, *Chem. Rev.* **2014**, *114*, 10575.
[20] A. J. Howarth, Y. Liu, P. Li, Z. Li, T. C. Wang, J. T. Hupp, O. K. Farha, *Nat. Rev. Mater.* **2016**, *1*, 15018.
[21] C. Serre, F. Millange, C. Thouvenot, M. Noguès, G. Marsolier, D. Louër, G. Férey, *J. Am. Chem. Soc.* **2002**, *124*, 13519.
[22] G. Férey, C. Serre, C. Mellot-Draznieks, F. Millange, S. Surble, J. Dutour, I. Margiolaki, *Angew. Chem., Int. Ed.* **2004**, *43*, 6296.
[23] J. H. Cavka, S. Jakobsen, U. Olsbye, N. Guillou, C. Lamberti, S. Bordiga, K. P. Lillerud, *J. Am. Chem. Soc.* **2008**, *130*, 13850.
[24] K. S. Park, Z. Ni, A. P. Côté, J. Y. Choi, R. Huang, F. J. Uribe-Romo, H. K. Chae, M. O'Keeffe, O. M. Yaghi, *Proc. Natl. Acad. Sci. USA* **2006**, *103*, 10186.
[25] A. Demessence, D. M. D'Alessandro, M. L. Foo, J. R. Long, *J. Am. Chem. Soc.* **2009**, *131*, 8784.
[26] H. J. Choi, M. Dincă, J. R. Long, *J. Am. Chem. Soc.* **2008**, *130*, 7848.
[27] C. Yang, U. Kaipa, Q. Z. Mather, X. Wang, V. Nesterov, A. F. Venero, M. A. Omary, *J. Am. Chem. Soc.* **2011**, *133*, 18094.
[28] W. J. Rieter, K. M. L. Taylor, W. Lin, *J. Am. Chem. Soc.* **2007**, *129*, 9852.
[29] S. J. Yang, C. R. Park, *Adv. Mater.* **2012**, *24*, 4010.
[30] G. Distefano, H. Suzuki, M. Tsujimoto, S. Isoda, S. Bracco, A. Comotti, P. Sozzani, T. Uemura, S. Kitagawa, *Nat. Chem.* **2013**, *5*, 335.
[31] W. Zhang, Y. Hu, J. Ge, H.-L. Jiang, S.-H. Yu, *J. Am. Chem. Soc.* **2014**, *136*, 16978.
[32] Z. Li, H. C. Zeng, *J. Am. Chem. Soc.* **2014**, *136*, 5631.
[33] C. V. McGuire, R. S. Forgan, *Chem. Commun.* **2015**, *51*, 5199.
[34] T. Kitao, Y. Zhang, S. Kitagawa, B. Wang, T. Uemura, *Chem. Soc. Rev.* **2017**, *46*, 3108.
[35] M. A. Nasalevich, R. Becker, E. V. Ramos-Fernandez, S. Castellanos, S. L. Veber, M. V. Fedin, F. Kapteijn, J. N. H. Reek, J. I. van der Vlugt, J. Gascon, *Energy Environ. Sci.* **2015**, *8*, 364.
[36] Y. H. Fu, D. R. Sun, Y. J. Chen, R. K. Huang, Z. X. Ding, X. Z. Fu, Z. H. Li, *Angew. Chem., Int. Ed.* **2012**, *51*, 3364.
[37] H. Furukawa, F. Gándara, Y.-B. Zhang, J. Jiang, W. L. Queen, M. R. Hudson, O. M. Yaghi, *J. Am. Chem. Soc.* **2014**, *136*, 4369.
[38] In *Elaboration and Applications of Metal–Organic Frameworks*, (Eds.: S. Ma, J. A. Perman), World Scientific, Singapore **2017**.
[39] J. J. Low, A. I. Benin, P. Jakubczak, J. F. Abrahamian, S. A. Faheem, R. R. Willis, *J. Am. Chem. Soc.* **2009**, *131*, 15834.
[40] D. Feng, Z.-Y. Gu, J.-R. Li, H.-L. Jiang, Z. Wei, H.-C. Zhou, *Angew. Chem., Int. Ed.* **2012**, *51*, 10307.
[41] D. Feng, W.-C. Chung, Z. Wei, Z.-Y. Gu, H.-L. Jiang, Y.-P. Chen, D. J. Darensbourg, H.-C. Zhou, *J. Am. Chem. Soc.* **2013**, *135*, 17105.
[42] H.-L. Jiang, D. Feng, K. Wang, Z.-Y. Gu, Z. Wei, Y.-P. Chen, H.-C. Zhou, *J. Am. Chem. Soc.* **2013**, *135*, 13934.
[43] K. Wang, D. Feng, T.-F. Liu, J. Su, S. Yuan, Y.-P. Chen, M. Bosch, X. Zou, H.-C. Zhou, *J. Am. Chem. Soc.* **2014**, *136*, 13983.

[44] K. Wang, X.-L. Lv, D. Feng, J. Li, S. Chen, J. Sun, L. Song, Y. Xie, J.-R. Li, H.-C. Zhou, *J. Am. Chem. Soc.* **2016**, *138*, 914.
[45] X.-L. Lv, K. Wang, B. Wang, J. Su, X. Zou, Y. Xie, J.-R. Li, H.-C. Zhou, *J. Am. Chem. Soc.* **2017**, *139*, 211.
[46] P. Horcajada, S. Surble, C. Serre, D.-Y. Hong, Y.-K. Seo, J.-S. Chang, J.-M. Greneche, I. Margiolaki, G. Férey, *Chem. Commun.* **2007**, 2820.
[47] S. Surble, C. Serre, C. Mellot-Draznieks, F. Millange, G. Férey, *Chem. Commun.* **2006**, 284.
[48] L. Valenzano, B. Civalleri, S. Chavan, S. Bordiga, M. H. Nilsen, S. Jakobsen, K. P. Lillerud, C. Lamberti, *Chem. Mater.* **2011**, *23*, 1700.
[49] S. Øien-Ødegaard, B. Bouchevreau, K. Hylland, L. Wu, R. Blom, C. Grande, U. Olsbye, M. Tilset, K. P. Lillerud, *Inorg. Chem.* **2016**, *55*, 1986.
[50] X. Huang, J. Zhang, X. Chen, *Chin. Sci. Bull.* **2003**, *48*, 1531.
[51] T. M. McDonald, D. M. D'Alessandro, R. Krishna, J. R. Long, *Chem. Sci.* **2011**, *2*, 2022.
[52] V. Colombo, S. Galli, H. J. Choi, G. D. Han, A. Maspero, G. Palmisano, N. Masciocchi, J. R. Long, *Chem. Sci.* **2011**, *2*, 1311.
[53] P.-Q. Liao, X.-Y. Li, J. Bai, C.-T. He, D.-D. Zhou, W.-X. Zhang, J.-P. Zhang, X.-M. Chen, *Chem. Eur. J.* **2014**, *20*, 11303.
[54] W. Morris, B. Volosskiy, S. Demir, F. Gándara, P. L. McGrier, H. Furukawa, D. Cascio, J. F. Stoddart, O. M. Yaghi, *Inorg. Chem.* **2012**, *51*, 6443.
[55] G. Mouchaham, L. Cooper, N. Guillou, C. Martineau, E. Elkaïm, S. Bourrelly, P. L. Llewellyn, C. Allain, G. Clavier, C. Serre, T. Devic, *Angew. Chem., Int. Ed.* **2015**, *54*, 13297.
[56] D. R. Lide, *CRC Handbook of Chemistry and Physics*, CRC Press **2001**.
[57] J. Speight, *Lang's Handbook of Chemistry*, McGraw-Hill, New York **2005**.
[58] O. K. Farha, J. T. Hupp, *Acc. Chem. Res.* **2010**, *43*, 1166.
[59] K. W. Chapman, G. J. Halder, P. J. Chupas, *J. Am. Chem. Soc.* **2009**, *131*, 17546.
[60] T.-F. Liu, D. Feng, Y.-P. Chen, L. Zou, M. Bosch, S. Yuan, Z. Wei, S. Fordham, K. Wang, H.-C. Zhou, *J. Am. Chem. Soc.* **2015**, *137*, 413.
[61] J. B. DeCoste, G. W. Peterson, H. Jasuja, T. G. Glover, Y.-g. Huang, K. S. Walton, *J. Mater. Chem. A* **2013**, *1*, 5642.
[62] N. M. Padial, E. Quartapelle Procopio, C. Montoro, E. López, J. E. Oltra, V. Colombo, A. Maspero, N. Masciocchi, S. Galli, I. Senkovska, S. Kaskel, E. Barea, J. A. R. Navarro, *Angew. Chem., Int. Ed.* **2013**, *52*, 8290.
[63] B. Wang, X.-L. Lv, D. Feng, L.-H. Xie, J. Zhang, M. Li, Y. Xie, J.-R. Li, H.-C. Zhou, *J. Am. Chem. Soc* **2016**, *138*, 6204.
[64] D. Sun, Y. Ke, D. J. Collins, G. A. Lorigan, H.-C. Zhou, *Inorg. Chem.* **2007**, *46*, 2725.
[65] A. Schaate, P. Roy, A. Godt, J. Lippke, F. Waltz, M. Wiebcke, P. Behrens, *Chem. Eur. J.* **2011**, *17*, 6643.
[66] L. Rozes, C. Sanchez, *Chem. Soc. Rev.* **2011**, *40*, 1006.
[67] H. Assi, G. Mouchaham, N. Steunou, T. Devic, C. Serre, *Chem. Soc. Rev.* **2017**, *46*, 3431.
[68] V. Guillerm, S. Gross, C. Serre, T. Devic, M. Bauer, G. Férey, *Chem. Commun.* **2010**, *46*, 767.
[69] D. Feng, K. Wang, Z. Wei, Y.-P. Chen, C. M. Simon, R. K. Arvapally, R. L. Martin, M. Bosch, T.-F. Liu, S. Fordham, D. Yuan, M. A. Omary, M. Haranczyk, B. Smit, H.-C. Zhou, *Nat. Commun.* **2014**, *5*, 5723.
[70] S. M. Cohen, *Chem. Rev.* **2012**, *112*, 970.
[71] S. Couck, J. F. M. Denayer, G. V. Baron, T. Rémy, J. Gascon, F. Kapteijn, *J. Am. Chem. Soc.* **2009**, *131*, 6326.
[72] S. Bauer, C. Serre, T. Devic, P. Horcajada, J. Marrot, G. Férey, N. Stock, *Inorg. Chem.* **2008**, *47*, 7568.
[73] P. Serra-Crespo, E. V. Ramos-Fernandez, J. Gascon, F. Kapteijn, *Chem. Mater.* **2011**, *23*, 2565.
[74] T. Ahnfeldt, N. Guillou, D. Gunzelmann, I. Margiolaki, T. Loiseau, G. Férey, J. Senker, N. Stock, *Angew. Chem., Int. Ed.* **2009**, *121*, 5265.
[75] S. J. Garibay, S. M. Cohen, *Chem. Commun.* **2010**, *46*, 7700.
[76] T. Ahnfeldt, D. Gunzelmann, T. Loiseau, D. Hirsemann, J. Senker, G. Férey, N. Stock, *Inorg. Chem.* **2009**, *48*, 3057.
[77] C. Volkringer, S. M. Cohen, *Angew. Chem., Int. Ed.* **2010**, *49*, 4644.
[78] E. D. Bloch, D. Britt, C. Lee, C. J. Doonan, F. J. Uribe-Romo, H. Furukawa, J. R. Long, O. M. Yaghi, *J. Am. Chem. Soc.* **2010**, *132*, 14382.
[79] T. Zhang, K. Manna, W. Lin, *J. Am. Chem. Soc.* **2016**, *138*, 3241.
[80] M. I. Gonzalez, E. D. Bloch, J. A. Mason, S. J. Teat, J. R. Long, *Inorg. Chem.* **2015**, *54*, 2995.
[81] J. E. Mondloch, W. Bury, D. Fairen-Jimenez, S. Kwon, E. J. DeMarco, M. H. Weston, A. A. Sarjeant, S. T. Nguyen, P. C. Stair, R. Q. Snurr, O. K. Farha, J. T. Hupp, *J. Am. Chem. Soc.* **2013**, *135*, 10294.
[82] L. C. Gallington, I. S. Kim, W.-G. Liu, A. A. Yakovenko, A. E. Platero-Prats, Z. Li, T. C. Wang, J. T. Hupp, O. K. Farha, D. G. Truhlar, A. B. F. Martinson, K. W. Chapman, *J. Am. Chem. Soc.* **2016**, *138*, 13513.
[83] T. C. Wang, N. A. Vermeulen, I. S. Kim, A. B. F. Martinson, J. F. Stoddart, J. T. Hupp, O. K. Farha, *Nat. Protocols* **2016**, *11*, 149.
[84] Y. Hu, W. M. Verdegaal, S.-H. Yu, H.-L. Jiang, *ChemSusChem* **2014**, *7*, 734.
[85] M. Banerjee, S. Das, M. Yoon, H. J. Choi, M. H. Hyun, S. M. Park, G. Seo, K. Kim, *J. Am. Chem. Soc.* **2009**, *131*, 7524.
[86] P. Deria, J. E. Mondloch, E. Tylianakis, P. Ghosh, W. Bury, R. Q. Snurr, J. T. Hupp, O. K. Farha, *J. Am. Chem. Soc.* **2013**, *135*, 16801.
[87] P. Deria, W. Bury, J. T. Hupp, O. K. Farha, *Chem. Commun.* **2014**, *50*, 1965.
[88] S. Yuan, Y.-P. Chen, J.-S. Qin, W. Lu, L. Zou, Q. Zhang, X. Wang, X. Sun, H.-C. Zhou, *J. Am. Chem. Soc.* **2016**, *138*, 8912.
[89] S. Yuan, W. Lu, Y.-P. Chen, Q. Zhang, T.-F. Liu, D. Feng, X. Wang, J. Qin, H.-C. Zhou, *J. Am. Chem. Soc.* **2015**, *137*, 3177.
[90] M. Kim, J. F. Cahill, H. Fei, K. A. Prather, S. M. Cohen, *J. Am. Chem. Soc.* **2012**, *134*, 18082.
[91] S. Pullen, H. H. Fei, A. Orthaber, S. M. Cohen, S. Ott, *J. Am. Chem. Soc.* **2013**, *135*, 16997.
[92] T. F. Liu, L. F. Zou, D. W. Feng, Y. P. Chen, S. Fordham, X. Wang, Y. Y. Liu, H. C. Zhou, *J. Am. Chem. Soc.* **2014**, *136*, 7813.
[93] M. Dan-Hardi, C. Serre, T. Frot, L. Rozes, G. Maurin, C. Sanchez, G. Férey, *J. Am. Chem. Soc.* **2009**, *131*, 10857.
[94] S. Yuan, T. F. Liu, D. W. Feng, J. Tian, K. C. Wang, J. S. Qin, Q. Zhang, Y. P. Chen, M. Bosch, L. F. Zou, S. J. Teat, S. J. Dalgarno, H. C. Zhou, *Chem. Sci.* **2015**, *6*, 3926.
[95] B. Bueken, F. Vermoortele, D. E. P. Vanpoucke, H. Reinsch, C.-C. Tsou, P. Valvekens, T. De Baerdemaeker, R. Ameloot, C. E. A. Kirschhock, V. Van Speybroeck, J. M. Mayer, D. De Vos, *Angew. Chem., Int. Ed.* **2015**, *127*, 14118.
[96] H. L. Nguyen, F. Gándara, H. Furukawa, T. L. H. Doan, K. E. Cordova, O. M. Yaghi, *J. Am. Chem. Soc.* **2016**, *138*, 4330.
[97] H. L. Nguyen, T. T. Vu, D. Le, T. L. H. Doan, V. Q. Nguyen, N. T. S. Phan, *ACS Catal.* **2017**, *7*, 338.
[98] C. H. Hendon, D. Tiana, M. Fontecave, C. Sanchez, L. D'Arras, C. Sassoye, L. Rozes, C. Mellot-Draznieks, A. Walsh, *J. Am. Chem. Soc.* **2013**, *135*, 10942.
[99] Y. Horiuchi, T. Toyao, M. Saito, K. Mochizuki, M. Iwata, H. Higashimura, M. Anpo, M. Matsuoka, *J. Phys. Chem. C* **2012**, *116*, 20848.

[100] J. Gao, J. Miao, P.-Z. Li, W. Y. Teng, L. Yang, Y. Zhao, B. Liu, Q. Zhang, *Chem. Commun.* **2014**, *50*, 3786.
[101] H. Assi, L. C. Pardo Pérez, G. Mouchaham, F. Ragon, M. Nasalevich, N. Guillou, C. Martineau, H. Chevreau, F. Kapteijn, J. Gascon, P. Fertey, E. Elkaim, C. Serre, T. Devic, *Inorg. Chem.* **2016**, *55*, 7192.
[102] J. A. Mason, L. E. Darago, W. W. Lukens, J. R. Long, *Inorg. Chem.* **2015**, *54*, 10096.
[103] D. Feng, Z.-Y. Gu, Y.-P. Chen, J. Park, Z. Wei, Y. Sun, M. Bosch, S. Yuan, H.-C. Zhou, *J. Am. Chem. Soc.* **2014**, *136*, 17714.
[104] M. Zhang, Y.-P. Chen, M. Bosch, T. Gentle, K. Wang, D. Feng, Z. U. Wang, H.-C. Zhou, *Angew. Chem., Int. Ed.* **2014**, *53*, 815.
[105] R. Wang, Z. Wang, Y. Xu, F. Dai, L. Zhang, D. Sun, *Inorg. Chem.* **2014**, *53*, 7086.
[106] D. Feng, K. Wang, J. Su, T.-F. Liu, J. Park, Z. Wei, M. Bosch, A. Yakovenko, X. Zou, H.-C. Zhou, *Angew. Chem., Int. Ed.* **2015**, *54*, 149.
[107] V. Bon, I. Senkovska, M. S. Weiss, S. Kaskel, *CrystEngComm* **2013**, *15*, 9572.
[108] V. Guillerm, F. Ragon, M. Dan-Hardi, T. Devic, M. Vishnuvarthan, B. Campo, A. Vimont, G. Clet, Q. Yang, G. Maurin, G. Férey, A. Vittadini, S. Gross, C. Serre, *Angew. Chem., Int. Ed.* **2012**, *51*, 9267.
[109] M. J. Cliffe, E. Castillo-Martínez, Y. Wu, J. Lee, A. C. Forse, F. C. N. Firth, P. Z. Moghadam, D. Fairen-Jimenez, M. W. Gaultois, J. A. Hill, O. V. Magdysyuk, B. Slater, A. L. Goodwin, C. P. Grey, *J. Am. Chem. Soc.* **2017**, *139*, 5397.
[110] P. Ji, K. Manna, Z. Lin, X. Feng, A. Urban, Y. Song, W. Lin, *J. Am. Chem. Soc.* **2017**, *139*, 7004.
[111] L. Cao, Z. Lin, W. Shi, Z. Wang, C. Zhang, X. Hu, C. Wang, W. Lin, *J. Am. Chem. Soc.* **2017**, *139*, 7020.
[112] S. Yuan, J.-S. Qin, L. Zou, Y.-P. Chen, X. Wang, Q. Zhang, H.-C. Zhou, *J. Am. Chem. Soc.* **2016**, *138*, 6636.
[113] Y. H. Xiong, S. H. Chen, F. G. Ye, L. J. Su, C. Zhang, S. F. Shen, S. L. Zhao, *Chem. Commun.* **2015**, *51*, 4635.
[114] M. Lammert, H. Reinsch, C. A. Murray, M. T. Wharmby, H. Terraschke, N. Stock, *Dalton Trans.* **2016**, *45*, 18822.
[115] M. Lammert, M. T. Wharmby, S. Smolders, B. Bueken, A. Lieb, K. A. Lomachenko, D. De Vos, N. Stock, *Chem. Commun.* **2015**, *51*, 12578.
[116] R. Dalapati, B. Sakthivel, A. Dhakshinamoorthy, A. Buragohain, A. Bhunia, C. Janiak, S. Biswas, *CrystEngComm* **2016**, *18*, 7855.
[117] T. Loiseau, C. Serre, C. Huguenard, G. Fink, F. Taulelle, M. Henry, T. Bataille, G. Férey, *Chem. Eur. J.* **2004**, *10*, 1373.
[118] I. Senkovska, F. Hoffmann, M. Froba, J. Getzschmann, W. Bohlmann, S. Kaskel, *Microporous Mesoporous Mater.* **2009**, *122*, 93.
[119] Q. Yang, S. Vaesen, M. Vishnuvarthan, F. Ragon, C. Serre, A. Vimont, M. Daturi, G. De Weireld, G. Maurin, *J. Mater. Chem.* **2012**, *22*, 10210.
[120] S. H. Lo, C. H. Chien, Y. L. Lai, C. C. Yang, J. J. Lee, D. S. Raja, C. H. Lin, *J. Mater. Chem. A* **2013**, *1*, 324.
[121] Z. W. Wang, M. Chen, C. S. Liu, X. Wang, H. Zhao, M. Du, *Chem. Eur. J.* **2015**, *21*, 17215.
[122] C. Volkringer, T. Loiseau, N. Guillou, G. Férey, M. Haouas, F. Taulelle, E. Elkaim, N. Stock, *Inorg. Chem.* **2010**, *49*, 9852.
[123] C. Volkringer, T. Loiseau, N. Guillou, G. Férey, M. Haouas, F. Taulelle, N. Audebrand, I. Margiolaki, D. Popov, M. Burghammer, C. Riekel, *Cryst. Growth Des.* **2009**, *9*, 2927.
[124] C. Volkringer, T. Loiseau, M. Haouas, F. Taulelle, D. Popov, M. Burghammer, C. Riekel, C. Zlotea, F. Cuevas, M. Latroche, D. Phanon, C. Knofelv, P. L. Llewellyn, G. Férey, *Chem. Mater.* **2009**, *21*, 5783.
[125] S. H. Yang, J. L. Sun, A. J. Ramirez-Cuesta, S. K. Callear, W. I. F. David, D. P. Anderson, R. Newby, A. J. Blake, J. E. Parker, C. C. Tang, M. Schroder, *Nat. Chem.* **2012**, *4*, 887.
[126] A. Fateeva, P. A. Chater, C. P. Ireland, A. A. Tahir, Y. Z. Khimyak, P. V. Wiper, J. R. Darwent, M. J. Rosseinsky, *Angew. Chem., Int. Ed.* **2012**, *51*, 7440.
[127] T. Loiseau, L. Lecroq, C. Volkringer, J. Marrot, G. Férey, M. Haouas, F. Taulelle, S. Bourrelly, P. L. Llewellyn, M. Latroche, *J. Am. Chem. Soc.* **2006**, *128*, 10223.
[128] C. Volkringer, D. Popov, T. Loiseau, G. Férey, M. Burghammer, C. Riekel, M. Haouas, F. Taulclle, *Chem. Mater.* **2009**, *21*, 5695.
[129] D. W. Feng, T. F. Liu, J. Su, M. Bosch, Z. W. Wei, W. Wan, D. Q. Yuan, Y. P. Chen, X. Wang, K. C. Wang, X. Z. Lian, Z. Y. Gu, J. Park, X. D. Zou, H. C. Zhou, *Nat. Commun.* **2015**, *6*, 5979.
[130] X. Z. Lian, Y. P. Chen, T. F. Liu, H. C. Zhou, *Chem. Sci.* **2016**, *7*, 6969.
[131] D. Lupu, O. Ardelean, G. Blanita, G. Borodi, M. D. Lazar, A. R. Biris, C. Ioan, M. Mihet, I. Misan, G. Popeneciu, *Int. J. Hydrogen Energy* **2011**, *36*, 3586.
[132] D. Alezi, Y. Belmabkhout, M. Suyetin, P. M. Bhatt, L. J. Weselinski, V. Solovyeva, K. Adil, I. Spanopoulos, P. N. Trikalitis, A. H. Emwas, M. Eddaoudi, *J. Am. Chem. Soc.* **2015**, *137*, 13308.
[133] T. Ahnfeldt, N. Guillou, D. Gunzelmann, I. Margiolaki, T. Loiseau, G. Férey, J. Senker, N. Stock, *Angew. Chem., Int. Ed.* **2009**, *48*, 5163.
[134] H. Reinsch, M. Feyand, T. Ahnfeldt, N. Stock, *Dalton Trans.* **2012**, *41*, 4164.
[135] T. R. Whitfield, X. Q. Wang, L. M. Liu, A. J. Jacobson, *Solid State Sci* **2005**, *7*, 1096.
[136] A. Fateeva, P. Horcajada, T. Devic, C. Serre, J. Marrot, J. M. Greneche, M. Morcrette, J. M. Tarascon, G. Maurin, G. Férey, *Eur. J. Inorg. Chem.* **2010**, *2010*, 3789.
[137] A. Fateeva, J. Clarisse, G. Pilet, J. M. Greneche, F. Nouar, B. K. Abeykoon, F. Guegan, C. Goutaudier, D. Luneau, J. E. Warren, M. J. Rosseinsky, T. Devic, *Cryst. Growth Des.* **2015**, *15*, 1819.
[138] C. Serre, C. Mellot-Draznieks, S. Surble, N. Audebrand, Y. Filinchuk, G. Férey, *Science* **2007**, *315*, 1828.
[139] P. Horcajada, H. Chevreau, D. Heurtaux, F. Benyettou, F. Salles, T. Devic, A. Garcia-Marquez, C. H. Yu, H. Lavrard, C. L. Dutson, E. Magnier, G. Maurin, E. Elkaim, C. Serre, *Chem. Commun.* **2014**, *50*, 6872.
[140] Y. L. Liu, J. F. Eubank, A. J. Cairns, J. Eckert, V. C. Kravtsov, R. Luebke, M. Eddaoudi, *Angew. Chem., Int. Ed.* **2007**, *46*, 3278.
[141] X. Z. Lian, D. W. Feng, Y. P. Chen, T. F. Liu, X. Wang, H. C. Zhou, *Chem. Sci.* **2015**, *6*, 7044.
[142] T. M. Reineke, M. Eddaoudi, M. Fehr, D. Kelley, O. M. Yaghi, *J. Am. Chem. Soc.* **1999**, *121*, 1651.
[143] C. Serre, C. Férey, *J. Mater. Chem.* **2002**, *12*, 3053.
[144] F. Millange, C. Serre, J. Marrot, N. Gardant, F. Pelle, G. Férey, *J. Mater. Chem.* **2004**, *14*, 642.
[145] T. Devic, C. Serre, N. Audebrand, J. Marrot, G. Férey, *J. Am. Chem. Soc.* **2005**, *127*, 12788.
[146] H. L. Jiang, N. Tsumori, Q. Xu, *Inorg. Chem.* **2010**, *49*, 10001.
[147] D. X. Xue, A. J. Cairns, Y. Belmabkhout, L. Wojtas, Y. Liu, M. H. Alkordi, M. Eddaoudi, *J. Am. Chem. Soc.* **2013**, *135*, 7660.
[148] D. Alezi, A. M. P. Peedikakkal, L. J. Weselinski, V. Guillerm, Y. Belmabkhout, A. J. Cairns, Z. J. Chen, L. Wojtas, M. Eddaoudi, *J. Am. Chem. Soc.* **2015**, *137*, 5421.
[149] D. X. Xue, Y. Belmabkhout, O. Shekhah, H. Jiang, K. Adil, A. J. Cairns, M. Eddaoudi, *J. Am. Chem. Soc.* **2015**, *137*, 5034.
[150] V. Guillerm, L. J. Weselinski, Y. Belmabkhout, A. J. Cairns, V. D'Elia, L. Wojtas, K. Adil, M. Eddaoudi, *Nat. Chem.* **2014**, *6*, 673.
[151] A. H. Assen, Y. Belmabkhout, K. Adil, P. M. Bhatt, D. X. Xue, H. Jiang, M. Eddaoudi, *Angew. Chem. Int. Ed.* **2015**, *54*, 14353.

[152] A. Lieb, H. Leclerc, T. Devic, C. Serre, I. Margiolaki, F. Mahjoubi, J. S. Lee, A. Vimont, M. Daturi, J. S. Chang, *Microporous Mesoporous Mater.* **2012**, *157*, 18.
[153] I. J. Kang, N. A. Khan, E. Haque, S. H. Jhung, *Chem. Eur. J.* **2011**, *17*, 6437.
[154] J. P. Zhang, Y. B. Zhang, J. B. Lin, X. M. Chen, *Chem. Rev.* **2012**, *112*, 1001.
[155] Y. Pan, Y. Liu, G. Zeng, L. Zhao, Z. Lai, *Chem. Commun.* **2011**, *47*, 2071.
[156] H. Wu, X. Qian, H. Zhu, S. Ma, G. Zhu, Y. Long, *RSC Adv.* **2016**, *6*, 6915.
[157] X. C. Huang, Y. Y. Lin, J. P. Zhang, X. M. Chen, *Angew. Chem., Int. Ed. Engl.* **2006**, *45*, 1557.
[158] C. Montoro, F. Linares, E. Q. Procopio, I. Senkovska, S. Kaskel, S. Galli, N. Masciocchi, E. Barea, J. A. Navarro, *J. Am. Chem. Soc.* **2011**, *133*, 11888.
[159] C. Heering, I. Boldog, V. Vasylyeva, J. Sanchiz, C. Janiak, *CrystEngComm* **2013**, *15*, 9757.
[160] M. Tonigold, Y. Lu, B. Bredenkotter, B. Rieger, S. Bahnmuller, J. Hitzbleck, G. Langstein, D. Volkmer, *Angew. Chem., Int. Ed. Engl.* **2009**, *48*, 7546.
[161] N. Masciocchi, S. Galli, V. Colombo, A. Maspero, G. Palmisano, B. Seyyedi, C. Lamberti, S. Bordiga, *J. Am. Chem. Soc.* **2010**, *132*, 7902.
[162] K. Wang, X. L. Lv, D. Feng, J. Li, S. Chen, J. Sun, L. Song, Y. Xie, J. R. Li, H. C. Zhou, *J. Am. Chem. Soc.* **2016**, *138*, 914.
[163] H. J. Choi, M. Dincă, J. R. Long, *J. Am. Chem. Soc.* **2008**, *130*, 7848.
[164] J. A. Mason, J. Oktawiec, M. K. Taylor, M. R. Hudson, J. Rodriguez, J. E. Bachman, M. I. Gonzalez, A. Cervellino, A. Guagliardi, C. M. Brown, P. L. Llewellyn, N. Masciocchi, J. R. Long, *Nature* **2015**, *527*, 357.
[165] V. Colombo, C. Montoro, A. Maspero, G. Palmisano, N. Masciocchi, S. Galli, E. Barea, J. A. Navarro, *J. Am. Chem. Soc.* **2012**, *134*, 12830.
[166] S. Rojas, F. J. Carmona, C. R. Maldonado, P. Horcajada, T. Hidalgo, C. Serre, J. A. Navarro, E. Barea, *Inorg. Chem.* **2016**, *55*, 2650.
[167] N. Mosca, R. Vismara, J. A. Fernandes, S. Casassa, K. V. Domasevitch, E. Bailón-García, F. J. Maldonado-Hódar, C. Pettinari, S. Galli, *Cryst. Growth Des.* **2017**, *17*, 3854.
[168] M. Dincă, A. Dailly, Y. Liu, C. M. Brown, D. A. Neumann, J. R. Long, *J. Am. Chem. Soc.* **2006**, *128*, 16876.
[169] X. F. Lu, P. Q. Liao, J. W. Wang, J. X. Wu, X. W. Chen, C. T. He, J. P. Zhang, G. R. Li, X. M. Chen, *J. Am. Chem. Soc.* **2016**, *138*, 8336.
[170] M. Grzywa, C. Gessner, D. Denysenko, B. Bredenkotter, F. Gschwind, K. M. Fromm, W. Nitek, E. Klemm, D. Volkmer, *Dalton Trans.* **2013**, *42*, 6909.
[171] Z. Li, Z. Zhang, Y. Ye, K. Cai, F. Du, H. Zeng, J. Tao, Q. Lin, Y. Zheng, S. Xiang, *J. Mater. Chem. A* **2017**, *5*, 7816.
[172] F. Nouar, J. F. Eubank, T. Bousquet, L. Wojtas, M. J. Zaworotko, M. Eddaoudi, *J. Am. Chem. Soc.* **2008**, *130*, 1833.
[173] J. F. Eubank, F. Nouar, R. Luebke, A. J. Cairns, L. Wojtas, M. Alkordi, T. Bousquet, M. R. Hight, J. Eckert, J. P. Embs, P. A. Georgiev, M. Eddaoudi, *Angew. Chem., Int. Ed.* **2012**, *51*, 10099.
[174] V. Guillerm, D. Kim, J. F. Eubank, R. Luebke, X. Liu, K. Adil, M. S. Lah, M. Eddaoudi, *Chem. Soc. Rev.* **2014**, *43*, 6141.
[175] B. Tu, Q. Pang, E. Ning, W. Yan, Y. Qi, D. Wu, Q. Li, *J. Am. Chem. Soc.* **2015**, *137*, 13456.
[176] B. Tu, Q. Pang, H. Xu, X. Li, Y. Wang, Z. Ma, L. Weng, Q. Li, *J. Am. Chem. Soc.* **2017**, *139*, 7998.
[177] S. D. Burd, S. Ma, J. A. Perman, B. J. Sikora, R. Q. Snurr, P. K. Thallapally, J. Tian, L. Wojtas, M. J. Zaworotko, *J. Am. Chem. Soc.* **2012**, *134*, 3663.
[178] P. Nugent, Y. Belmabkhout, S. D. Burd, A. J. Cairns, R. Luebke, K. Forrest, T. Pham, S. Ma, B. Space, L. Wojtas, M. Eddaoudi, M. J. Zaworotko, *Nature* **2013**, *495*, 80.
[179] O. Shekhah, Y. Belmabkhout, Z. Chen, V. Guillerm, A. Cairns, K. Adil, M. Eddaoudi, *Nat. Commun.* **2014**, *5*, 4228.
[180] A. Cadiau, Y. Belmabkhout, K. Adil, P. M. Bhatt, R. S. Pillai, A. Shkurenko, C. Martineau-Corcos, G. Maurin, M. Eddaoudi, *Science* **2017**, *356*, 731.
[181] A. Cadiau, K. Adil, P. M. Bhatt, Y. Belmabkhout, M. Eddaoudi, *Science* **2016**, *353*, 137.
[182] E. Alvarez, N. Guillou, C. Martineau, B. Bueken, B. Van de Voorde, C. Le Guillouzer, P. Fabry, F. Nouar, F. Taulelle, D. de Vos, J. S. Chang, K. H. Cho, N. Ramsahye, T. Devic, M. Daturi, G. Maurin, C. Serre, *Angew. Chem., Int. Ed.* **2015**, *54*, 3664.
[183] M. Gaab, N. Trukhan, S. Maurer, R. Gummaraju, U. Muller, *Microporous Mesoporous Mater.* **2012**, *157*, 131.
[184] T. Loiseau, C. Mellot-Draznieks, H. Muguerra, G. Férey, M. Haouas, F. Taulelle, *C. R. Chim.* **2005**, *8*, 765.
[185] C. Volkringer, D. Popov, T. Loiseau, N. Guillou, G. Férey, M. Haouas, F. Taulelle, C. Mellot-Draznieks, M. Burghammer, C. Riekel, *Nat. Mater.* **2007**, *6*, 760.
[186] C. Volkringer, T. Loiseau, N. Guillou, G. Férey, E. Elkaim, *Solid State Sci* **2009**, *11*, 1507.
[187] H. Reinsch, M. Kruger, J. Wack, J. Senker, F. Salles, G. Maurin, N. Stock, *Microporous Mesoporous Mater.* **2012**, *157*, 50.
[188] H. Reinsch, M. Kruger, J. Marrot, N. Stock, *Inorg. Chem.* **2013**, *52*, 1854.
[189] H. Reinsch, M. A. van der Veen, B. Gil, B. Marszalek, T. Verbiest, D. de Vos, N. Stock, *Chem. Mater.* **2013**, *25*, 17.
[190] P. P. Long, H. W. Wu, Q. Zhao, Y. X. Wang, J. X. Dong, J. P. Li, *Microporous Mesoporous Mater.* **2011**, *142*, 489.
[191] A. Sonnauer, F. Hoffmann, M. Froba, L. Kienle, V. Duppel, M. Thommes, C. Serre, G. Férey, N. Stock, *Angew. Chem., Int. Ed.* **2009**, *48*, 3791.
[192] D. W. Feng, K. C. Wang, Z. W. Wei, Y. P. Chen, C. M. Simon, R. K. Arvapally, R. L. Martin, M. Bosch, T. F. Liu, S. Fordham, D. Q. Yuan, M. A. Omary, M. Haranczyk, B. Smit, H. C. Zhou, *Nat. Commun.* **2014**, *5*, 5723.
[193] Z. Wei, Z.-Y. Gu, R. K. Arvapally, Y.-P. Chen, R. N. McDougald, J. F. Ivy, A. A. Yakovenko, D. Feng, M. A. Omary, H.-C. Zhou, *J. Am. Chem. Soc.* **2014**, *136*, 8269.
[194] H. L. Jiang, D. Feng, K. Wang, Z. Y. Gu, Z. Wei, Y. P. Chen, H. C. Zhou, *J. Am. Chem. Soc.* **2013**, *135*, 13934.
[195] V. Bon, V. Senkovskyy, I. Senkovska, S. Kaskel, *Chem. Commun.* **2012**, *48*, 8407.
[196] V. Bon, I. Senkovska, I. A. Baburin, S. Kaskel, *Cryst. Growth Des.* **2013**, *13*, 1231.
[197] O. V. Gutov, W. Bury, D. A. Gomez-Gualdron, V. Krungleviciute, D. Fairen-Jimenez, J. E. Mondloch, A. A. Sarjeant, S. S. Al-Juaid, R. Q. Snurr, J. T. Hupp, T. Yildirim, O. K. Farha, *Chem. Eur. J.* **2014**, *20*, 12389.
[198] T. C. Wang, W. Bury, D. A. Gómez-Gualdrón, N. A. Vermeulen, J. E. Mondloch, P. Deria, K. Zhang, P. Z. Moghadam, A. A. Sarjeant, R. Q. Snurr, J. F. Stoddart, J. T. Hupp, O. K. Farha, *J. Am. Chem. Soc.* **2015**, *137*, 3585.
[199] A. Schaate, S. Dühnen, G. Platz, S. Lilienthal, A. M. Schneider, P. Behrens, *Eur. J. Inorg. Chem.* **2012**, *2012*, 790.
[200] X.-L. Lv, M. Tong, H. Huang, B. Wang, L. Gan, Q. Yang, C. Zhong, J.-R. Li, *J. Solid State Chem.* **2015**, *223*, 104.
[201] A. Schaate, P. Roy, T. Preuße, S. J. Lohmeier, A. Godt, P. Behrens, *Chem. Eur. J.* **2011**, *17*, 9320.

[202] M. Yoon, D. Moon, *Microporous Mesoporous Mater.* **2015**, *215*, 116.
[203] S. B. Kalidindi, S. Nayak, M. E. Briggs, S. Jansat, A. P. Katsoulidis, G. J. Miller, J. E. Warren, D. Antypov, F. Corà, B. Slater, M. R. Prestly, C. Martí-Gastaldo, M. J. Rosseinsky, *Angew. Chem. Int. Ed.* **2015**, *54*, 221.
[204] A. Tăbăcaru, S. Galli, C. Pettinari, N. Masciocchi, T. M. McDonald, J. R. Long, *CrystEngComm* **2015**, *17*, 4992.
[205] H. J. Choi, M. Dincă, A. Dailly, J. R. Long, *Energy Environ. Sci.* **2010**, *3*, 117.
[206] W. Morris, C. J. Doonan, H. Furukawa, R. Banerjee, O. M. Yaghi, *J. Am. Chem. Soc.* **2008**, *130*, 12626.
[207] A. Henschel, K. Gedrich, R. Kraehnert, S. Kaskel, *Chem. Commun.* **2008**, 4192.
[208] A. Dhakshinamoorthy, M. Alvaro, H. Chevreau, P. Horcajada, T. Devic, C. Serre, H. Garcia, *Catal. Sci. Technol.* **2012**, *2*, 324.
[209] O. V. Zalomaeva, A. M. Chibiryaev, K. A. Kovalenko, O. A. Kholdeeva, B. S. Balzhinimaev, V. P. Fedin, *J. Catal.* **2013**, *298*, 179.
[210] A. Dhakshinamoorthy, M. Alvaro, H. Garcia, *Chem. Eur. J.* **2010**, *16*, 8530.
[211] A. Dhakshinamoorthy, M. Alvaro, H. Garcia, *Adv. Synth. Catal.* **2010**, *352*, 711.
[212] F. Vermoortele, B. Bueken, G. Le Bars, B. Van de Voorde, M. Vandichel, K. Houthoofd, A. Vimont, M. Daturi, M. Waroquier, V. Van Speybroeck, C. Kirschhock, D. E. De Vos, *J. Am. Chem. Soc.* **2013**, *135*, 11465.
[213] F. Vermoortele, R. Ameloot, A. Vimont, C. Serre, D. De Vos, *Chem. Commun.* **2011**, *47*, 1521.
[214] F. Vermoortele, M. Vandichel, B. Van de Voorde, R. Ameloot, M. Waroquier, V. Van Speybroeck, D. E. De Vos, *Angew. Chem., Int. Ed.* **2012**, *51*, 4887.
[215] M. J. Katz, R. C. Klet, S.-Y. Moon, J. E. Mondloch, J. T. Hupp, O. K. Farha, *ACS Catal.* **2015**, *5*, 4637.
[216] M. J. Katz, J. E. Mondloch, R. K. Totten, J. K. Park, S. T. Nguyen, O. K. Farha, J. T. Hupp, *Angew. Chem., Int. Ed.* **2014**, *53*, 497.
[217] M. J. Katz, S.-Y. Moon, J. E. Mondloch, M. H. Beyzavi, C. J. Stephenson, J. T. Hupp, O. K. Farha, *Chem. Sci.* **2015**, *6*, 2286.
[218] P. Li, R. C. Klet, S.-Y. Moon, T. C. Wang, P. Deria, A. W. Peters, B. M. Klahr, H.-J. Park, S. S. Al-Juaid, J. T. Hupp, O. K. Farha, *Chem. Commun.* **2015**, *51*, 10925.
[219] Y. Liu, S.-Y. Moon, J. T. Hupp, O. K. Farha, *ACS Nano* **2015**, *9*, 12358.
[220] S.-Y. Moon, A. J. Howarth, T. Wang, N. A. Vermeulen, J. T. Hupp, O. K. Farha, *Chem. Commun.* **2016**, *52*, 3438.
[221] S.-Y. Moon, Y. Liu, J. T. Hupp, O. K. Farha, *Angew. Chem., Int. Ed.* **2015**, *54*, 6795.
[222] S.-Y. Moon, G. W. Wagner, J. E. Mondloch, G. W. Peterson, J. B. DeCoste, J. T. Hupp, O. K. Farha, *Inorg. Chem.* **2015**, *54*, 10829.
[223] J. E. Mondloch, M. J. Katz, W. C. Isley III, P. Ghosh, P. Liao, W. Bury, G. W. Wagner, M. G. Hall, J. B. DeCoste, G. W. Peterson, R. Q. Snurr, C. J. Cramer, J. T. Hupp, O. K. Farha, *Nat. Mater.* **2015**, *14*, 512.
[224] F. Vermoortele, R. Ameloot, L. Alaerts, R. Matthessen, B. Carlier, E. V. R. Fernandez, J. Gascon, F. Kapteijn, D. E. De Vos, *J. Mater. Chem.* **2012**, *22*, 10313.
[225] A. Herbst, A. Khutia, C. Janiak, *Inorg. Chem.* **2014**, *53*, 7319.
[226] J. Jiang, F. Gándara, Y.-B. Zhang, K. Na, O. M. Yaghi, W. G. Klemperer, *J. Am. Chem. Soc.* **2014**, *136*, 12844.
[227] C. M. McGuirk, M. J. Katz, C. L. Stern, A. A. Sarjeant, J. T. Hupp, O. K. Farha, C. A. Mirkin, *J. Am. Chem. Soc.* **2015**, *137*, 919.
[228] M. G. Goesten, J. Juan-Alcañiz, E. V. Ramos-Fernandez, K. B. Sai Sankar Gupta, E. Stavitski, H. van Bekkum, J. Gascon, F. Kapteijn, *J. Catal.* **2011**, *281*, 177.
[229] Z. Hasan, J. W. Jun, S. H. Jhung, *Chem. Eng. J.* **2015**, *278*, 265.
[230] Q.-L. Zhu, Q. Xu, *Chem. Soc. Rev.* **2014**, *43*, 5468.
[231] Y. K. Hwang, D.-Y. Hong, J.-S. Chang, S. H. Jhung, Y.-K. Seo, J. Kim, A. Vimont, M. Daturi, C. Serre, G. Férey, *Angew. Chem., Int. Ed.* **2008**, *47*, 4144.
[232] X. Gu, Z.-H. Lu, H.-L. Jiang, T. Akita, Q. Xu, *J. Am. Chem. Soc.* **2011**, *133*, 11822.
[233] Q.-L. Zhu, J. Li, Q. Xu, *J. Am. Chem. Soc.* **2013**, *135*, 10210.
[234] B. An, J. Zhang, K. Cheng, P. Ji, C. Wang, W. Lin, *J. Am. Chem. Soc.* **2017**, *139*, 3834.
[235] M. Zhao, K. Yuan, Y. Wang, G. Li, J. Guo, L. Gu, W. Hu, H. Zhao, Z. Tang, *Nature* **2016**, *539*, 76.
[236] H. Noh, Y. Cui, A. W. Peters, D. R. Pahls, M. A. Ortuño, N. A. Vermeulen, C. J. Cramer, L. Gagliardi, J. T. Hupp, O. K. Farha, *J. Am. Chem. Soc.* **2016**, *138*, 14720.
[237] K. Manna, P. Ji, F. X. Greene, W. Lin, *J. Am. Chem. Soc.* **2016**, *138*, 7488.
[238] S. Yuan, Y.-P. Chen, J. Qin, W. Lu, X. Wang, Q. Zhang, M. Bosch, T.-F. Liu, X. Lian, H.-C. Zhou, *Angew. Chem., Int. Ed.* **2015**, *54*, 14696.
[239] Z. Li, N. M. Schweitzer, A. B. League, V. Bernales, A. W. Peters, A. B. Getsoian, T. C. Wang, J. T. Miller, A. Vjunov, J. L. Fulton, J. A. Lercher, C. J. Cramer, L. Gagliardi, J. T. Hupp, O. K. Farha, *J. Am. Chem. Soc.* **2016**, *138*, 1977.
[240] A. Dhakshinamoorthy, A. M. Asiri, H. Garcia, *Angew. Chem., Int. Ed.* **2016**, *55*, 5414.
[241] L. Zeng, X. Y. Guo, C. He, C. Y. Duan, *ACS Catal.* **2016**, *6*, 7935.
[242] C. G. Silva, I. Luz, F. Xamena, A. Corma, H. Garcia, *Chem. Eur. J.* **2010**, *16*, 11133.
[243] D. R. Sun, W. J. Liu, Y. H. Fu, Z. X. Fang, F. X. Sun, X. Z. Fu, Y. F. Zhang, Z. H. Li, *Chem. Eur. J.* **2014**, *20*, 4780.
[244] J. Long, S. Wang, Z. Ding, S. Wang, Y. Zhou, L. Huang, X. Wang, *Chem. Commun.* **2012**, *48*, 11656.
[245] J. D. Xiao, Q. C. Shang, Y. J. Xiong, Q. Zhang, Y. Luo, S. H. Yu, H. L. Jiang, *Angew. Chem., Int. Ed.* **2016**, *55*, 9389.
[246] H. Q. Xu, J. H. Hu, D. K. Wang, Z. H. Li, Q. Zhang, Y. Luo, S. H. Yu, H. L. Jiang, *J. Am. Chem. Soc.* **2015**, *137*, 13440.
[247] H. Zhang, J. Wei, J. Dong, G. Liu, L. Shi, P. An, G. Zhao, J. Kong, X. Wang, X. Meng, J. Zhang, J. Ye, *Angew. Chem., Int. Ed. Engl.* **2016**, *55*, 14310.
[248] L. Chi, Q. Xu, X. Liang, J. Wang, X. Su, *Small* **2016**, *12*, 1351.
[249] Y. W. Gao, S. M. Li, Y. X. Li, L. Y. Yao, H. Zhang, *Appl. Catal., B* **2017**, *202*, 165.
[250] R. W. Liang, F. F. Jing, L. J. Shen, N. Qin, L. Wu, *J. Hazard. Mater.* **2015**, *287*, 364.
[251] Y. An, Y. Y. Liu, P. F. An, J. C. Dong, B. Y. Xu, Y. Dai, X. Y. Qin, X. Y. Zhang, M. H. Whangbo, B. B. Huang, *Angew. Chem., Int. Ed.* **2017**, *56*, 3036.
[252] C. Wang, Z. G. Xie, K. E. deKrafft, W. L. Lin, *J. Am. Chem. Soc.* **2011**, *133*, 13445.
[253] K. M. Choi, D. Kim, B. Rungtaweevoranit, C. A. Trickett, J. T. D. Barmanbek, A. S. Alshammari, P. D. Yang, O. M. Yaghi, *J. Am. Chem. Soc.* **2017**, *139*, 356.
[254] C. Wang, J. L. Wang, W. B. Lin, *J. Am. Chem. Soc.* **2012**, *134*, 19895.
[255] Z. M. Zhang, T. Zhang, C. Wang, Z. K. Lin, L. S. Long, W. B. Lin, *J. Am. Chem. Soc.* **2015**, *137*, 3197.
[256] Q. Y. Li, Z. Ma, W. Q. Zhang, J. L. Xu, W. Wei, H. Lu, X. S. Zhao, X. J. Wang, *Chem. Commun.* **2016**, *52*, 11284.
[257] H. G. T. Nguyen, L. Mao, A. W. Peters, C. O. Audu, Z. J. Brown, O. K. Farha, J. T. Hupp, S. T. Nguyen, *Catal. Sci. Technol.* **2015**, *5*, 4444.
[258] D. Shi, C. He, B. Qi, C. Chen, J. Niu, C. Duan, *Chem. Sci.* **2015**, *6*, 1035.
[259] X. J. Kong, Z. K. Lin, Z. M. Zhang, T. Zhang, W. B. Lin, *Angew. Chem., Int. Ed.* **2016**, *55*, 6411.
[260] A. W. Peters, Z. Y. Li, O. K. Farha, J. T. Hupp, *ACS Appl. Mater. Interfaces* **2016**, *8*, 20675.

[261] Y. H. Fu, L. Sun, H. Yang, L. Xu, F. M. Zhang, W. D. Zhu, *Appl. Catal., B* **2016**, *187*, 212.
[262] Y. Su, Z. Zhang, H. Liu, Y. Wang, *Appl. Catal., B* **2017**, *200*, 448.
[263] Q. Lan, Z. M. Zhang, C. Qin, X. L. Wang, Y. G. Li, H. Q. Tan, E. B. Wang, *Chem. Eur. J.* **2016**, *22*, 15513.
[264] D. K. Wang, Z. H. Li, *J. Catal.* **2016**, *342*, 151.
[265] D. R. Sun, Z. H. Li, *J. Phys. Chem. C* **2016**, *120*, 19744.
[266] X. Zeng, L. Q. Huang, C. N. Wang, J. S. Wang, J. T. Li, X. T. Luo, *ACS Appl. Mater. Interfaces* **2016**, *8*, 20274.
[267] C. Yang, X. You, J. H. Cheng, H. D. Zheng, Y. C. Chen, *Appl. Catal., B* **2017**, *200*, 673.
[268] Z. W. Yang, X. Q. Xu, X. X. Liang, C. Lei, Y. L. Wei, P. Q. He, B. L. Lv, H. C. Ma, Z. Q. Lei, *Appl. Catal., B* **2016**, *198*, 112.
[269] D. Tilgner, R. Kempe, *Chem. Eur. J.* **2017**, *23*, 3184.
[270] M. H. Li, Z. J. Zheng, Y. Q. Zheng, C. Cui, C. X. Li, Z. Q. Li, *ACS Appl. Mater. Interfaces* **2017**, *9*, 2899.
[271] B. Nohra, H. El Moll, L. M. Rodriguez Albelo, P. Mialane, J. Marrot, C. Mellot-Draznieks, M. O'Keeffe, R. Ngo Biboum, J. Lemaire, B. Keita, L. Nadjo, A. Dolbecq, *J. Am. Chem. Soc.* **2011**, *133*, 13363.
[272] J. S. Qin, D. Y. Du, W. Guan, X. J. Bo, Y. F. Li, L. P. Guo, Z. M. Su, Y. Y. Wang, Y. Q. Lan, H. C. Zhou, *J. Am. Chem. Soc.* **2015**, *137*, 7169.
[273] X. Dai, M. Liu, Z. Li, A. Jin, Y. Ma, X. Huang, H. Sun, H. Wang, X. Zhang, *J. Phys. Chem. C* **2016**, *120*, 12539.
[274] N. Kornienko, Y. Zhao, C. S. Kley, C. Zhu, D. Kim, S. Lin, C. J. Chang, O. M. Yaghi, P. Yang, *J. Am. Chem. Soc.* **2015**, *137*, 14129.
[275] J. Q. Shen, P. Q. Liao, D. D. Zhou, C. T. He, J. X. Wu, W. X. Zhang, J. P. Zhang, X. M. Chen, *J. Am. Chem. Soc.* **2017**, *139*, 1778.
[276] I. Hod, M. D. Sampson, P. Deria, C. P. Kubiak, O. K. Farha, J. T. Hupp, *ACS Catal.* **2015**, *5*, 6302.
[277] C. W. Kung, J. E. Mondloch, T. C. Wang, W. Bury, W. Hoffeditz, B. M. Klahr, R. C. Klet, M. J. Pellin, O. K. Farha, J. T. Hupp, *ACS Appl. Mater. Interfaces* **2015**, *7*, 28223.
[278] Z. Tao, T. Wang, X. Wang, J. Zheng, X. Li, *ACS Appl. Mater. Interfaces* **2016**, *8*, 35390.
[279] X. Wang, H. Zhang, H. Lin, S. Gupta, C. Wang, Z. Tao, H. Fu, T. Wang, J. Zheng, G. Wu, X. Li, *Nano Energy* **2016**, *25*, 110.
[280] W. Zhang, Z. Y. Wu, H. L. Jiang, S. H. Yu, *J. Am. Chem. Soc.* **2014**, *136*, 14385.
[281] A. Mahmood, W. Guo, H. Tabassum, R. Zou, *Adv. Energy Mater.* **2016**, *6*, 1600423.
[282] S.-N. Zhao, X.-Z. Song, S.-Y. Song, H.-J. Zhang, *Coord. Chem. Rev.* **2017**, *337*, 80.
[283] C. R. Wade, T. Corrales-Sanchez, T. C. Narayan, M. Dincaˇ, *Energy Environ. Sci.* **2013**, *6*, 2172.
[284] Y.-K. Seo, J. W. Yoon, J. S. Lee, Y. K. Hwang, C.-H. Jun, J.-S. Chang, S. Wuttke, P. Bazin, A. Vimont, M. Daturi, S. Bourrelly, P. L. Llewellyn, P. Horcajada, C. Serre, G. Férey, *Adv. Mater.* **2012**, *24*, 806.
[285] A. Khutia, H. U. Rammelberg, T. Schmidt, S. Henninger, C. Janiak, *Chem. Mater.* **2013**, *25*, 790.
[286] H. Kim, S. Yang, S. R. Rao, S. Narayanan, E. A. Kapustin, H. Furukawa, A. S. Umans, O. M. Yaghi, E. N. Wang, *Science* **2017**, *356*, 430.
[287] E. Barea, C. Montoro, J. A. R. Navarro, *Chem. Soc. Rev.* **2014**, *43*, 5419.
[288] T. Grant Glover, G. W. Peterson, B. J. Schindler, D. Britt, O. Yaghi, *Chem. Eng. Sci.* **2011**, *66*, 163.
[289] Y. Liu, A. J. Howarth, J. T. Hupp, O. K. Farha, *Angew. Chem., Int. Ed.* **2015**, *54*, 9001.
[290] H. Jasuja, G. W. Peterson, J. B. Decoste, M. A. Browe, K. S. Walton, *Chem. Eng. Sci.* **2015**, *124*, 118.
[291] L. Hamon, C. Serre, T. Devic, T. Loiseau, F. Millange, G. Férey, G. D. Weireld, *J. Am. Chem. Soc.* **2009**, *131*, 8775.
[292] L. Hamon, H. Leclerc, A. Ghoufi, L. Oliviero, A. Travert, J.-C. Lavalley, T. Devic, C. Serre, G. Férey, G. De Weireld, A. Vimont, G. Maurin, *J. Phys. Chem. C* **2011**, *115*, 2047.
[293] X. J. Liu, Y. H. Zhang, Z. Chang, A. L. Li, D. Tian, Z. Q. Yao, Y. Y. Jia, X. H. Bu, *Inorg. Chem.* **2016**, *55*, 7326.
[294] O. Yassine, O. Shekhah, A. H. Assen, Y. Belmabkhout, K. N. Salama, M. Eddaoudi, *Angew. Chem., Int. Ed.* **2016**, *55*, 15879.
[295] P. Horcajada, T. Chalati, C. Serre, B. Gillet, C. Sebrie, T. Baati, J. F. Eubank, D. Heurtaux, P. Clayette, C. Kreuz, J.-S. Chang, Y. K. Hwang, V. Marsaud, P.-N. Bories, L. Cynober, S. Gil, G. Férey, P. Couvreur, R. Gref, *Nat. Mater.* **2009**, *9*, 172.
[296] P. Horcajada, C. Serre, G. Maurin, N. A. Ramsahye, F. Balas, M. Vallet-Regí, M. Sebban, F. Taulelle, G. Férey, *J. Am. Chem. Soc.* **2008**, *130*, 6774.
[297] Z. Dong, Y. Sun, J. Chu, X. Zhang, H. Deng, *J. Am. Chem. Soc.* **2017**, *139*, 14209.
[298] X. Lian, Y. Fang, E. Joseph, Q. Wang, J. Li, S. Banerjee, C. Lollar, X. Wang, H.-C. Zhou, *Chem. Soc. Rev.* **2017**, *46*, 3386.

